Antisense-oligonucleotides targeting tumor necrosis factor-alpha in murine herpes simplex virus type 1 retinitis

Jin Li

From Wuhan, China

Medizinische Fakultät

der

Universität Duisburg-Essen

Augenabteilung am St. Franziskus-Hospital, Ophtha-Lab., Münster

Antisense-oligonucleotides targeting tumor necrosis factor-alpha in murine herpes simplex virus type 1 retinitis

Inaugural-Dissertation

zur

Erlangung des Doktorgrades der Medizin

durch die Medizinische Fakultät

der Universität Duisburg-Essen

Vorgelegt von

Jin Li

aus Wuhan, China

2006

Dekan: Univ.-Prof. Dr. rer. nat. Karl-Heinz Jöckel

1. Gutachter: Prof. Dr. med. Arnd Heiligenhaus

2. Gutachter: Univ.-Prof. Dr. rer. nat. Ulf Dittmer

Tag der mündlichen Prüfung: 15. August 2006

Contents

1. INTRODUCTION

1.1 Acute retinal necrosis (ARN)

ARN syndrome is a well-known clinical entity that was first described in 1971 (Urayama et al., 1971). ARN is a type of retinitis that affects both healthy and immunocompromised patients (Silverstein et al., 1997; Batisse et al., 1996; Nussenblatt et al., 1989). Patients typically experience blurred vision, eye pain, and light sensitivity, in one or sometimes both eyes. Several members of the herpes virus family including herpes simplex virus (HSV)-1, HSV-2, varicella zoster virus (VZV) and, rarely, cytomegalovirus (CMV) are the main causing viruses (Silverstein et al., 1997; Atherton et al., 2001; Lewis et al., 1989; Thompson et al., 1994; Hellinger et al., 1993; Ganatra et al., 2000).

1.1.1 Virology of herpes viruses

They all have a large number of enzymes available that are involved in nucleic acid metabolism, DNA synthesis, and possibly the procession of proteins. The synthesis of DNA and the assembly of the capsid take place in the nucleus. The production of infectious virus particles may lead to the destruction of the infected cell. Furthermore, the herpes viruses establish latent infection in their natural hosts (Roizman et al., 1996). During latency, the herpes virus genomes form closed circular molecules, and only a small number of viral proteins are expressed. There is evidence that selected regulatory genes are active and may maintain latency, but neither the mechanisms to keep the status of latency nor the factors that cause reactivation of viral replication are yet completely known. After reactivation, infectious viruses are transported to peripheral tissues, e.g., by axonal transport in HSV infection (or retrograde transport back to the locus of primary infection). The immune response of the host may determine whether reactivation may result in a symptomatic or asymptomatic course

of herpetic disease (Roizman et al., 1996; Roizman & Sears , 1996)

1.1.2 Pathogenesis of HSV-1 induced experimental acute retinal necrosis

The acute stage of ARN is characterized by necrotizing retinitis of all retinal layers. The retinal vessels in the diseased area show fibrinoid necrosis of the vessel wall and vascular occlusion. The retinal pigment epithelium (RPE) shows focal necrosis and is occasionally separated from Bruch's membrane. The necrotizing retinal cells may reach the overlying vitreous body, where inflammatory cells group around it. The necrotizing retina is mostly sharply demarcated adjacent to the intact retina. In the marginal areas, intranuclear inclusions can be noted histologically, and by electron microscopy, virus particles can be detected in the retinal cells (Minckler et al., 1976; Cibis et al.,1978; Johnson et al.,1977). The adjacent choroid shows severe choroiditis with vascular occlusions. At the same time, optic nerve neuritis and papillitis arises. Inflammatory cells are infiltrating the aqueous humor and the anterior chamber angle. The iris and ciliary body show non-granulomatous and granulomatous cell infiltration and perivasculitis (Culbertson et al., 1982; Naumann et al., 1968; Culbertson et al., 1986). In the healing phase, the process leads to complete disintegration of the retina and the optic nerve, with reactive metaplasia of the retinal pigment epithelium (Cogan et al., 1964; Rummelt et al., 1992).

Herpes viruses were demonstrated in the retinal lesions and vitreous body in ARN patients by culture methods, histology, electron microscopy, immunohistochemistry, and by polymerase chain-reaction methods (Lewis et al., 1989; Culbertson et al., 1982; Pavan-Langston & Dunkel, 1989; Forster et al., 1990; Culbertson et al., 1986; Pepose & Whittum-Hudson, 1987). After primary infection or reactivation from latency, herpes virus replication follows. From animal experiments (Forster et al., 1990) it is known that viruses migrate through the ipsilateral parasympathetic fibers of the oculomotor nerve that serve the iris and ciliary bodies in the central nervous system. The viral replication within the CNS is fairly well limited to the nucleus of

the visual system and to the suprachiasmatic area of the hypothalamus. Viruses than migrate from the brain to the retina via retrograde axonal transport through the optic nerve, along the endocrine-optic path between the retina and the suprachiasmatic nucleus of the hypothalamus.

At this site, the viral invasion can spread out to the contralateral regions, which may explain the involvement of the fellow eye in patients with bilateral acute retinal necrosis (BARN). Along the optic nerve, the viruses may also reach the ganglionic cells of the contralateral retina (Pettit et al., 1965).

The retinal pathology represents a viral-induced cytopathology (Holland et al., 1987; Whittum-Hudson & Pepose, 1987). However, the accompanying immune reactions are decisive for the further inflammatory process that finally results in the development of retinal necrosis (Holland et al., 1987.; Whittum et al., 1984). Local as well as systemic factors come into effect here (Whittum et al., 1984). It has been shown that the retinal HSV infection is under the control of T lymphocytes in experimental herpetic retinitis (Whittum-Hudson et al., 1985). A contribution of T lymphocytes in the pathogenesis of human ARN has been suggested (Verjans et al., 1998).

The severe vascular occlusions lead to ischemia of the retina and choroid and further promote the development of necrosis. The massive breakdown of the blood-retina barrier with the resulting increase of the protein content in the vitreous is associated with a proliferative effect on the pigment epithelium and the fibroblasts. This may further support the development of proliferative vitreoretinopathy (PVR). The necrotic-related retinal tears and the developing traction from the vitreous space then finally result in the emergence of retinal detachment.

1.2 von Szily model

von Szily was the first scientist who reported about acute retinal necrosis syndrome in rabbits in 1924 (Von Szily, 1924). After injecting replication herpes simplex virus into the right anterior chamber of a rabbit, a rapidly destructive retinitis of the opposite (left) eye developed. The histopathologic analysis of the inoculated eye, however, disclosed that the retina of the injected (right) eye was more or less completely spared of this destructive phenomenon.

It has been shown that inoculation of the KOS strain of HSV-1 into the anterior chamber of one eye of BALB/c mice induced characteristic retinal changes, including a devastating inflammatory reaction within the posterior segment of the uninoculated eye, resulting in pan-necrosis of the retina 10 to 14 days post inoculation (PI) (Whittum et al., 1984).

Diverse inbred strains of mice have been shown to vary considerably in their resistance and susceptibility to that HSV induced retinal necrosis syndrome. The different strains of BALB/c, C57BL/6 and F1 hybrid had been studied to define the resistance and susceptibility to HSV retinitis. Injected eyes of BALB/c mice showed an anterior uveitis with HSV-1 antigens in the anterior segment and an intact retina that was free of HSV antigens. The retina of the contralateral uninjected eye, in contrast, was necrotic and contained HSV-1 antigens. In both, C57BL/6 and F1 mice, HSV antigens were limited to the structures of the anterior segment in the injected eye, whereas, in contrast to BALB/c mice, the contralateral retina appeared histologically normal and contained no viral antigens. Furthermore, these strains also remained relatively resistant to retinal infection despite being immunosuppressed by radiation (Pepose et al., 1987; Whittum & Pepose, 1988). Another study showed that DBA/2 mice were mildly resistant to HSV-1 retinitis in the uninoculated eye (Kielty et al., 1987).

Although HSV inoculated into anterior chamber of mouse in general induced retinitis, the different strains of HSV induced different courses of that disease. Whereas HSV-1 produces a rapid, explosive retinitis that led to destruction of all cell layers of contralateral retina, HSV-2 induced a retinitis in the ipsilateral eye that was more

gradual in onset (Dix et al., 1987).

Inoculation of HSV-1 (KOS) into the anterior chamber of BALB/c mouse eyes produces an intense inflammatory reaction at the inoculation site. Intensity and speed of the inflammatory reaction are dose-dependent over a wide range: 2×10^2 to 2×10^5 plaque forming units (PFU) HSV-1. The dose of 2×10^4 PFU was chosen by the researchers for the following reasons: (1) this particular dose of virus induced anterior chamber-associated immune deviation (ACAID), i.e., recipient mice produced high titers of circulating anti-HSV-1 antibody, but failed to develop T-cell immunity as measured by the capacity to express HSV-1 specific delayed type hypersensitivity (DTH); (2) when inoculated subcutaneously, this dose of virus regularly induced vigorous DTH to HSV-1 as well as humoral anti-HSV-1 responses; and (3) lid vesicles were observed uncommonly after AC inoculation of 2×10^4PFU HSV, whereas at higher doses lid lesions regularly occurred, raising the possibility that auto-inoculation of virus by infected mice would unduly confound the analysis. Within this dose range, the only visible manifestation of disease in AC-inoculated mice was in the injected eye. None of the mice died or developed signs of disease at other sites (Whittum et al., 1983; Whittum et al.,1984).

In the HSV-1 inoculated eyes, the inflammatory reaction commonly involves the entire anterior segment. The cornea rapidly becomes edematous, and an inflammatory cell infiltration and neovascularization occurs. The central stromal infiltrate peaks by day 7 and resolved completely by day 21. The extensive neovascularization reaches its maximum intensity by day 14. The extensive loss of corneal clarity observed by slit lamp corresponds with the edema and disruption of the stromal architecture. By day 5, the corneal endothelium is destroyed. The anterior chamber of injected eyes contains an increasingly severe cell and flare reaction that is already visible by 1 day after virus inoculation. Over 21 days, the anterior chamber becomes progressively more shallow (loss of form or depth), and it is occupied by a fibrovascular tissue development between day 14 and 21 PI. Iris infiltration and loss of iris integrity are both evident at day 1. Iris atrophy (loss of iris stroma and vessels) occurs by day 3

(Whittum et al., 1984).

In contralateral eye, the inflammatory reaction involves mainly the posterior segment. The infectious process in the retina of the uninoculated eye has been divided in three phases: acute retinitis, retinal necrosis, and resolution (Cousins et al., 1989). Acute retinitis is observed between days 7 and 9 PI. The retina remains normal until day 7 PI. At this time, small foci of inflammatory cells appear around one or two small vessels in the ganglion cell layer (GCL). These foci are limited generally to one lateral aspect of the GCL per eye, midway between the optic nerve and the anterior edge of the retina (ora serrata). The remainder of the GCL appears normal at this time, as do the outer layers of the retina and underlying choroid.

The retinal necrosis begins on day 10 PI. By day 10, a large necrotic area containing a mixed inflammatory infiltrate extends posteriorly through the entire retina. The choroid underlying the necrotic area also is infiltrated. Inflammatory cells can occasionally be seen around the optic nerve at this time. By day 14 PI, the retina is completely necrotic with inflammatory cells, debris and numerous plasma cells interspersed throughout the disrupted retinal cells. In addition, the choroid is infiltrated extensively.

The resolution phase usually begins on or about day 15 PI. The remnants of the retina are organized into a fibrocellular scar, and the ocular inflammation is gradually resolved (Azumi et al., 1994; Zaltas et al., 1992; Azumi & Atherton, 1998; Cousins et al., 1989).

Following anterior chamber inoculation of HSV-1 into one eye of BALB/c mice, a certain pattern of ocular pathology as well as systemic immune response emerges. It is a suppression of DTH responses to the injected HSV with an intact HSV-1 neutralizing antibody response. This phenomenon is termed anterior chamber associated immune deviation (Whittum et al., 1983). However, compared with the BALB/c strain, the AC infection in C57BL/6 mice was not followed by a contralateral retinitis, while the mice showed a vigorous HSV-1 specific DTH response. Therefore,

is has been suggested that the absence of contralateral retinitis might be linked to the induction of virus-specific DTH response. It has been speculated that DTH inducing T-effector cells or other mechanisms might limit the amount of virus that reaches the CNS, which in turn affects the amount of second wave of virus which reaches to uninoculated contralateral eye (Kielty et al., 1987)

The virus culture studies have revealed that virus reaches the uninoculated eye in two temporally separate waves after uniocular anterior chamber inoculation. The first wave of virus is detected in the uninoculated eye as early as one day PI, long before virus is found in either of the optic nerves or the brain. The second wave of virus arrives in the uninoculated eye between 7 and 10 days PI (Atherton & Streilein, 1987).

Kahn (1993) investigated the effect of light onto von Szily model. His findings suggested that virus does not reach the contralateral retina in dark-reared mice. He found a decrease in neuronal firing and retrograde axoplasmic flow during darkness (Kahn et al., 1993). Colchicine is known for its axonal-transport-blocking capabilities. It was used to examine whether virus is transported via the optic nerve to the uninoculated eye after anterior chamber inoculation of HSV-1. The results demonstrated that blocking the optic nerve with colchicine prevented the entry of only the second-wave of virus, while the first-wave of virus was not affected. This observation supported the hypothesis that the second-wave of virus reaches the contralateral eye from the central nervous system via the optic nerve (Bosem et al., 1990).

The route of second wave of virus spread was also studied by Vann and Atherton (Vann & Atherton, 1991) in BALB/c mice. The data showed that virus spreads from the injected eye to the central nervous system (CNS) through parasympathetic fibers of the oculomotor nerve that supply the iris and ciliary body. The virus spread in the CNS is limited primarily to the nuclei of the visual system and the suprachiasmatic area of the hypothalamus. Subsequently, the virus is transmitted from the CNS to the retina of the contralateral eye by retrograde axonal transport through the optic nerve

along the endocrine-optic pathway between the retina and the suprachiasmatic nucleus (SCN) of the hypothalamus (Fig 1).

1.3 Participation of the immune response to the injected virus

Researchers have concluded that immune response participates in the course of the HSV-1-induced contralateral retinitis (Atherton et al., 1989; Whittum-Hudson et al., 1985). Using flow cytometry and immunohistochemistry, Azumi (Azumi & Atherton, 1998) documented that T cell play a role in the disease. At day 9 PI (acute retinitis), T cells were observed in the uvea but not in the retina of contralateral eye. The $CD4^+$ and $CD8^+$ T cells were found in the sensory retina coincident with the onset of retinal necrosis (day 11 PI), and $CD4^+$ and $CD8^+$ T cells were then detected in the remnants of the retina until day 63 PI. The maximum number of infiltrating cell, both of the $CD4^+$ and $CD8^+$ subgroups were observed at day 21 PI.

Another investigation by the same group of researchers suggested that the $CD4^+$ T cell subset contributes to the destruction of the retina, and may accelerate the cellular infiltration and inflammation-induced retinal destruction at day 14 (retinal necrosis phase). At least 2 weeks before inoculation of virus, T-cell-depleted BALB/c mice were injected intravenously with anti-CD4 monoclonal antibody. Indeed, the treatment with an anti-CD4 monoclonal antibody in the von Szily model modified the virus recovery from the posterior segment of the contralateral eye significantly. By day 14 PI, significantly higher titers of virus were recovered from the mice that were depleted of $CD4^+$ cells. In conclusion, the $CD4^+$ T cells are involved in virus clearance from contralateral eye (Azumi et al., 1994).

The Mac-1 positive cells (macrophages, natural-killer cells, and polymorphonuclear neutrophils) appear in contralateral ciliary body between day 8 and 10 PI. On day 10, a large number of Mac-1 positive cells infiltrate the retina, and mainly the inner retinal layers. Simultaneously, Mac-1 positive cells also infiltrated the choroid. The

finding of a predominance of Mac-1 cells in the contralateral retina of susceptible BALB/c mice on day 10 led the researchers to speculate that the cells might be important mediators of necrotizing in contralateral retinal necrosis phase (Zaltas et al., 1992). The DNA microarray results showed that macrophage-related genes were up-regulated in the contralateral eye at day 9 PI. Additional immunohistochemical studies also showed the presence of F4/80-positive cells in the retina (Zheng et al., 2003). In further experiments, an anti-CD11b mAB was injected intravitreally before the first wave of inflammatory cells arrived to the eye. This resulted in a profound suppression of retinal necrosis with significant decrease in both the incidence and the severity of the retinitis, even though herpes simplex viral particles could be detected in the chorioretinal layers of unaffected eyes by indirect immunofluorescence. In agreement with these data, a suppression of retinal necrosis was also noted when macrophages were depleted from mice by the treatment with Cl_2MDP-liposomes. The timing of the anti-CD11b mAb injection appeared to be critical for the inhibition of contralateral retinitis. Suppression of retinal necrosis was effective only when the antibody was administered before the onset of clinical signs. Once the initial clinical signs of contralateral retinitis were observed, anti-CD11b mAb did not alter the course of the disease (Berra et al.,1994). These findings suggested that macrophages are important participants in the effector phase of the inflammatory immune response in HSV-1 induced contralateral retinitis. Macrophages probably play a multifunctional role in the pathogenesis of the disease by direct cytotoxic action and indirectly by releasing chemotactic and immunoregulatory cytokines that finally contribute to retinal destruction. Other possibilities are that they are acting as antigen presenting cells (APC) to increase T-cell function (accessory function of macrophages). They can also provide costimulatory signals to increase effector T-cell function by B7.1/B7.2.

Beside the inflammatory cells, various cytokines and chemokines are actively involved in the course of HSV-1 retinitis. DNA microarray was used to analyze the expression patterns of genes in the uninoculated eye following uniocular anterior chamber inoculation of HSV-1. The most abundant cytokines and chemokines in the

contralateral eyes of mice with HSV-1 retinitis were the IFN-family and their receptors, the interleukins IL-1, IL-6, and IL-4 and their receptors, and macrophage inflammatory protein (MIP-1 and MIP-2) and their receptors. Since these cytokine and cytokine-receptor genes were up-regulated in the uninoculated eye at the peak of acute retinal infection, these results suggested that they are likely to be the modulators most closely related to ARN (Zheng et al., 2003). From RT-PCRs assay, the transcriptions of some cytokines were investigated. IFN-g-mRNA was moderately elevated on day 6 PI, increased slightly between days 6 and 8 PI, and then increased slightly again between day 8 and 11 PI. On day 6 and 8 PI, the level of mRNA for IL-4 was only slightly above that observed in the uninjected eyes of the mock-infected mice. Between day 8 and 11 PI, the amount of IL-4 mRNA increased approximately three fold. IFN-γ^+ and IL-4^+ cells were observed throughout the retina. Most of $CD4^+$, Gr-1^+, $CD19^+$ and $F4/80^+$ cells expressed IFN-γ and IL-4 (Zheng et al., 2005).

1.4 Tumor necrosis factor-alpha

The proinflammatory cytokine tumor necrosis factor alpha (TNF-α) originally was identified as a serum factor causing hemorrhagic necrosis of tumors and inducing cachexia. TNF-α is now known to possess many cell-activating and pro-inflammatory activities. TNF-α is produced by many cell types, among them are macrophages, T cells, and natural killer cells. The pro-inflammatory effects include induction of expression or up-regulation of major histocompatibility complex molecules (Sartani et al., 1996; Fong & Lowry, 1990; Fleisher et al., 1990). TNF-α exerts its actions through two distinct receptors: TNF RI (P55) and TNF RII (P75). The TNF-induced cytotoxicity has been attributed in the past to the p55 receptor, and TNF-induced proliferation to the p75 receptor. However, it has been shown, that p75 can greatly enhance p55-induced cell death (Koizumi et al., 2003; Bigda et al., 1994; Tartaglia et al., 1991).

The TNF/TNF-R family plays a key role in the activation, differentiation and effector responses of T-cells. Subsequent analysis of TNF-R expression revealed that antigen activation was required for the up-regulation of p75 and to a lesser extent p55 TNF-R and the acquisition of TNF responsiveness by different T-cell subsets in vitro, but more importantly at sites of inflammation (Ware et al., 1991; Brennan et al.,1992; Cope et al.,1995). Both in vitro and in vivo co-stimulatory effects may arise through different mechanisms, including activation and differentiation of antigen-presenting cells, such as dendritic cells, as well as antigen-presenting function (Sallusto et al., 1995). The treatment with rabbit anti-TNF-α serum in experimental autoimmune uveoretinitis (EAU) during the afferent stage significantly reduced the autoantigen specific lymphocyte proliferation and DTH (Sartani et al., 1996). Greiner and co-workers investigated 15 patients with posterior segment intraocular inflammation (PSII) refractory to conventional immunosuppressive therapy and who then received a single infusion of a recombinant protein generated by fusing the p55 TNF-α receptor with human IgG1. Interestingly, the authors found that the anti-TNF-α agent induced an up-regulation of IL-10-expression in peripheral blood $CD4^+$ T cells and an alteration in the ratio of IL-10- and IFN-γ-producing $CD4^+$ T cells (Greiner et al., 2004).

Macrophages are versatile cells that are intimately involved in diverse aspects of the immune response and inflammation. The cytotoxic macrophages and production of nitric oxide (NO) or reactive oxygen species (ROS) might cause cell membrane peroxidation and destruction. Classic macrophage activation after stimulation with IFN-γ and TNF refers to the ability of a macrophage to express nitric oxide synthase (NOS2) and generate nitrite, peroxynitrites, and superoxides, which in turn induce lipid peroxidation of cell membranes and cell death (Robertson et al., 2002; Erwing et al., 1998; Li & Verma, 2002; van Strijp et al., 1991). In experimental cutaneous leishmaniasis, the blockade of the TNF activity resulted in a reduced NOS2 expression from draining lymph nodes and macrophages (Engwerda et al., 2002; Fonseca et al., 2003). With a treatment of mice with sTNFr-IgG in the EAU model,

infiltrating macrophages reduced expression nitrite production at the height of disease, and the level of apoptosis within the retina was reduced too (Robertson, 2003).

In the von Szily model, TNF-α mRNA and protein was up-regulated during the evolution of ARN (from day 6 to 14 PI) in the contralateral eyes compared with levels in control subjects (Zheng et al., 2005). The DNA microarray results showed that among the most up-regulated cytokines and chemokines in contralateral eye of mice with HSV-1 retinitis was the TNF family cytokines and their receptors (Zheng et al., 2003). The immunohistochemical stainings revealed that TNF-α was produced by infiltrating cells such as $CD4^+$, $Gr\text{-}1^+$, $CD19^+$, and $F/80^+$ cells. Approximately one third of the RPE cells produced TNF-α at day 9 PI. In addition, a smaller number (4-14%) of Müller cells also produced TNF-α at the same time (Zheng et al., 2005).

Latently infected trigeminal ganglia (strain KOS) were excised and placed in vitro. TNF-α was added daily. The reactivation replication rate in the TNF-α treated group was higher than the control group. These experiments demonstrated that TNF-α enhanced the reactivation frequency and replication of HSV (Walev et al., 1995). Also, the number of TNF-α producing cells was investigated during the acute replication phase of HSV in trigeminal ganglia. The appearance of TNF-α producing cells in the trigeminal ganglia was correlated to virulence and replication of HSV dependent on the time of appearance. The higher the virulence the earlier commenced replication and the more increased the number of TNF-α- producing cells (Walev et al., 1995).

In conclusion, it appears that TNF-α is an one of the most important pro-inflammatory cytokines in ARN (Oettinger & D'Szouza, 2003).

1.5 Antisense technologies

Scientists have been working on strategies to selectively turn off specific genes in diseased tissues for the past thirty years. The potential of oligodeoxynucleotides to act

as antisense agents that inhibit viral replication in cell culture was discovered by Zamecnik and Stephenson in 1978 (Zamecnik et al., 1978). Since then antisense technology has been developed as a powerful tool for target validation and therapeutic purposes. Theoretically, antisense molecules could be used to cure any disease that is caused by the expression of a deleterious gene, such as viral infections, cancer growth and inflammatory diseases. In the 1980's, oligodeoxynucleotides with unique chemistries were tested in experimental model systems both in vitro and in vivo with varying degrees of success. In the 1990's, ribozymes with both antisense and catalytic properties were successfully introduced to the field. Ribozymes were shown to selectively knock-down targeted genes in human tumors grown in mice, but delivery issues for these therapeutic anti-genes limited their clinical utility. Short interfering RNA (siRNA) is currently a growing sector of this anti-gene research field for target validation and therapeutic applications.

Three types of anti-mRNA strategies are summarized in Fig 2. Most of conventional drugs bind to proteins and thereby modulate their function. In contrast, antisense agents act at the mRNA level, preventing its translation into protein. Antisense oligonucleotides pair with their complementary mRNA, whereas ribozymes and DNA enzymes are catalytically active oligonucleotides that not only bind, but also cleave their target RNA. In recent years, the development of novel chemical modifications stabilized oligonucleotides. It enhanced the target affinity too. RNA interference is an efficient method for suppressing gene expression by the use of 21-23-mer small interfering RNA (siRNA) molecules (Elbashir et al., 2001).

Antisense molecules are commonly composed of single-stranded DNA, which they are termed antisense oligonucleotides (ASON). The ASON usually consist of 15-20 nucleotides, which is complementary to their target mRNA. The mechanisms of action include blockage of translation and splicing. The RNA-DNA hybrid can also be recognized and cleaved by RNase H, yielding an additional mechanism of repression of gene expression. Alternatively, ASON that do not induce RNase H cleavage can be used to inhibit translation by blockade of the ribosome. When the ASON are targeted

to the 5'-terminus, binding and assembly of the translation machinery can be prevented (Fig 3). The antisense-mediated inhibition of gene expression raised considerable interest in the potential of antisense molecules not just as a molecular tool in biomedical research, but also as a novel class of therapeutic agent (Scanlon, 2004).

One of the major challenges for antisense approaches is the stabilization of oligonucleotides. If used in their unmodified form as phosphodiesters, they are rapidly degraded in biological fluids by nucleases. There are a vast number of chemically modified nucleotides that have been used previously in antisense experiments. In general, three types of modifications of ribonucleotides can be distinguished: analogs with unnatural bases, modified sugars or altered phosphate backbones. In the recent years, a variety of modified nucleotides have been developed to improve properties such as target affinity, nuclease resistance and pharmacokinetics. DNA and RNA analogs with modified phosphate linkages or riboses, as well as nucleotides with a completely different chemical moiety substituting the furanose ring (Galderisi & Cascino, 1999; Pierce et al., 2005; Da Ros et al., 2005).

An important hurdle that has to be overcome for successful antisense applications, is the cellular uptake of the molecules. In cultured cells, internalization of naked DNA is usually inefficient, due to the fact that charged oligonucleotides have to cross a hydrophobic cell membrane. A number of methods have, therefore, been developed for in vitro and in vivo delivery on oligonucleotides. By far the most commonly and successfully used delivery systems are liposomes and charged lipids, which can either encapsulate nucleic acids within their aqueous center, or form lipid-nucleic acid complexes as a result of opposing charges. These complexes are usually internalized by endocytosis (Kurreck, 2003).

It has been recently shown that TNF-α-ASON diminishes the release of TNF-α from cultured draining lymph node cells or splenocytes (Wasmuth et al., 2003). Furthermore, the corneal injection of TNF-α-ASON significantly improved the course

of herpetic stromal keratitis (HSK). TNF-α-ASON effectively suppressed the content of TNF-α in the HSV-1 infected corneas.

1.6 Aim of this study

In this study, mice were infected in the AC of the right eyes with HSV-1 (von Szily model), and the left eyes were treated subconjunctivally with ASON targeting TNF-α Experiments were performed to answer the following questions:

1. Is TNF-α-ASON taken up into the eyes when injected subconjunctivally? (in the injected eyes, in regional lymph nodes and spleen)
2. Is TNF-α-ASON treatment influencing the expression of TNF-α in vivo? (in the injected eyes)
3. Is TNF-α-ASON able to modify the severity of contralateral retinitis? What is an appropriate treatment plan?
4. What is the effective way of modifying the course of contralateral retinitis by TNF-α-ASON administration? (comparison of subconjunctival and intraocular injections)
5. Is TNF-α-ASON modifying the intraocular inflammatory cell infiltration?
6. Is TNF-α-ASON affecting the systemic immune response against HSV-1?

2. MATERIALS AND METHODS

2.1 Reagents

[^{3}H]Thymidine	Amersham Bioscience, Buckinghamshire, UK
3-Amino-9-Ethylcarbazol	Sigma-Aldrich Chemie GmbH, Germany
β-Mercaptoethanol	Sigma-Aldrich Chemie GmbH, Germany
Acetic acid	Merck KGaA,, Germany
Acetone	Merck KGaA,, Germany
Agarose	Sigma-Aldrich Chemie GmbH, Germany
APES (3-aminopropyltriethoxysilane)	Sigma-Aldrich Chemie GmbH, Germany
Aquatex	Merck KgaA, Germany
Concanavalin (Con) A	Sigma-Aldrich Chemie GmbH, Germany
Crystal violet	Merck KGaA, Germany
Ethanol	Carl Roth GmbH, Germany
Eosin	Sigma Diagnostics, USA
Eukitt	Sigma-Aldrich Chemie GmbH, Germany
Fetal calf serum	DAKO, A/S, Denmark
Formaldehyde sodium 37%	Merck KGaA, Germany
Hematoxylin solution, Gill No.3	Sigma Diagnostics, USA
HEPES	Roth, Karlsruhe, Germany
Hydrogen Peroxide	PharMingen, Heidelberg, Germany
Ketamine hydrochloride	CuraMED Pharma GmbH, Germany
Mepivacaine hydrochloride	CuraMED Pharma GmbH, Germany
Natrium chlorid	Merck KGaA, Germany
N,N-Dimethylformamid	Sigma-Aldrich Chemie GmbH, Germany
Normal mouse serum	DAKO, A/S, Denmark
PBS	Gibco Brc, Germany
Paraformaldehyde	Sigma-Aldrich Chemie GmbH, Germany
RPMI	YIB CO, Germany
Scandicain 2%	AstraZeneca GmbH, Germany
Sterile saline solution	Bayer, Germany
Sodium acetate	Sigma-Aldrich Chemie GmbH, Germany
Tetramethylbenzidine (TMB)	PharMingen, Heidelberg, Germany
Tween-20 0.05%	PharMingen, Heidelberg, Germany
Xylol	Merck KGaA,, Germany

2.2 Instruments

Frigocut cryostat	Reichert-Jung 2800N, Germany
Flow cytometry	FACScan Flow Analyser (Becton Dickinson San Jose, CA)
Microscope	Olympus BX40F4, Japan
Microtome	Leica RM 2135, Germany
Fluorescence microscopy	Olympus BX40F4, Japan
Microtiter Plate Reader MRX	Dynatech Laboratories, Chantilly, VA, USA
Scintillation Counter	Top Count NTX; Packard Bioscience, Meriden, CT

2.3 Animals

BALB/c mice were obtained for the entire study. The animals were aged 6~8 weeks and were maintained according to the ARVO Statement for Use of Animals in Ophthalmic and Vision Research and according to the guidelines approved by the institutional animal care and use committee, and according to the Institutional Board (Genehmigung eines Versuchsvorhabens, nach § 8 Abs. 1 des Tierschutzgesetzes).

2.4 Virus

HSV-1 KOS strain was kindly provided by David Knipe (Harvard Medical School, Boston, MA). The virus was isolated and expanded on Vero cells (CCL 81; American Type Tissue Collection, Manassas, VA). When confluent effects appeared, virus infected vero cell monolayers were harvested. After three times freeze-thawed, homogenized and centrifuged, the virus-containing supernatants were collected.

2.5 Plaque assay

1 Dilute Vero cells (CCL 81: American Type Tissue Collection, Manassas, VA) to a density of 1.5×10^5 cells/ml with RPMI and 10% fetal calf serum

2 Transfer 0.5 ml of this cell suspension to each well and incubate for 24 hours

3 The homogenized virus-containing solution were 10 folds step diluted in RPMI medium as 10^{-1}-10^{-8}

4 Discard the medium over Vero cells and add 0.2ml of diluted virus solution quickly

5 Standard virus suspension of 2×10^8PFU/ml was add as positive controls

6 RPMI medium was add as negative controls

7 Incubate for 1 hour at 37°C

8 Melt the agarose completely in a microwave being careful to allow air to escape to avoid exploding glassware

9 Mix 50ml agarose, 50 ml 2×RPMI and 1ml Ciprobay, keep in 35-37°C until use

10 Remove the suspension in the wells and cover well with 0.7ml RPMI/agarose medium

11 Place the plate in a 37°C, 98% humidity controlled incubator for at least 2-3 days

12 Incubate with 200μl 37% formalin solution to fixing the cell layers for 1 days

13 Discard the RPMI/agarose carefully in each well

14 Stain the cells with 200μl 2% crystal violet for 30 seconds

15 Wash with water and dry them

16 Count the plaques under microscope fields

17 The titer (PFU/ml) may be calculated by the following formula: PFU/ml (of

original stock) = Counts×5×dilution factor (ml of inoculum/plate)

2.6 Infection of the anterior chamber with HSV-1

The animals were anesthetized with ketamin (2mg) and mepivacaine hydrochloride (400ng) intraperitoneally. The AC of the right eyes were inoculated with $2x10^4$ PFU of HSV-1 contained in a total volume of 5 µl PBS. The experiments were repeated to test the reproducibility of the results.

2.7 Injection technique into the vitreous

2µl ASON solution (100nMol) was injected into the vitreous of the left eyes by three-direction tap system. Injections were performed using glass pipettes with a diameter of approximately 150µm at the tip made with a standard pipette puller. The pipette was connected to a three direction tap with a 10µl Hamilton syringe and a normal syringe. ASON was stored in the normal syringe. Before injection, 2µl of ASON solution were uploaded in the Hamilton syringe. The lid fissure was opened and the eye proptosed by gentle pressure on the temporal upper eyelid. Under an operation microscope, the eye was punctured directly at the pars plana, and the 2µl were then injected into the vitreous behind the lens. Since reflux of a certain amount of intraocular fluid is unavoidable when removing the pipette from the injection site, the pipette was kept in place for 10 seconds to allow diffusion of the solution.

2.8 Injection technique for subconjunctival injection

Mice received a subconjunctival injection of ASON at the right eye. Under an

operation microscope, the conjunctiva was elevated with an iris forceps, Bonn model (Geuder, Germany). 50 µl (2.5 µMol) of the ASON solution was injected into the conjunctiva using a 30-gauge needle. The injection resulted in a circular bleb formation around the corneal limbus.

2.9 Antisense oligonucleotides

ASON targeted to TNF-α and control oligonucleotides (CON) were designed and manufactured by Biognostik (Göttingen, Germany). For against enzymatic cleavage by DNases, the full-length backbone was modified. In these phosphorothioates one of the nonbridging oxygens of the phosphate backbone is replaced by a sulfur atom. This is achieved through postcoupling oxidation with a sulfurizing reagent (EDITH (3-ethoxy-1,2,4-dithiazoline-5-one); PE Applied Biosystems, Weiterstadt, Germany). The ASON (CGA AGT TCA GTA GAC AG) used in the present study is the reverse complement to the bases 300 to 316 of the total sequence of murine TNF-α, and it targets an exon of the coding region. The mixed antisense oligonucleotides in a randomized fashion are obtained as the controls. Cross homologies with other genes were excluded for both sequences in the GenBank database (http://www.ncbi.nlm.nih.gov/Genbank; provided in the public domain by the National Center for Biotechnology Information, Bethesda, MD). ASON and CON (GCT CTA TGA CTC TTC AG) have identical chemical modification.

2.10 ASON in vitro uptake by lymphatic cells from the lymph nodes and spleen

Regional lymph nodes and spleens were harvested from HSV-infected mice at days 10 PI (Bauer et al., 2002). The spleens or lymph nodes were homogenized and centrifugated at 1500 rpm for 10 min. Single-cell suspensions were prepared, and

cells were cultured in 96-well plates ($1x10^5$ cells/well). The culture medium contained RPMI, 5%FCS, HEPES and β-mercaptoethanol. The cells were treated with 2μM fluorescein isothiocyanate (FITC)-labeled ASON from 15 minutes to 48 hours in dark, then washed 3 times by adding 150μl PBS and centrifuged 5 minutes at 1000 rpm. All of the cells were separated in 2 groups for fluorescence microscopy and flow cytometry assay.

2.11 Fluorescence microscopy assay

1 50μl single-cell suspension was scattered on APES coated slides

2 Dry the slides in air at room temperature

3 Fix the cells in RPMI with 4% paraformaldehyde

4 Place the slides in graded ethanol series (70%, 80%, 96%, 100%) 2 minutes for dehydrating

5 Exam them under fluorescence microscopy in dark room

2.12 Flow cytometry assay

The flow cytometer (FacsCan BD) was calibrated by standard fluoresent beads before assay. For each sample, 20,000 events were measured. Cells without FITC-ASON served as the negative control. The data was analysis with Facs Scan software.

2.13 Uptake of ASON in vivo

50μl FITC-labeled TNF-α-ASON (50nMol/μl) was injected subconjunctivally in mouse. In another group, 2μl FITC-labeled TNF-α-ASON (50nMol/μl) was treated

with mouse by intraocular injection. The eyes were harvested after 1, 2¤ 3, 7 and 10 days. Specimens were then dehydrated in ascending ethanol series, fixed in acetone, and embedded in paraffin. The specimens were then cut into 5μm sections and fixed on APES (3-aminopropyltriethoxysilane) covered slides. The distribution of the FITC-positive staining was observed by fluorescence microscopy.

2.14 TNF-α expression in eyes

Animals were killed on day 8 PI. The left eyes were removed and snap frozen in liquid nitrogen. They were then thawed and homogenized by manual treatment. The supernatants were collected after centrifugation for TNF-α assay by standard ELISA (PharMingen, Heidelberg, Germany).

2.15 Enzyme-linked immunosorbent assay

1 Coat microwells with 100 μL per well of capture antibody

2 Seal plate and incubate overnight at 4° C

3 Aspirate wells and wash 3 times with ≥ 300 μL/well PBS with 0.05% Tween-20

4 Block plates with ≥ 200 μL/well PBS with 10% FCS

5 Incubate at room temperature for 1 hour

6 Aspirate wells and wash 3 times

7 Pipette 100 μL of each standard, sample, and control into appropriate wells

8 Seal plate and incubate for 2 hours at room temperature

9 Aspirate wells and wash 5 times

10 Add 100 µL of detection antibody and HRP in each well

11 Seal plate and incubate for 1 hour at room temperature

12 Aspirate wells and wash 7 times

13 Add 100 µL of substrate solution containing tetramethylbenzidine and hydrogen peroxide to each well

14 Incubate plate (without plate sealer) for 30 minutes at room temperature in the dark

15 Add 50 µL of stop solution (1 M H_3PO_4 or 2 N H_2SO_4) to each well

16 Read absorbance at 450 nm within 30 minutes of stopping reaction

(Bauer et al., 2002).

2.16 Experimental Design

In all of the mice, HSV-1 solution was injected into the right eyes on day 0. The left eyes were treated on days –1, +1 and +4 with subconjunctival injections. The mice from group 1 (n=20) received 2.5µM of ASON in 50µL PBS. The mice from group 2 (n=20) served as the control for substance-specific bystander effects and, therefore, received 2.5µM of CON in 50µL PBS. The mice from group 3 (n=20) were given 50µL PBS.

2.17 Clinical Examination

Ipsilateral and contralateral eyes were examined every day with a binocular operation microscope. The development of intraocular inflammation, particularly contralateral

chorioretinitis, was evaluated in a masked fashion. Anterior chamber inflammatory reaction, papillary and iris vessel dilation, cataract formation, vitreal haziness and whitening of fundus reflex were examined by two observers.

2.18 Histology

Animals were killed on day 8 and 10 after the HSV-1 was injected into anterior chamber.

1 Remove the left eyes and fix for 6 hours in 4% formalin.

2 For dehydrating, keep specimens in graded ethanol series (70%, 80%, 96%, 100%,100%), each for 1.5 hours

3 Keep specimens in acetone for 1.5 hours twice

4 Keep specimens in xylol for 2 hours

5 Keep specimens in paraffin three times for 1 hour at 60° C

6 Embedded in paraffin

7 Cut the tissue cross-sections into 5-μm thick.

8 Fix the sections on the APES coated slides

9 For deparaffination, keep the sections in xylol 10 minutes for 3 times

10 For rehydrating, keep the sections in degrade ethanol series (100%, 100%,96%, 80%, 70%), each for 3 minutes

11 Rinse in distilled water twice

12 Stain with hematoxylin for 30 seconds

13 Rinse in distill water twice

14 Stain in eosin for 30 seconds

15 Rinse in 96% ethanol for 3 minutes 3 times

16 Rinse in 100% ethanol for 3 minutes 3 times

17 Rinse in xylol for 3 minutes 3 times

18 Mount sections in eukitt and coverslips

The infiltrating cells in ciliary body, retina and choroid were enumerated by means of brightfield microscopy under a 10×10 grid high-power (×250) (n=5/Group).
The severity of retinitis was graded on a scale of 0 to 2+.

Grade 0: no retinitis present.

Grade 1+: infiltrating inflammatory cells in the inner 1/3 of the retina, especially perivascularly. Foci of retinitis
Grade 2+: infiltrating inflammatory cells in the entire depth of the retina, involving at least half of retina.

2.19 Glass slide coating protocol

1 Place the precleaned slides in slide rack in the plastic slide box

2 Rinse slides in 96% ethanol

3 Place slide rack into acetone in slide box for 2 minutes

4 Transfer slide rack into 2% APES in slide box for 20 seconds

5 Place slide rack into acetone for 2 minutes

6 Rinse slides in distilled water

7 Dry the slides in 80°C oven for 1 hour

2.20 Immunohistochemistry

The eyes, regional lymph nodes or spleens were removed, snap frozen in liquid nitrogen, and were kept at –70°C until use. The 5μm sections were prepared with a cryostat, and were fixed on the APES coated slides.

1 Dry sections on slides in the air at room temperature

2 For blocking the non-specific binding sites, incubate sections with 5% secondary antibody animal's serum in PBS

3 Remove serum

4 Rat anti-mouse CD3, CD11b or F4/80 (Pharmingen, Germany) as the primary antibody were diluted to 1:50, 1:100, or 1:200 in PBS with 1% FCS

5 Incubate sections with primary antibody at room temperature for 20 minutes

6 Replace the primary antibody by PBS in control sections

7 Incubate in 3% hydrogen peroxide for 5 minutes for blocking the endogenous peroxidase activity

8 Rinse sections with PBS 3 times

9 Biotinylated rabbit anti-mouse immunoglobulins (DAKO, A/S, Denmark) as the second antibody was diluted to 1:200 in PBS with 1% FCS

10 Incubate sections with the second antibody at room temperature for 20 minutes

11 Rinse sections with PBS 3 times

12 Incubate sections with peroxidase-conjugated streptavidin (1:500) (DAKO, A/S, Denmark) for 20 min

13 Rinse sections with PBS 5 times

14 Mount sections in substrate

15 Observe under the microscope and stop after 10-15 minutes

16 Stop the reaction by 4% formalin in acetate buffer (pH5)

17 Rinse in 1% acetic acid

18 Stain with hematoxylin for 15 seconds

19 Mount with aquatex and cover with glass coverslip

2.21 Delayed-Type Hypersensitivity Reaction

Ten days following virus inoculation, mice were received in right footpad with 1×10^7 PFU HSV-1 in 50µl RPMI, and in the left footpad with 50µl RPMI. Footpad thickness was measured 24 hours later with a micrometer. The difference between the swelling in left and right footpads was calculated as the HSV-1-specific DTH.

2.22 Detection of Virus titer in the Eye

Virus titer was studied with a plaque assay, as reported previously (Bauer et al., 2001). Whole eyes were collected and were snap frozen in liquid nitrogen on days 10 PI. The HSV-infected tissue specimens were thawed and homogenized. After centrifugation at 2000rpm for 20 min to remove the cell debris, the supernatant of each sample was serially diluted. The samples were cultured on Vero cell monolayers. After 1 hour of incubation at 37°C, the supernatants were discarded. Each well was covered with RPMI-agarose medium and incubated in a 5% CO_2 atmosphere at 37°C for 2 to 3 days. The cells were fixed with 37% buffered formalin and stained with 2% crystal violet, and the plaques were counted (respective details described in section “Plaque assay”).

2.23 Proliferation Assay with [^{3}H]thymidine

1 The left regional lymph node were homogenized and a single cell suspension was

prepared ($1x10^6$ cell/ml).The cells were cultured in 96-well plates for 3 days at a density of 1×10^5 cells in 100µl medium per well.

2 Add 2µl UV-inactivated HSV (2×10^6 PFU before inactivation per well) into wells directly.

3 Add 2µl ConA (0.5µg/ml) into wells as the positive controls.

4 Add 2µl 10% FCS into wells as the negative controls

5 All of the cells treated with different stimulants were cultured for 3 day at 37°C

6 1µCi of [^{3}H]thymidine were incubated with cells for 24 hours

7 Spot lysates on a glass filter with a cell harvester and wash out unincorporated [^{3}H]thymidine with sterile water

8 Determine radioactivity in a scintillation counter

(Bauer et al., 2002)

2.24 Statistical analysis

Unpaired two-tail Student's t-test was used to determine the significance of the differences in number of cells in the eye, retinitis grade, DTH, ELISA, plaque assay and proliferation assays. Fisher's test was used for statistical analysis of the difference in the incidence of retinitis. $P<0.05$ was considered statistically significant.

3. Results

3.1 ASON uptake in vitro

To study the uptake of FITC-ASON in vitro, regional lymph nodes and spleens were harvested from HSV-infected mice and single-cell suspensions were collected. The cells were cultured with FITC-labeled ASON (2μM/L) and examined under fluorescence microscopy or flow cytometry. After 15 minutes, the fluorescence was easily detectable in the cells. The maximum of fluorescence was observed between 8 and 12 hours of incubation (95% fluorescence positive cells). Even 48 hours later, it was still detectable in the cultured cells. (Fig 4)

Flow cytometric analysis disclosed that more than 67% of the lymph node cells were fluorescence positive after incubating them with FITC-ASON for 15 minutes. There were still fluorescence positive cells after 48 hours of incubation (Fig 5). Similar results were found in both lymph node and spleen cells.

3.2 Subconjunctival Injection of ASON

3.2.1 ASON uptake in vivo

To study the uptake of ASON in vivo mice were treated with a single subconjunctival injection of 50μl FITC-labeled TNF-α-ASON, and were then enucleated after different time-points. Sections from the eyes were studied with a fluorescence microscope. On day 1 after the injection, the sclera and subconjunctival tissue were strongly fluorescent positive. In addition, the fluorescent staining was also found in

the choroid, in the retinal vessels and few cells within the retina, which are most probably the Müller cells (Fig 6). This staining pattern was not markedly different on day 2 PI. FITC-TNF-α-ASON was detected in the choroid and retinal vessels up to 7 days after injection, but the staining was less intense. A few cells in lymph node were stained positively just on day 1 PI (Fig 6). In contrastingly, intracellular fluorescence was undetectable in the spleen.

3.2.2 TNF-α-ASON reduced the TNF-α expression in vivo

To study the TNF-α-expression after injection of ASON eyes were infection with 2µl HSV. TNF-α-ASON, CON or PBS was injected subconjunctivally on the days -1, +1 and +4. The eyes were harvested on day 8 PI. The cytokine expression in the eye was measured by an ELISA technique. The levels of TNF-α in the eye were markedly diminished after subconjunctival injection with TNF-α-ASON compared with other groups. Otherwise, the TNF-α level in the PBS and CON groups were not significantly different (Fig 7).

3.2.3 Clinical course of the retinitis on day 8 PI in the contralateral eyes after administration of TNF-α-ASON

Inflammatory cell infiltration in the contralateral eye in the v. Szily model can be found after 7-8 days PI. The following tests were done to determine, if the administration of ASON would be able to decrease the incidence or severity of ARN. For the induction of the disease, the right eyes were injected with HSV-1. The TNF-α-ASON, CON or PBS was injected subconjunctivally on the days -1, +1 and +4. The eyes were harvested on day 8 PI.

Fig 8 shows the incidence of contralateral retinitis in the different treatment groups. In the PBS treatment group, 6 out of 12 mice (50%) had developed clinical signs of contralateral retinitis by day 8. The CON treatment group had a similar incidence (7 out of 14, 50%) of contralateral retinitis. In contrast, after TNF-α-ASON treatment, only 2 out of the 14 mice (14.29%) had developed retinitis by day 8 ($P<0.05$).

3.2.4 Histological findings in the contralateral eyes on day 8 PI after administration of TNF-α-ASON

Eye specimens were analyzed histologically to determine if the clinical findings could also be found in the eye specimens obtained from the animals.

By day 8 PI, there was a severe acute retinitis in the left eyes in the mice from the PBS and CON treatment group. Photoreceptor layer collapse and outer nuclear layer disruption was seen in the retina. The inflammatory cell infiltration varied between the individual mice. While retinitis was focal in some mice, it involved the entire retina in others. Vitritis was present in all mice from these 2 groups. The underlying choroid had a profound inflammatory cell infiltration in all mice.

In contrast, TNF-α-ASON treated mice had only a mild retinitis. It was typically focal and involved only the inner 1/3 of the retinal layers. The retinal structure was still well organized, and contained a quite small number of inflammatory cells, primarily polymorphonuclear leukocytes (PMN) and lymphocytes. Only few inflammatory cells were found in the vitreous (Fig 9).

In order to quantify the severity of contralateral retinitis, the inflammatory cells in retina were enumerated. The healthy retina contains ganglion cells, Müller cells, photoreceptor cells and others. The inflamed retina contains additional inflammatory cells.

The infiltrating inflammatory cells cannot be clearly distinguished from the retinal cells in the inflamed retina. Therefore, the total number of cells was enumerated, and

the mean number of cells that are generally present in healthy retina was subtracted in order to determine the number of inflammatory cells. However, the number of cells counted in the highly inflamed retina may be mistakenly too low, as retinal cells damaged by inflammation might have been remove by phagocytes.

In order to quantify the severity of contralateral retinitis, the inflammatory cells in retina were enumerated in the technique described above. The mean retinitis severity was 0.76 in TNF-α-ASON group, and was 1.50 in the PBS and 1.56 in the CON group. The severity of retinitis in animals treated with TNF-α-ASON was markedly reduced as compared to the other groups ($P<0.05$) (Fig 10).

Furthermore, the inflammatory cell infiltration in the ciliary body and choroid were determined on day 8. While the ciliary body and choroid was highly infiltrated by inflammatory cells both in the PBS and CON treated mice, only a mild inflammation was seen in the TNF-α-ASON treated group. The number of inflammatory cells in ciliary body in mice that were treated with PBS was significantly higher ($P<0.05$) than TNF-α-ASON (29.96±30.52 vs. 7.48±9.52). Correspondingly, the choroid from the mice that were treated with TNF-α-ASON had also significantly fewer ($P<0.05$) inflammatory cells than in the PBS (28.14±31.44 vs. 75.33±75.78) (Fig 11).

3.2.5 Immunohistochemical studies of the contralateral eyes on day 8 PI after administration of TNF-α-ASON

To examine the cell populations in the ASON treated eyes, immunohistochemical stainings against the cell marker CD11b, CD3, F4/80, or IA/IE were performed.

1 CD11b

Large numbers of CD11b positive cells were observed in the retina and choroid of mice from the PBS group and CON group (Fig 12). The positive cells were mainly found in the ganglion cell layer and inner plexiform layer of retina, in the ciliary body

and choroid. In the retina of mice from the TNF-α-ASON treatment group, only few CD11b positive cells were found in the retina, choroid and ciliary body.

The numbers of CD11b cells found in the 3 experimental groups are summarized in figure 13. The number of CD11b positive cells in the ciliary body was reduced in the TNF-α-ASON treated group as compared to the CON and PBS groups, the difference did not reach the level of significance. Compared with the PBS and CON treatment group, the infiltration with CD11b positive cells in contralateral retina and choroid of the TNF-α-ASON treated mice was significantly reduced ($P<0.05$).

2 CD3

The CD3 positive cells were found in PBS group and CON group predominantly in the choroid and ciliary body(Fig 14). In the TNF-α-ASON treatment group, only few such cells were found in the choroid. In the 3 groups of mice, no significant CD3 cell numbers were found in the retina.

Following TNF-α-ASON treatment, the number of CD3 positive cells in ciliary body decreased significantly as compared to the control group ($P<0.05$). Compared with the PBS treated group, the number of positively stained cells in choroid from the TNF-α-ASON treated mice was reduced. However, due to the small numbers of cells found in all of the groups and tissue areas, the differences did not reach the level of significance (Fig 15).

3 F4/80

F4/80 positive cells were found in the eyes from the PBS group (Fig 16). Most of the F4/80 positive cells were located in ciliary body, choroid, and in the inner nuclear and ganglion cell layers of the retina. In the TNF-α-ASON group, only a few F4/80 positive cells were found in the choroid.

Compared with the mice of the PBS treatment group, there was the tendency that the

cellular infiltration with F4/80+ cells in retina with TNF-α-ASON and CON treatment was reduced. In general, only few such cells were found in the eyes of the mice from the 3 experimental groups (Fig 17).

4 IA/IE

IA/IE positive cells were observed in PBS and CON group (Fig 18). The positive cells were mainly found in the ciliary body and choroid. The retina had a faint and diffuse positive staining with this antibody. In the mice from the TNF-α-ASON treatment group, no IA/IE positive cells were found in the retina, and only few IA/IE positive cells were detected in the choroid.

Compared with the PBS treatment group, the number of IA/IE positive cells in the ciliary body was reduced in the TNF-α-ASON and CON treatment ($P<0.05$). No such cells were found in the retina in all three groups. In the choroid, the number of IA/IE-positive cells was lower in the TNF-α-ASON group than in the other 2 groups, however, the difference did not reach the level of significance (Fig 19).

3.2.6 Clinical course of retinitis on day 10 PI in the contralateral eyes after administration of TNF-α-ASON

The following tests were performed to determine if the ASON-treatment of mice with ARN could be used as a therapeutic treatment option.

Fig 20 summarizes the incidence of contralateral retinitis following the different treatment regiments. In the PBS treatment group, 9 of 12 mice (75%) had developed clinical signs of contralateral retinitis by day 10. In the CON treatment group, a similar incidence of contralateral retinitis was found (8 of 11, 72.7%). And after TNF-α-ASON treatment, 11 of 14 mice (78.6%) had developed retinitis by day 10 PI. The difference in the incidence of retinitis in the contralateral eyes between TNF-α-

ASON-treated mice and control groups was not significant (P>0.05). Retinitis included severe vitreous opacity, retinal veins dilated and tortuous. Tractional detachment of the retina was a prominent clinical feature.

3.2.7 Histological findings of retinitis on day 10 PI in the contralateral eyes after administration of TNF-α-ASON

In order to further analyze the effect of TNF-α-ASON treatment on the course of contralateral inflammation, we studied the histological findings on day 10 PI. Retinal necrosis was typically detected in the PBS, CON and TNF-α-ASON treatment group. Compared with the findings on day 8 PI, the inflammation was now more severe in all of the three groups. In addition, large areas of retinal necrosis were noted, and vasculitis, perivasculitis, vascular occlusions and fibrin deposition were prominent. The ganglion cell layer, inner and outer nuclear layers were disarranged. The inflammatory infiltrate, containing mainly PMN, but also monocytes and lymphocytes, now involved the entire depth of the retina. The choroid underlying the necrotic area was also heavily infiltrated with inflammatory cells. Inflammatory cells, phagocytes and necrotic cell particles were found in the vitreous. (Fig 21). Tractional retinal detachment was noted. No obvious difference in the histopathological appearance was obvious between the 3 treatment groups.

3.2.8 Immunohistochemical studies of the contralateral eyes on day 10 PI after administration of TNF-α-ASON

1 CD11b

Many CD11b positive cells were observed in PBS, CON and TNF-α-ASON group (Fig 22). The positive cells were mainly found in retina, ciliary body and choroid. The

CD11b positive cell numbers in posterior segment on day 10 PI were increased when compared to the observations on day 8 PI. Similar to both of the control groups, the numbers of CB11b+ cells in the retina and choroid were reduced in the TNF-α-ASON group.

As shown in Fig 23, many CD11b positive cells were observed in ciliary body, retina and choroid on day 10 PI. In ciliary body, the number of CD11b positive cells in TNF-α-ASON treated group was smaller than in the CON group, but the difference did not reach the level of significance. Compared with the PBS and CON treatment groups, the number of CD11b+ cells in contralateral retina and choroid was significantly decreased in the TNF-α-ASON treatment group ($P<0.05$).

2 CD3

A large number of CD3 positive cells was noted in the PBS, CON and TNF-α-ASON groups (Fig 24). The positive cells were located in ciliary body and choroid, and some CD3+ cells were also located in the retina. Compared with the immunohistochemical findings on day 8 PI, the number of CD3+ cells infiltrating the ciliary body, choroid and retina were increased ($P<0.05$).

As shown in Fig 25, the CD3 positive cells were observed in ciliary body, retina and choroid on day 10 PI. With TNF-α-ASON treatment, the positive cell number in retina was significantly lower than in the PBS and CON group ($P<0.05$). However, the number of CD3+ cells in the ciliary body and choroid did not differ between the treatment groups.

Taken together, the total number of infiltrating cells increased between day 8 and 10 PI, and this was associated with an increased number of CD3+ cells.

3 F4/80

Many F4/80 positive cells were found in the PBS and CON group (Fig 26). Most of

the positive cells were located in choroid and retina. Only a few F4/80 positive cells were observed in ciliary body. In the TNF-α-ASON group, few positive cells were observed in contralateral posterior segment.

Compared with the immunohistochemical findings on day 8 PI, the number of F4/80+ cells was increased in the retina from the contralateral eyes on day 10 PI, while the F4/80+ cell numbers were not changed in the ciliary body and choroid. Compared with PBS and CON treatment groups, the cellular infiltration in the retina and choroid from the TNF-α-ASON treatment group was suppressed significantly ($P<0.05$) (Fig 27).

As the numbers of infiltrating CD11b cells in the choroid and retina of the TNF-α-ASON treated mice are higher than the numbers of F4/80+ cells, it may be concluded, that the infiltrating CD11b+ cells are not macrophages but primarily PMN.

4 IA/IE

The IA/IE positive cells were found primarily in the ciliary body and in the choroid, but some IA/IE cells were also found in the necrotic retina. The immunohistochemical appearance did not profoundly differ between the mice in the PBS, CON and TNF-α-ASON groups (Fig 28).

The numbers of IA/IE + cells in the contralateral eyes did not differ significantly between the three groups. Compared to the findings on day 8 PI, the numbers of IA/IE+ cell were slightly increased on day 10 PI, however, the difference did not reach the level of significance (Fig 29).

3.2.9 Delayed-type hypersensitivity reaction on day 10 PI after administration of TNF-α-ASON

As shown in Fig 30, the HSV-1 specific DTH response did not differ significantly between mice that received PBS, CON or TNF-α-ASON ($P>0.05$).

3.2.10 T cell proliferation assay with [^{3}H]thymidine on day 10 PI after administration of TNF-α-ASON

To evaluate the effect of TNF-α-ASON on the systemic immune response against HSV-1, the antigen specific proliferation of lymphocytes obtained from the regional lymph nodes was detected on day 10 PI. As shown in Fig 31, the HSV-1 specific T cell response was lower in the mice after TNF-α-ASON treatment as compared to the PBS and CON treated groups ($P<0.05$) (Fig 31).

3.2.11 Virus titer in eyes on day 10 after administration of TNF-α-ASON

As the clinical and histological findings revealed an acceleration of herpetic retinitis between the day 8 and 10 PI, we wondered whether this might be associated with an increased virus titer at this time point. The PFU content was studied with a standard plaque assay. The results show that virus titers were increased in the TNF-α-ASON treatment group as compared to the PBS and CON group of mice (Fig 32, $P<0.05$).

3.3 Intraocular Injection of TNF-α-ASON

3.3.1 ASON uptake in vivo

The mice were treated with a single intraocular injection of 2µl FITC-labeled TNF-α-

ASON, and were then enucleated after different time points. Sections from the eyes were studied with a fluorescence microscope. On day 1 after the injection, the corneal endothelium, iris, ciliary body, vessels of retina, ganglion cells and choroid were strongly fluorescent positive (Fig 33). This staining pattern was not markedly different on day 2 PI. However, on day 2, the staining in the endothelium was absent already, and the staining was less intense in the iris, ciliary body, choroid and retina. While the inner ganglion cells were still fluorescent positive, the nuclear layer was negative for the FITC staining. On day 3 after injection, only a staining of the ganglion cells was present, while the other tissues were fluorescent negative. No positive staining was detected after 7 days.

It was, therefore, concluded that the injections should either be repeated at least every 3 days. For the first set of experiments, the injections were planed for the first experiments on the days –1, +1, and +4 PI, as the up-regulation of TNF-α was detected in previous experiments by 6 to 8 days PI, and before the onset on retinitis. Also, the regional lymph nodes and spleen were removed after 1 and 3 days and were studied by fluorescence microscopy. TNF-α was not detected in the samples at different time point (Fig 33).

3.3.2 TNF-α-ASON reduced the TNF-α expression in vivo

The right eyes of the mice were infected intraocularly with 2µl HSV, and TNF-α-ASON, CON or PBS was injected into the vitreous cavity of the left eyes on the days -1, +1 and +4. The left eyes were harvested on day 8 PI. The cytokine expression in the eye was measured by an ELISA technique. The levels of TNF-α in the eye were markedly diminished after treatment with TNF-α-ASON as compared with other groups. Otherwise, the TNF-α level in PBS and CON groups showed no significant differences (Fig 34).

3.3.3 Clinical course of retinitis on day 8 PI in the contralateral eyes after administration of TNF-α-ASON

The viral retinitis was induced by intracameral injection of the right eyes with HSV-1. In order to modify the course of the disease in the contralateral eyes, TNF-α-ASON was injected into the vitreous cavity of the left eyes. CON or PBS was injected in the mice of the control groups. The eyes were injected 3 times (days -1, 1 and 4 PI) and were then harvested on day 8 PI.

Fig 35 shows the incidence of contralateral retinitis following the treatment in the three experimental groups. In the PBS treatment group, 10 of 18 mice (55%) had developed clinical signs of contralateral retinitis by day 8. The CON treatment group showed a lower incidence of contralateral retinitis. After TNF-α-ASON treatment, 7 of 17 mice (41.18%) had developed retinitis by day 8 PI. No significant differences were found between the groups.

It was obvious that some of the mice developed a retinal detachment after the repeated injections. This untoward side effect from the injection occurred following the second or third injections in approximately 2 out of 3 animals. Retinal detachment was the most frequent side effect observed in PBS (11 of 18 animals), CON (10 of 15) and TNF-α-ASON (12 of 17) group. This suggested that repeated injections might be followed by severe complications that are related to the injection method. In conclusion, single injections at a critical time-point directly before the up-regulation of the HSV-1 induced TNF-α peak in the contralateral eyes might be superior to the repeated injection regiment used herein.

3.3.4 Histological findings in the contralateral eyes on day 8 PI after administration of TNF-α-ASON

By day 8 PI, there was an acute retinitis in the left eyes in the mice from the PBS,

CON and TNF-α-ASON treatment group. Photoreceptor layer collapse and outer nuclear layer disruption was seen in the retina. The inflammatory cell infiltration, however, varied considerably between the individual mice. In some mice, the retinitis was focal and involved only the inner 1/3 of the retinal layers. The retinal structure was still well organized, and contained a small number of inflammatory cells, primarily PMN and other leukocytes. A few inflammatory cells were found in the vitreous (Fig 36). The retinitis involved the entire retina in other mice. In sharp contrast, some of the mice did not have any contralateral retinitis. Vitritis was present in all mice from these 2 groups. The underlying choroid had a marked inflammatory cell infiltration in all mice.

In order to quantify the severity of contralateral retinitis, the inflammatory cells in the retina were enumerated in the technique described above. The mean retinitis severity was 1.25 in TNF-α-ASON group, and was 1.0 in the PBS and CON group (Fig 37). The difference was not significant ($P>0.05$).

Also, the inflammation of the ciliary body and choroid varied considerably between the individual mice. A heavy infiltration by inflammatory cells was seen in some mice, while only a mild inflammation was seen in other groups. The ciliary body and choroid was highly infiltrated by inflammatory cells both in the PBS and TNF-α-ASON treated mice. The numbers of inflammatory cells in ciliary body in mice that were treated with PBS and TNF-α-ASON were not significantly different (75.96 ± 16.09 vs. 66.68 ± 15.78, $P>0.05$). Correspondingly, the choroid from the mice that were treated with PBS and TNF-α-ASON had similar inflammatory cells (145.87 ± 32.65 vs. 124.86 ± 30.22, $P>0.05$) (Fig 38).

Frank retinal detachment and proliferative vitreoretinopathy adjacent to the areas of scleral puncture was noted in some of the mice. This supports the clinical observation of this complication that is resulting from the injection technique.

3.3.5 Clinical course of retinitis on day 10 PI in the contralateral eyes after

administration of TNF-α-ASON

The Fig 39 summarizes the clinical findings that were obtained in the 3 groups at day 10 PI. A considerable number of animals developed the typical signs of contralateral retinitis. Compared with the PBS and CON treatment group, the retinitis rate was reduced in the TNF-α-ASON group. However, the difference between the groups did not reach the level of significance.

As noted already on day 8 PI, a great number of mice showed the typical signs of retinal detachment.

3.3.6 Delayed-type hypersensitivity reaction on day 10 PI after administration of TNF-α-ASON

As shown in Fig 40, compared with mice that received PBS treatment, those that received TNF-α-ASON had a significantly reduced DTH reaction ($P<0.05$).

3.3.7 T cell proliferation assay with [^{3}H]thymidine on day 10 PI after administration of TNF-α-ASON

As shown in Fig 41, the HSV-1 specific proliferative response of cells obtained from the regional lymph nodes was significantly reduced both with CON and with TNF-α-ASON treatment as compared to the PBS treatment.

4. Discussion

4.1 Background of the study

Previously it has been shown that TNF-α-mRNA and -protein was upregulated during the progression of ARN (from day 6 to 14 PI) in HSV-1 infected contralateral eyes (Zheng et al., 2005). The TNF/TNF-R family plays a particular key role in the activation, differentiation and effector responses of T-cells. As TNF-α plays an important part in the development of ARN, the elimination of TNF-α-may be candidate therapeutic approach.

4.2 Alternative: systemic TNF-α inhibition

4.2.1 Disadvantages:

There are several possible ways of blocking TNF-α functions in vivo. Etanercept (Enbrel®) is a soluble TNF-receptor-immunogobuline-fusion-protein. Soluble TNF-receptors can bind and inactivate the soluble TNF-α. Infliximab is a monoclonal chimeric mouse-human antibody that is binding with high affinity to soluble and transmembranaous forms of TNF-α. In vivo, infliximab quickly builds up stable complexes with human TNF-α. Adalimumab is a monoclonal human anti-TNF-antibody.

The administration of all of the commercially available TNF-α inhibitors by antibodies may be complicated by the development of humoral immune responses directed against the therapeutic antibodies after repeated application. Hypersensitivity reactions and severe infusion reactions especially when using the chimeric antibody of infliximab may occur. In addition, antibody production directed against TNF-α might be associated with reduced treatment effects.

In addition, systemic treatment with TNF-α inhibitors resulted in an increased rate of

tuberculosis. Previously, it has been reported that 70 out of 12,100 patients that were under therapy with Infliximab developed tuberculosis. Until 2001, 12 cases of tuberculosis out of 117,000 patients treated with etanercept were reported (Keane, 2001; Wallis et al., 2001; Reimold, 2003). In some patients, the development of auto-antibodies has also been noted, and especially antinuclear antibodies or antibodies against ds-DNA, but also a lupus-like syndrome appeared. In 17 patients treated with etanercept and in another 2 patients treated with infliximab, demyelinating disease could be observed (Mohan et al., 2001). Infliximab led to the aggravation of moderately or severe heart insufficiency. The FDA Arthritis Drug Advisory Commitee reported about 16 infliximab patients and 19 etanercept patients with lymphomas. The follow-up period is yet too short to assess the long-term-risk of TNF-alpha inhibitors with a certain accuracy. In addition, antibody production directed against TNF-α might be associated with reduced treatment effects.

4.2.2 Advantages:

While side effects from systemic TNF-α inhibition might be untoward, modulation of the general immune response against HSV-1 may be of importance to the alteration of the course of acute contralateral HSV-1 retinitis.

Previous experiments in experimental autoimmune uveitis have revealed contradictionary results about the role of TNF-α in the development of uveitis. There has been profound evidence that TNF-α inhibition may lead to an improvement of EAU (Robertson et al,. 2003). However, TNF-α application has also been associated with an improvement of uveitis.

There are several lines of evidence that TNF-α participates in the pathogenesis of contralateral HSV-1 retinitis. 1. TNF-α expression is increased in the contralateral eyes during the development of acute HSV-1 retinitis. 2. The inhibition of TNF-α led to an improvement of acute retinitis. However, the role of TNF-α in the diverse compartments of the body, e.g in the eye, draining lymph node and spleen, and within

the different cell types in the diverse compartment of the body, have not been defined in detail. As a consequent, it cannot be completely excluded, that TNF-α inhibition may also be associated with a worsening of the course of experimental HSV-1 retinitis.

4.3 Cells and soluble factors in regional lymph node

It has been previously shown that cells in the regional lymph nodes are of critical importance for the antigen presentation. The cells in the regional lymph nodes may also be of importance for the course of experimental ARN.

We intended to design a topical TNF-α inhibition in our experiments. However, we observed that FITC-positive cells were present in the regional lymph nodes after subconjunctival injection. The FITC-TNF-α-ASON was detected in the regional lymph nodes on the first day after subconjunctival injection. This drainage of dye to the regional lymph nodes is not unexpected, as the subconjunctival space is drained via the lymphatic system to the submandibular lymph nodes. Also, the secretion of TNF-α was reduced in lymphocytes obtained from the regional lymph nodes. We can only speculate about the relevance of this observation on the course of acute retinitis. It might be speculated that TNF-α expression is also decreased in the antigen presenting cells. Indeed, nearly 95% of the cells from the rLN were FITC positive, and this was true for small lymphocytes as well as larger phagocytes. As a consequence, early activated dendritic cells may be of relevance to the improvement of Th-1 induced disease in the retina.

4.4 Cells and soluble factors in the spleen

It has been previously shown that cells in the spleen are of critical importance for

ACAID. Furthermore, ACAID has been suggested to be critical for the course of acute retinitis. Interestingly, fluorescent positive cells were not found in the spleen after subconjunctival FITC-TNF-α-ASON injection. It may, therefore, be speculated that cells or soluble factors that are critical for the course of acute retinitis may not be influenced by the subconjunctival treatment in the spleen.

4.5 Antisense oligonucleotides

In principle, there are several action mechanisms of ASON. Beside a sequence specific activity from a binding to target mRNA, ASON can bind to other factors and they exert sequence unspecific interactions.

Antisense oligonucleotides have great therapeutic potential because of their ability to inhibit the synthesis of specific proteins. The discovery that complementary nucleotide bases synthesized in 12-25 mer sequences can bind with specific mRNA synthesized to produce unique proteins, such as cytokines, in response to regulatory physiologic stimuli has enormous potential to alter the inflammatory response (Agrawal & Kandimalla, 2000; Scanoon, 2004). The covalent hydrogen binding of antisense compounds to mRNA can effectively prohibit translation of specific mRNA. The construction of antisense oligonucleotides may be useful for the prevention of individual protein synthesis, thus permitting a wide variety of potential therapeutic application.

4.5.1 TNF-α-ASON for the treatment of inflammatory disease

ASON targeting TNF-α has been used to treat immune mediated disease such as allergy, Crohn's disease (van Hogezand & Verspaget, 1998; Popescu et al., 2005). Wasmuth reported that topical treatment with TNF-α-ASON can reduced the severity of HSK (Wasmuth et al., 2003).

4.5.2 Use of ASON in eye diseases

Inhibition of gene expression with ASON has been previously applied for the treatment of some ocular diseases. Henry reported that fomivirsen (Vitravene, also known as ISIS 2922; Isis Pharmaceuticals, inc., Carlsbad, CA) which was designed to inhibit human CMV was approved for treatment of CMV retinitis (Henry et al., 2001). An ASON against vascular endothelial growth factor was delivered to the retina via intravitreal injection reduced iris neovascularization in monkey models (Bhisitkul et al., 2005).

4.5.3 Uptake

It was indicated that the FITC-labeled ASON were taken up after 15 minutes in vitro by cells taken from the regional lymph node and spleen. It was still detectable in the cultured cells even 48 hours later.

The ASON are taken up by nearly 95% of the cells ion vitro. The larger cells are most likely macrophages / monocytes. Cells with granular nuclei are neutrophils. Small cells were most likely lymphocytes. As described in the literature, TNF-α secretion is reduced in the T cell line H2T2 as in the macrophage cell line (Taylor et al., 1997)

As epithelial barriers are bypassed by subconjunctival and intraocular injections, uptake enhances have not been applied for our experiments. When treated with a single subconjunctival injection, the intracellular fluorescence staining was found in the eye tissue such as choroid, retinal vessels and few cells within retina (most likely Müller cells) till on day 2PI. Although the staining was less intense, FITC-TNF-α-ASON was still detected in the choroid and retinal vessels up to 7 days after injection.

Transscleral delivery has been considered to be an alternative for the intraocular delivery of macromolecules, because sclera has a large and accessible surface area, a

high degree of hydration rendering it conducive to water-soluble substances, and a hypocellularity with an attendant paucity of proteolytic enzymes and protein-binding sites. It appears that transscleral influx and intrachoroidal dispersion of macromolecules in the mouse eye is not precluded by either transscleral aqueous flow or by choroidal blood flow (Kim et al., 2002). The fluorescence in the retinal vessels indicated that the hematogenous pathway may have also contributed to the intraocular dispersion of FITC-TNF-α-ASON. Most probably it penetrated the arterial wall in the retrobulbar region and mixed with the blood stream as the blood was about to enter the retina.

As compared with the recent findings in the cornea (Wasmuth et al., 2003), the uptake of FITC-TNF-α-ASON in the retinal tissue and uvea was not as stable as in the cornea. The long presence of ASON in the cornea might be related to the slow tissue turn over and metabolism in the cornea. The axoplasmatic transport mechanisms, the transport in the vessels and in the uvea might have caused the faster decrease of fluorescence.

The staining pattern of most of the cells suggests that the FITC-ASON is incorporated not only into the cell membrane, but also into the cytoplasm.

Previously, a relation between the uptake of ASON and cell activity has been suggested (Zhao et al., 1996). Although no such studies were performed herein, we have seen that FITC-ASON was taken up into the eye.

4.5.4 Toxicity

The concentration of the TNF-α-ASON solution was used as designed in our previous experiments in the HSK model (Wasmuth et al., 2003). As no toxic effects were noted in the treated eyes in the previous studies, a similar dye was applied for our present experiments. Accordingly, toxic effects to the treated ocular tissues, by means of clinical nor histological methods, have not been seen from the control ASON used in

our studies. Additionally, no systemic side effects were noted in any of the mice treated in our experiments.

4.5.5 Stabilization against enzymatic cleavage

One of the most difficult challenges facing the anti-gene field is ASON that will stabilize, transducer and express a transgene in the target tissue. As described in the Methods, the TNF-α-ASON we used was modified to protect it against enzymatic cleavage by DNases.

4.5.6 Decreased TNF-α protein expression after TNF-α-ASON treatment

It was reported that TNF-α-ASON down-regulated the TNF-α protein in vitro (Wasmuth et al., 2003). Furthermore, the secretion of TNF-α in the cornea was significantly impaired after ASON treatment given three times in vivo (Wasmuth, 2003). In our study, when the animals were treated with TNF-α-ASON subconjunctival, the cytokine expression in the eyes that develop acute HSV-1 retinitis was diminished significantly. As no such effect has been noted with the treatment of CON, this shows that this is a sequence specific ASON effect.

4.6 Design of the treatment protocol

We thought to block the TNF-α secretion in the contralateral eyes by the TNF-α-ASON injections. The concentration used was adjusted to our previous studies, as discussed before.

The amount of dye that was injected subconjunctivally was chosen: 1. as the volume could be easily injected into the subconjunctival space without significant prompt leakage from the injection site, and 2. it did not induce a significant proptosis of the eye. The frequency of the subconjunctival injections was chosen: 1. as the previous

FITC-ASON in vitro and in vivo uptake studies suggested stable uptake into cultured cells and eye's structures, e.g. choroid and retina, was achieved for the intervals applied, 2. no significant tissue damage of the eyes was noted in the cultured cells and eye tissues when these intervals were applied, 3. a significant reduction of the TNF-α secretion was achieved with this TNF-α-ASON amount.

The frequency of the intraocular injections was also chosen with consideration of these aspects. However, several major disadvantages occurred with the repeated intraocular injections. 1. The injections induced a significant damage of the intraocular tissues in the eyes. The pars plana area that was chosen for the injections is the preferred area of injecting dye into the vitreous cavity, as the lens is located anteriorly and the retina is attached more posteriorly. However, no needle is commercial available for this procedure, so that glass capillaries were used. While these smallest diameter needles were still patent for the dye, damage to the lens or the retina were still seen in several of the mice, and the probability of the tissue damage increased with the number of the injections; 2. The puncture side did not completely heal until the subsequent repeated injections, which consequently led to leakage of the ASON dye; 3. The leakage of injected ASON solution into the subconjunctival space and its subsequent drainage via the lymphatic system resulted in the untoward influence of immune system outside the eye, namely in the regional lymph nodes..

4.7 Influence of subconjunctival TNF-α-ASON treatment on the course of experimental HSV-1 retinitis

In our study, after three subconjunctival treatments with TNF-α-ASON, only 14.3% animals had developed retinitis by day 8. The incidence of retinitis in TNF-α-ASON treatment group was lower than in the control group. Additionally, the contralateral retinitis in treatment group was less severe than in control group by day 8. There was less inflammatory cell infiltration in the posterior segment.

There are several possible mechanisms by which TNF-α-ASON treatment may have achieved improvement of the contralateral retinitis. Antigen activation was required for the up-regulation of p75 and to a lesser extent p55 TNF-R and the acquisition of TNF responsiveness by different T-cell subsets in vitro, but more importantly at sites of inflammation (Ware et al., 1991; Brennan et al., 1992; Cope et al., 1995). $CD4^+$ T cell subsets contribute to the destruction of the retina, and may accelerate the cellular infiltration and inflammation-induced retinal destruction in von Szily model (Azumi et al., 1994). TNF-α-ASON can block the production of TNF-α that enhances T cell proliferation and differentiation.

Activated macrophages can express NOS2 and generate nitrite, peroxy-nitrites, and superoxides, which induce lipid peroxidation of cell membranes and cell death. TNF refers to stimulate macrophage together with IFN-g. In previous experiments, the blockade of TNF-α activity resulted in a reduced NOS2 expression from lymph nodes and macrophages (Engwerda et al., 2002; Fonseca et al., 2003).

It is tempting to speculate that the reduction of TNF-α secretion may also be apparent in resident cells of the retina and choroid. Zheng reported that RPE cells and activated Müller cells expressed TNF-α in von Szily model (Zheng et al., 2005). As a consequence, reduction of TNF-α expression in these cells may be in part responsible for the improvement of acute retinitis obtained by TNF-α-ASON treatment. Indeed, our studies with FITC-TNF-α-ASON indicated that Müller cells are able to take up ASON after subconjunctival injection

The histological results in our experiments showed that the numbers of PMN, lymphocytes and monocytes were reduced in the choroid and retina after TNF-α-ASON treatment. The immunohistochemical studies disclosed that CD11b positive cells were decreased in the choroid and retina after TNF-α-ASON treatment. Together with the finding that there were fewer F4/80 positive cells in the TNF-α-ASON mice this is suggesting that PMN and macrophage numbers are reduced in the choroid and retina by the treatment. The IA/IE expression was slightly reduced in the choroid and

retina after TNF-α-ASON treatment. Also, the CD3 positive cells were also reduced in the choroid and retina of the TNF-α-ASON treated mice.

Taken together, the TNF-α-ASON treatment influenced a broad array of inflammatory events in the choroid and retina. It is possible that TNF-α inhibition reduces the influx of inflammatory cells into the uvea and retina. By TNF-α inhibition, reduction of chemokines and adhesion molecules may be induced. It is also possible that TNF-α-ASON results in reduced leukocyte proliferation, reduced antigen presentation, reduced apoptosis of APC and reduced matrix metalloproteinase (MMP) secretion.

In the later phase of retinal necrosis (day 10 PI), the animals that received TNF-α-ASON treatment had increased incidence of retinitis and more severe retinitis. The histological studies showed that the number of inflammatory cells infiltrating in the posterior segment had increased. Our further immunohistochemical investigation supported the notion that the total number of infiltrating cells increased between day 8 and 10 PI. The inflammatory cells mainly belonged to PMN and T cells. Interestingly, the composition of the cells changed slightly after the subconjunctival TNF-α-ASON treatment as compared to the CON and PBS treated mice. After the TNF-α-ASON treatment, the number of CD-11b cells had decreased, while the percentage of CD3 T cells had increased.

The increasing retinitis incidence and severity between the days 8 and 10 PI might also be related to the ASON-administration that was chosen. It has been described previously that TNF-α mRNA and protein is up-regulated during the evolution of experimental retinal necrosis (from day 6 to 14 PI) in the contralateral eyes as compared with the levels in control subjects (Zheng et al., 2005). Our FITC-TNF-α-ASON experiments revealed a veining of fluorescence in retina at 3 days after injection. However, in our experiments, the last administration of TNF-α-ASON was performed on day 4 PI. in order to achieve profound TNF-α blockade in the development phase of retinal disease. Due to the increased sensitivity of mice to

general anesthesia and death during the later phase of the von Szily model, no additional injection was attempted. However, higher TNF-α-ASON concentration in the eye might have been achieved by additional subconjunctival injections at later time points. Consequently, application of TNF-α ASON at later time-points might have been superior in order to improve retinitis.

Interestingly, the virus titer in the eyes of the TNF-α-ASON treatment group was slightly higher than in the control group on day 10. It is well known that TNF-α plays an import role in antiviral during the virus infection. The role of TNF-α for the control of virus can be explained by several direct and indirect antiviral effects. It has been described that TNF-α induces NO/ROS and phagocytosis in macrophages. TNF-α induces expression of adhesion molecules an endothelial cells. TNF-α enhances maturation of Th1 cells and activates NK cells and macrophages. TNF-α enhances migration of APC and macrophages to regional lymph nodes and their maturation (Robertson et al., 2002; Cope et al., 1995).

TNF-α has synergy with IL-12 in enhancing NK cell IFNα production (Lucin et al., 1994; Heise & Virgin, 1995). The antiviral function of TNF-α may be of particular importance in the von Szily model, as the damage of retina in retinal necrosis phase is connected to the viral replication.

In our experiments, the subconjunctival TNF-α-ASON injection at the contralateral eye affected the systemic immune response against HSV-1. TNF-α-ASON reduced HSV-1 specific T cell-proliferation in cells from contralateral regional lymph nodes. The $CD4^+$ T cells are involved in virus clearance from contralateral eye (Azumi et al., 1994). This is another explanation why the virus titer was higher in TNF-α-ASON treatment group than in the control group. As a consequence, subconjunctival treatment with TNF-α-ASON combined with systemic antiviral drug might be more effective in improving the course of contralateral retinitis than the use of TNF-α inhibitors alone.

4.8 Influence of intraocular TNF-α-ASON treatment on the course of experimental HSV-1 retinitis

Our observations show that the incidence of contralateral retinitis did not differ significantly between PBS and TNF-α-ASON treatment group (55% and 41.18%) when intraocular injections were performed on the days –1, +1, +4 PI. Several issues must be discussed to explain the obvious difference between the treatment results of the subconjunctival and intraocular injection mode.

1. The intraocular injection induced a significant tissue damage of the eyes as compared to the subconjunctival mode of injections. 2. The leakage after i.o. injection resulted to a drainage to the regional lymph nodes, while the intraocular TNF-α-ASON may by particularly drained to the spleen.

2. The leakage from the subconjunctival space influenced the systemic immune responses, as the HSV-1 specific T cell proliferative response in the regional lymph nodes was reduced with TNF-α-ASON as compared to the PBS treatment. In contrast, the HSV-1 specific proliferation of T cells harvested from the spleen did not differ between the TNF-α-ASON and PBS treated groups of mice.

3. In our experiments, FITC-TNF-α-ASON was detected in the retinal vessels and the retinal cells up to 3 days after intraocular injection. Previous experiments have shown that the mRNA level of TNF-α is elevated on day 6 PI., and subsequently decreased. The TNF-α expression in contralateral is significantly increased on the days 6, 9 and 14 PI. (Zheng et al,. 2005). As a consequence of our experiments done so far, the intraocular injection should only be performed once in order to minimize tissue damage of the eye and may be performed on day 7 PI. in order to achieve a maximum of TNF-α inhibition.

4. The age of the mice that were used for the von Szily experiments may be of particular importance for the course of HSV-1 encephalitis and retinitis. Due to the

maturation of the immune responses, older mice may be more resistant against HSV-1 induced retinitis and encephalitis. In one of our experiments, the age of the mice varied between 6 and 12 weeks. The low incidence of contralateral disease noted in these experiments might be related to this notion. On the contrary, young mice are generally more susceptible to HSV-1 induced encephalitis and retinitis. Although the high retinitis incidence is favorable for the experiments, the high mortality of the young mice is a major disadvantage. Therefore, the use of mice between the ages of 6 and 8 weeks must be considered for the further experiments in experimental HSV-1 acute retinitis.

5. Summary

Antisense-oligonucleotides targeting tumor necrosis factor-alpha in murine herpes simplex virus type 1 retinitis.

Purpose: To investigated whether topical tumor necrosis factor-alpha (TNF-α)-antisense-oligonucleotides (ASON) treatment might affect the course of contralateral HSV-retinitis.

Methods: In vivo uptake was determined after subconjunctival (s.c.) injection of FITC-labeled TNF-α-ASON. BALB/c mice were injected in the AC of the right eyes with HSV-1 (KOS); the left eyes were injected s.c. 3 times with TNF-α-ASON; sequence-unspecific control (C) ON or buffer. The clinical course of HSV-R, ocular inflammatory cell-infiltration, uptake of [3H]thymidine from rLN cells and viral replication in the eyes were analyzed.

Results: In vivo, FITC-TNF-α-ASON was found in the choroid and retina up to 7 days after s.c. injection, but also in the rLN. After s.c. TNF-α-ASON injection, expression of TNF-α was reduced in the ipsilateral eyes and rNL. TNF-α-ASON injection reduced the incidence and severity of early chorioretinitis and of the inflammatory cell infiltration and CD-11b cells in the choroid and retina of the treated eye. On day 10 PI, the virus titers, inflammatory cell infiltration and HSV-R had increased in the TNF-α-ASON treated eyes, while the HSV-1 specific [3H]thymidine uptake from rLN cells was decreased and DTH response did not differ between the PBS, CON and TNF-α-ASON groups.

Conclusions: Topical TNF-α-ASON-injection reduced early ocular inflammatory cell infiltration, but delayed the virus clearance and increased the severity of HSV-retinitis in the treated eyes. The antisense technique is a useful experimental approach for the topical application of TNF-α in experimental HSV-1 retinitis.

6. References

1. Agrawal S, Kandimalla ER. (2000): Antisense therapeutics: is it as simple as complementary base recognition? Mol Med Today. 6,72-81.

2. Atherton SS. (2001): Acute retinal necrosis: insights into pathogenesis from the mouse model. Herpes. 8,69-71.

3. Atherton SS, Altman NG, Streilein JW. (1989): Histopathologic study of herpes virus-induced retinitis in athymic BALB/c mice: evidence for an immunopathogenic process. Curr Eye Res. 8,1179-1192.

4. Atherton SS, Streilein WJ. (1987): Two waves of virus following anterior chamber inoculation of HSV-1. Invest Ophthalmol Vis Sci. 28,571-579.

5. Azumi A, Atherton SS. (1998): T cells in the uninjected eye after anterior chamber inoculation of herpes simplex virus type 1. Invest Ophthalmol Vis Sci. 39,78-83.

6. Azumi A, Cousins SW, Kanter MY, Atherton SS. (1994): Modulation of murine HSV-1 retinitis in the uninoculated eye by $CD4^+$ lymphocytes. Invest Ophthalmol Vis Sci. 35,54-63.

7. Batisse D, Eliaszewicz M, Zazoun L, Baudrimont M, Pialoux G, Dupont B. (1996): Acute retinal necrosis in the course of AIDS: study of 26 cases. AIDS.

10,55-60.

8. Bauer D, Mrzyk S, Van Rooijen N, Steuhl KP, Heiligenhaus A. (2001): Incidence and severity of herpetic stromal keratitis: impaired by the depletion of lymph node macrophages. Exp Eye Res. 72,261-269.

9. Bauer D, Schmitz A, van Rooijen N, Steuhl KP, Heiligenhaus A. (2002): Conjunctival macrophage-mediated influence of the local and systemic immune response after corneal herpes simplex virus-1 infection. Immunology. 107,118-128.

10. Berra A, Rodriguez A, Heiligenhaus A, Pazos B, Van Rooijen N, Foster CS. (1994): The role of macrophages in the pathogenesis of HSV-1 induced chorioretinitis in BALB/c mice. Invest ophthalmol vis sci. 35,2990-2998.

11. Bhisitkul RB, Robinson GS, Moulton RS, Claffey KP, Gragoudas ES, Miller JW. (2005): An antisense oligodeoxynucleotide against vascular endothelial growth factor in a nonhuman primate model of iris neovascularization. Arch Ophthalmol. 123,214-219.

12. Bigda J, Beletsky I, Brakebusch C. (1994): Dual role of the p75 tumor necrosis factor (TNF) receptor in TNF cytotoxicity. J Exp Med. 180,445-460.

13. Bosem ME, Harris R, Atherton SS. (1990): Optic nerve involvement in viral spread in herpes simplex virus type 1 retinitis. Invest ophthalmol Vis Sci. 31,1683-1689.

14. Brennan FM, Gibbons DL, Mitchell T, Cope AP, Maini RN, Feldmann M. (1992): Enhanced ecpression of tumor necrosis factor receptor mRNA and protein in mononuclear cells isolated from rheumatoid arthritis synovial joints. Eur J Immunol. 22,1907-1912.

15. Cibis GW, Flynn JT, Davis B. (1978): Herpes simplex retinitis. Arch Ophthalmol. 96, 299-306.

16. Cogan DG, Kuwabara T, Young GF, Knox DL. (1964): Herpes simplex retinopathy in an infant. Arch Ophthalmol. 72, 641-649.

17. Cope AP, Aderka D, Wallach D, Kahan M, Chu NR, Brennan FM, Feldmann M. (1995): Soluble TNF receptor production by activated T lymphocytes: differential effects of acute and chronic exposure to TNF. Immunology. 84,21-30.

18. Cousins SW, Gonzalez A, Atherton SS. (1989): Herpes simplex retinitis in the mouse: Clinicopathologic correlation. Invest ophthalmol Vis Sci. 30,1485-1494.

19. Culbertson WW, Blumenkranz MS, Haines H, Gass DM, Mitchell KB, Norton EW. (1982): The acute retinal necrosis syndrome. Part 2: histopathology and etiology. Ophthalmology. 89, 1317-1325.

20. Culbertson WW, Blumenkranz MS, Pepose JS, Stewart JA, Curtin VT. (1986): Varicella zoster virus is a cause of the acute retinal necrosis syndrome. Ophthalmology. 93, 559-569.

21. Da Ros T, Spalluto G, Prato M, Saison-Behmoaras T, Boutorine A, Cacciari B. (2005): Oligonucleotides and oligonucleotide conjugates: a new approach for cancer treatment. Curr Med Chem. 12,71-88.

22. Dix RD, Streilein JW, Cousins S, Atherton SS. (1987): Histopathologic characteristics of two forms of experimental herpes simplex virus retinitis. Curr eye Res. 6,47-52.

23. Elbashir SM, Harborth J, Lendeckel W, Yalcin A, Weber K, Tuschl T. (2001): Duplexes of 21-nucleotide RNAs mediate RNA interference in cultured mammalian cells. Nature. 411,494-498.

24. Engwerda CR, Ato M, Cotterell SE, Mynott TL, Tschannerl A, Gorak-Stolinska PM, Kaye PM. (2002): A role for tumor necrosis factor-alpha in remodeling the splenic marginal zone during Leishmania donovani infection. Am J Pathol. 161,429-437.

25. Erwig L, Kluth DC, Walsh GM, Rees AJ. (1998): Initial cytokine exposure determines function of macrophages and renders them unresponsive to other cytokines. J Immunol. 161,1983-1988.

26. Fleisher LN, Ferrell JB, McGahan MC. (1990): Ocular inflammatory effects of intravitreally injected tumor necrosis factor-alpha and endotoxin. Inflammation. 14,325-335.

27. Fong Y, Lowry SF. (1990): Tumor necrosis factor in the pathophysiology of infection and sepsis. Clin Immunol Immunopathol. 55,157-170.

28. Fonseca SG, Romao PR, Figueiredo F, Morais RH, Lima HC, Ferreira SH, Cunha FQ. (2003): TNF-alpha mediates the induction of nitric oxide synthase in macrophages but not in neutrophils in experimental cutaneous leishmaniasis. Eur J Immunol. 33,2297-2306.

29. Forster DJ, Dugel PU, Frangieh GT, Liggett PE, Rao NA. (1990): Rapidly progressive outer retinal necrosis in the acquired immunodeficiency syndrome. Am J Ophthalmol. 110, 341-348.

30. Galderisi U, Cascino A, Giordano A. (1999): Antisense oligonucleotides as therapeutic agents. J Cell Physiol. 181,251-257.

31. Ganatra JB, Chandler D, Santos C, Kuppermann B, Margolis TP. (2000): Viral causes of the acute retinal necrosis syndrome. Am J Ophthalmol. 129,166-172.

32. Greiner K, Murphy CC, Willermain F, Duncan L, Plskova J, Hale G, Isaacs JD, Forrester JV, Dick AD. (2004): Anti- TNFα therapy modulates the phenotype of peripheral blood $CD4^+$ T cells in patients with posterior segment intraocular inflammation. Invest Ophthalmol Vis Sci. 45,170-176.

33. Heise MT, Virgin HW 4^{th}. (1995): The T-cell-independent role of gamma interferon and tumor necrosis factor alpha in macrophage activation during murine cytomegalovirus and herpes simplex virus infections. J Virol. 69,904-909.

34. Hellinger WC, Bolling JP, Smith TF, Campbell RJ. (1993): Varicella-zoster virus retinitis in a patient with AIDS-related complex: case report and brief review of the acute retinal necrosis syndrome. Clin Infect Dis. 16,208-212.

35. Henry SP, Miner RC, Drew WL, Fitchett J, York-Defalco C, Rapp LM, Levin AA. (2001): Antiviral activity and ocular kinetics of antisense oligonucleotides designed to inhibit CMV replication. Invest Ophthalmol Vis Sci. 42,2646-2651.

36. Holland GN, Togni BI, Briones OC, Dawson CR. (1987): A microscopic study of herpes simplex virus retinopathy in mice. Invest Ophthalmol Vis Sci. 28 ,1181-1190.

37. Johnson BL, Wisotzkey HM. (1977): Neuroretinitis associated with herpes simplex encephalitis in an adult. Am J Ophthalmol. 83, 481-489.

38. Kahn M, Kaplan HJ, Ferguson TA. (1993): The regulation by light of retinal necrosis and the immune response following anterior chamber inoculation of herpes simplex virus type-1. Arch Virol. 131,115-126.

39. Keane J, Gershon S, Wise RP, Mirabile-Levens E, Kasznica J, Schwieterman WD, Siegel JN, Braun MM. (2001): Tuberculosis associated with infliximab, a tumor necrosis factor alpha-neutralizing agent. N Engl J Med. 345,1098-104.

40. Kielty David, Cousins SW, Atherton SS. (1987): HSV-1 retinitis and delayed hypersensitivity in DBA/2 and C57BL/6 mice. Invest Ophthalmol Vis Sci. 28,1994-1999.

41. Kim TW, Lindsey JD, Aihara M, Anthony TL, Weinreb RN. (2002): Intraocular distribution of 70-kDa dextran after subconjunctival injection in mice. Invest Ophthalmol Vis Sci. 43,1809-1816.

42. Koizumi K, Poulaki V, Doehmen S, Welsandt G, Radetzky S, Lappas A, Kociok N, Kirchhof B, Joussen AM. (2003): Contribution of TNF-α to Leukocyte Adhension, Vascular Leakage, and Apoptotic Cell Death in Endotoxin-Induced Uveitis In Vivo. Invest Ophthalmol Vis Sci. 44,2184-2191.

43. Kurreck J. (2003): Antisense technologies. Improvement through novel chemical modifications. Eur J Biochem. 270,1628-44.

44. Lewis ML, Culbertson WW, Post JD, Miller D, Kokame GT, Dix RD. (1989): Herpes simplex virus type 1. A cause of the acute retinal necrosis syndrome. Ophthalmology. 96,875-878.

45. Li Q, Verma IM. (2002): NF-pappaB regulation in immune system. Nat Rev Immunol. 2,725-734.

46. Lucin P, Jonjic S, Messerl B Polic B, Hengel H, Koszinowski UH. (1994): Late phase inhibition of murine cytomegalovirus replication by synergistic action of interferon-gamma and tumor necrosis factor. J Gen Virol. 75,101-110.

47. Minckler DS, McLean EB, Shaw CM, Hendrickson A. (1976): Herpesvirus hominis encephalitis and retinitis. Arch Ophthalmol. 94, 89-95.

48. Mohan N, Edwards ET, Cupps TR, Oliverio PJ, Sandberg G, Crayton H, Richert JR, Siegel JN. (2001): Demydlination occurring during anti-tumor necrosis factor alpha therapy for inflammatory arthritides. Arthritis Rheum. 44,2862-2869.

49. Naumann G, Gass JD, Font RL. (1968): Histopathology of herpes zoster ophthalmicus. Am J Ophthalmol. 65, 533-541.

50. Nussenblatt RB, Palestine AG. (1989): Acute retinal necrosis. Uveitis: Fundamentals and clinical practice. Chicago: Year Book Mecical, pp407-414.

51. Oettinger C, D'Szouza M. (2003): Microencapsulation of tumor necrosis factor oligomers: a new approach to proinflammatory cytokine inhibition. J Interferon Cytokine Res. 23,533-543.

52. Pavan-Langston D, Dunkel EC. (1989): Ocular varicella-zoster virus infection in the guinea pig. A new in vivo model. Arch Ophthalmol. 107,1068-1073.

53. Pepose JS, Whittum-Hudson JA. (1987): An immunogenetic analysis of resistance to herpes simplex virus retinitis in inbred strains of mice. Invest Ophthalmol Vis Sci. 28,1549-1552.

54. Pettit TH, Kimura SJ, Uchida Y, Peters H. (1965): Herpes simplex uveitis: an experimental study with the fluorescein-labeled antibody technique. Invest Ophthalmol Vis Sci 4,349-357.

55. Pierce TL, White AR, Tregear GW, Sexton PM. (2005): Peptide-oligonucleotide hybrids in antisense therapy. Mini Rev med Chem. 5,41-55.

56. Popescu FD. (2005): Antisense- and RNA interference-based therapeutic strategies in allergy. J cell Mol Med. 9,840-853.

57. Reimold AM. (2003): New indications for treatment of chronic inflammation by TNF-alpha blockade. Am J Med Sci. 325,75-92.

58. Robertson MJ, Erwin LP, Liversidge J. (2002): Retinal microenvironment controls resident and infiltrating macrophage function during uveoretinitis. Invest Ophthalmol Vis Sci. 43,2250-2257.

59. Robertson M, Liversidge J, Forrester JV, Dick AD. (2003): Neutralizing tumor necrosis factor-α activity suppresses activation of infiltrating macrophages in experimental autoimmune uveoretinitis. Invest Ophthalmol Vis Sci. 44,3034-3041.

60. Roizman B, Herpesviridae. (1996): In Fields BN, Knipe DM, Howley PM (eds): Virology, 3d edition. Lippincott-Raven Publishers, Philadelphia.

61. Roizman B, Sears A. (1996): Herpes simplex viruses and their replication. In Fields BN, Knipe DM, Howley PM (eds): Virology, 3d edition. Lippincott-Raven Publishers, Philadelphia.

62. Rummelt V, Wenkel H, Rummelt C, Jahn G, Meyer HJ, Naumann GO. (1992):

Detection of varicella zoster virus DNA and viral antigen in the late stage of bilateral acute retinal necrosis syndrome. Arch Ophthalmol. 110, 1132-1136.

63. Sallusto F. Cella M, Danieli C, Lanzavecchia A. (1995): Dendritic cells use macropinocytosis and the mannose receptor to concentrate macromolecules in the major histocompatibility complex class □ compartment: downregulation by cytokines and bacterial products. J Exp Med. 182,389-400.

64. Sartani G, Silver PB, Rizzo LV, Chan CC, Wiggert B, Mastorakos G, Caspi RR. (1996): Anti-tumor necrosis factor alpha therapy suppresses the induction of experimental autoimmune uveoretinitis in mice by inhibiting antigen priming. Imvest ophthalmol vis sci.37,2211-2218.

65. Scanoon KJ. (2004): Anti-Genes: siRNA, Ribozymes and antisense. Curr Pharm Biotechnol. 5,415-420.

66. Silverstein BE, Conrad D, Margolis TP, Wong IG. (1997): Cytomegalovirus-associated acute retinal necrosis syndrome. Am J Ophthalmol. 123,257-258.

67. Tartaglia LA, Weber RF, Figari IS. (1991): Two different receptors for tumor necrosis factor mediate distinct cellular responses. Proc Natl Acad Sci USA.88,9292-9296.

68. Taylor MF, Paulauskis JD, Weller DD Kobzik L. (1997): Comparison of efficacy of antisense oligomers directed toward TNF-alpha in helper T and macrophage cell lines. Cytokine. 9,672-681.

69. Thompson WS, Culbertson WW, Smiddy WE, Robertson JE, Rosenbaum JT. (1994): Acute retinal necrosis caused by eactivation of herpes simplex virus type 2. Am J Ophthalmol. 118,205-211.

70. Urayama A, Yamada N, Susaki T. (1971): Unilateral acute uveitis with retinal periarteritis and detachment. Jpn J Clin Ophthalmol. 25,607-619.

71. van Hogezand RA, Verspaget HW. (1998): The future role of anti-tumour necrosis factor-alpha products in the treatment of Crohn's disease. Drugs. 56,299-305.

72. van Strijp JA, van der Tol ME, Miltenburg LA, van Kessel KP, Verhoef J. (1991): Tumor necrosis factor triggers granulocytes to internalize complement-coated virus particles. Immunology. 73,77-82.

73. Vann VR, Atherton SS. (1991): Neural spread of herpes simplex virus after anterior chamber inoculation. Invest Ophthalmol Vis Sci. 32,2462-2472.

74. Verjans GM, Feron EJ, Dings ME, Comelissen JG, Van der Lelij A, Baarsma GS, Osterhaus AD. (1998): T cells specific for the triggering virus infiltrate the eye in patients with herpes simplex virus-mediated acute retinal necrosis. J Infect Dis. 178, 27-34.

75. von Szily A. (1924): Experimental endogenous transmission of infection from bulbus to bulbus. Klin Monatsbl Augenheilkd. 72,592-602.

76. Walev I, Podlech J, Falke D. (1995): Enhancement by TNF-α of reactivation and replication of latent herpes simplex virus from trigeminal ganglia of mice. Arch Virol. 140,987-992.

77. Walev I, Podlech J, Falke D. (1995): Correlation of virus replication, cytokine (TNF-α and IL-1) producing cells, neuronal necrosis and inflammation after intranasal infection of mice with herpes simplex virus strains of different virulence. Arch Virol. 140,1957-1967.

78. Wallis WJ, Burge DJ, Holman J. (2001): Infection reports with entanercept (Enbrel) therapy. Arthritis Rheum. 44,S.78-85.

79. Ware CF, Crowe PD, Vanarsdale TL Andrews JL, Grayson MH, Jerzy R, Smith CA, Goodwin RG. (1991): Tumor necrosis factor (TNF) receptor expression in T lymphocytes. Differential regulation of the type ¤ TNF receptor during activation of resting and effecor T cells. J Immunol. 147,4229-4238.

80. Wasmuth S, Bauer D, Yang Y, Steuhl KP, Heiligenhaus A. (2003): Topical treatment with antisense oligonucleotides targeting tumor necrosis factor-alpha in herpetic stromal keratitis. Invest Ophthalmol Vis Sci. 44,5228-5234.

81. Whittum-Hudson J, Farazdaghi M, Prendergast RA. (1985): A role for T lymphocytes in preventing experimental herpes simplex virus type 1-induced retinitis. Invest Ophthalmol Vis Sci. 26, 1524-1532.

82. Whittum-Hudson JA, Pepose JS. (1987): Immunologic modulation of virus-

induced pathology in a murine model of acute herpetic retinal necrosis. Invest Ophthalmol Vis Sci. 28, 1541-1548.

83. Whittum-Hudson JA, Pepose JS. (1988): Herpes simples virus type 1 induces anterior chamber-associated immune deviation (ACAID) in mouse strains resistant to intraocular infection. Curr Eye Res. 7,125-130.

84. Whittum JA, McCulley JP, Niederkorn JY, Streilein JW. (1984): Ocular disease induced in mice by anterior chamber inoculation of herpes simplex virus. Invest Ophthalmol Vis Sci. 25,1065-1073.

85. Whittum JA, Niederkorn JY, Mcculley JP, Streilein JW. (1983): Intracameral inoculation of herpes simplex virus type 1 induces anterior chamber-associated immune deviaton. Curr Eye Res. 2,691-696.

86. Zaltas MM, Opremcak EM, Hemady R, Foster CS. (1992): Immunopathology of herpes simplex virus chorioretinitis in the von Szily model. Imvest Ophthalmol Vis Sci. 33,68-77.

87. Zamecnik PC, Stephenson ML. (1978): Inhibition of Rous sarcoma virus replication and cell trasformation by a specific oligodeoxynucleotide. Proc Natl Acad Sci USA. 75, 280-284.

88. Zhao Q, Song X, Waldschmidt T, Fisher E, Krieg AM. (1996): Oligonucleotide uptake in human hematopoietic cells is increased in leukemia and is related to cellular activation. Blood. 88,1788-1795.

89. Zheng M, Atherton SS. (2005): Cytokine profiles and inflammatory cells during HSV-1-induced acute retinal necrosis. Invest Ophthalmol Vis Sci. 46,1356-1363.

90. Zheng M, Qian H, Joshi RM, Nechtman J, Atherton SS. (2003): DNA microarray analysis of the uninoculated eye following anterior chamber inoculation of HSV-1. Ocul Immunol Inflamm. 11,187-195.

7. Figures

Figure 1

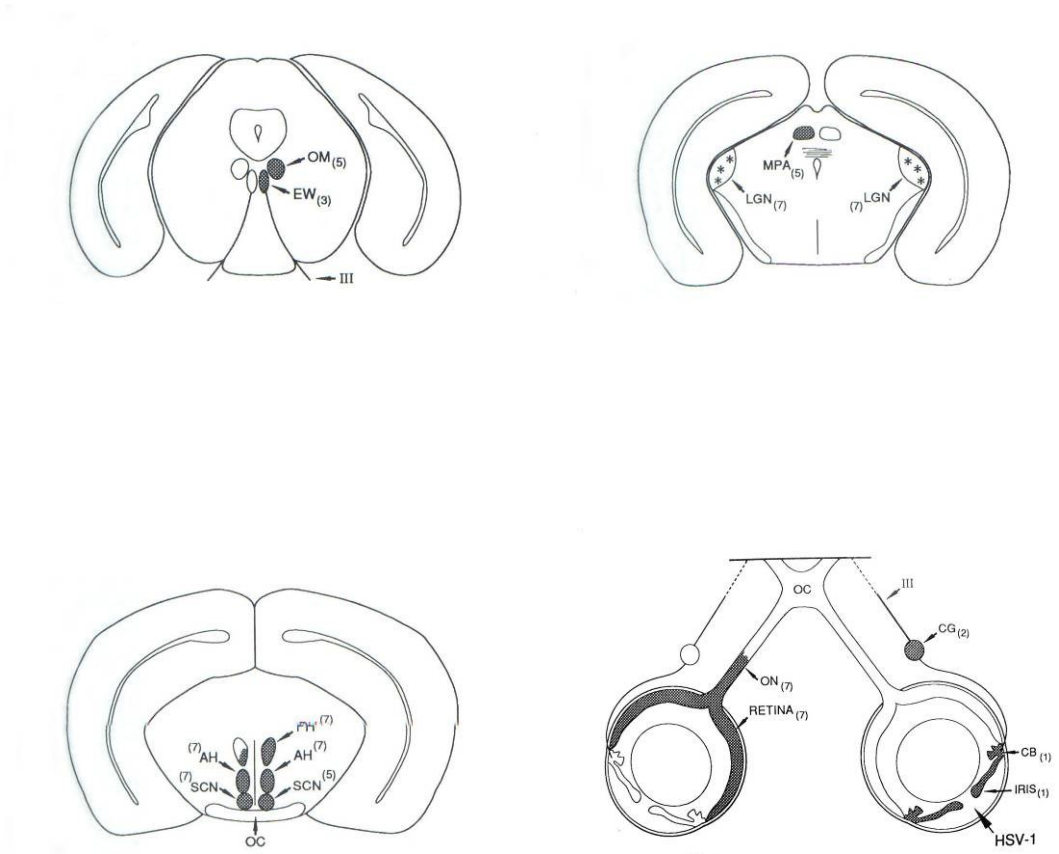

Fig 1 Distribution of HSV-1 antigen in the eyes, the optic nerve and autonomic structures at different time-points after infection. Infected areas are stippled. Numbers in parentheses indicate mean delay to detection of viral antigens (days PI). Abbreviations: AH, anterior hypothalamic nucleus; CB, ciliary body; CG, ciliary ganglion; EW, Edinger-Westphal nucleus; LGN, lateral geniculate nucleus; MPA, medial pretectal area; OC, optic chiasm; OM, nucleus of the oculomotor nerve; ON, optic nerve; PH, paraventricular hypothalamic nucleus; SCN, suprachiasmatic

nucleus; □, oculomotor nerve. (Fig. 13 in Vann et al., 1991).

Figure 2

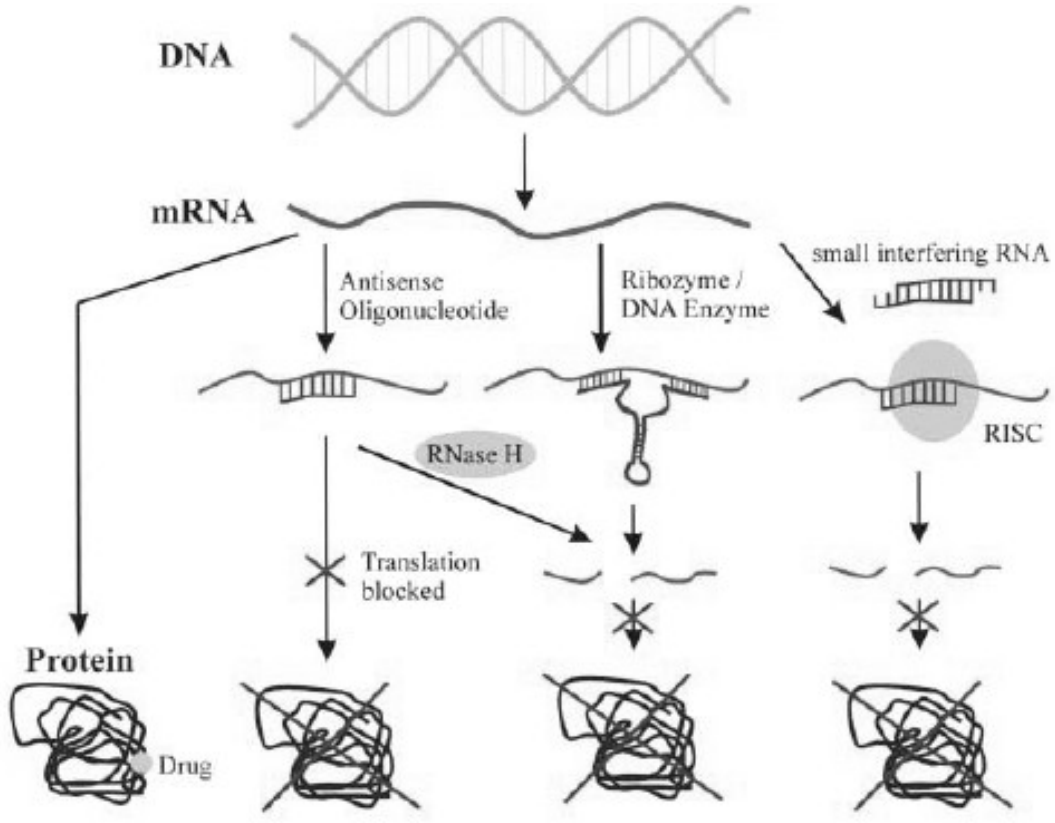

Fig 2 Comparison of different antisense strategies. While most of the conventional

drugs bind to proteins, antisense molecules pair with their complementary target RNA. Antisence-oligonucleotides block translation of the mRNA or induce its degradation by RNase H, while ribozymes and DNA enzymes possess catalytic activity and cleave their target RNA. RNA interference approaches are performed with siRNA molecules that are bound by the RISC and induce degradation of the target mRNA. (Fig. 1 in Kurreck et al., 2003).

Figure 3

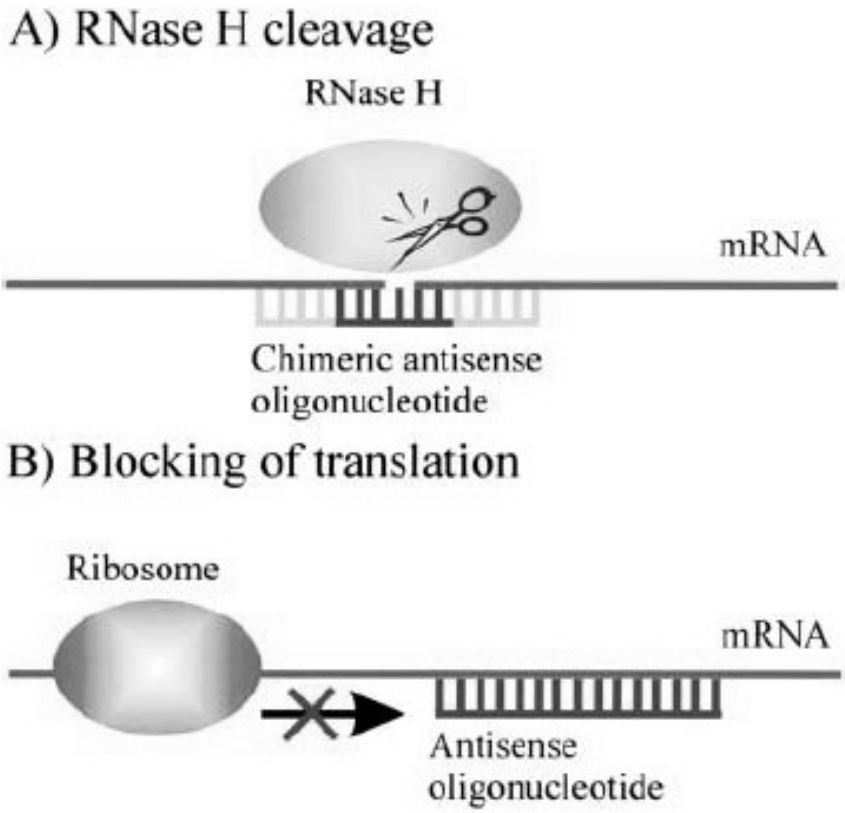

Fig 3 Mechanisms of antisense activity. (A) RNase H cleavage induced by ASON. (B) translational arrest by blocking the ribosome. (Fig. 2 in Kurreck et al., 2003).

Figure 4

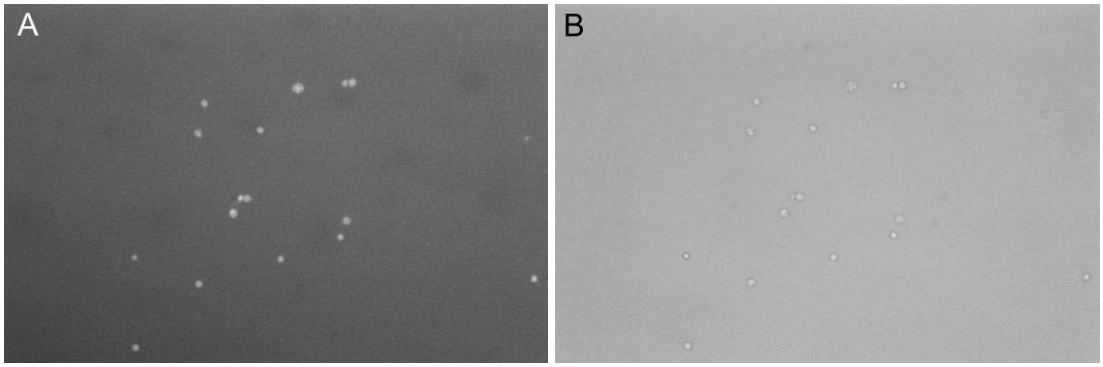

Fig 4 Fluorescence staining of cells derived from regional lymph nodes. After cultured with FITC-labeled ASON for 12 hours, the cells were examined by fluorescence- and light microscopy. (A) Fluorescence was observed in the cells of regional lymph nodes. (B) Lymph nodes cells were observed under light microscopy. (magnification, ×400).

Figure 5

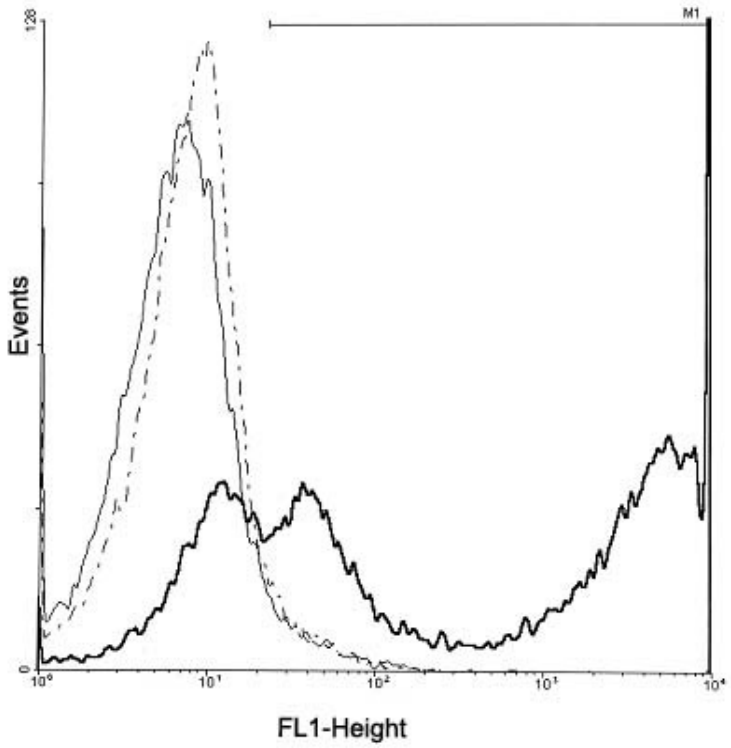

Fig 5 Flow cytometric analysis of cells derived from regional lymph nodes. Left trace: the negative control without FITC; broken trace: events after incubation solely with FITC (0.45% positive); thick trace: event with FITC-labeled oligonucleotide (67.17% positive). Incubation time, 15 minutes; concentration, 2μM. (Fig 1 in Wasmuth et al., 2003)

Figure 6

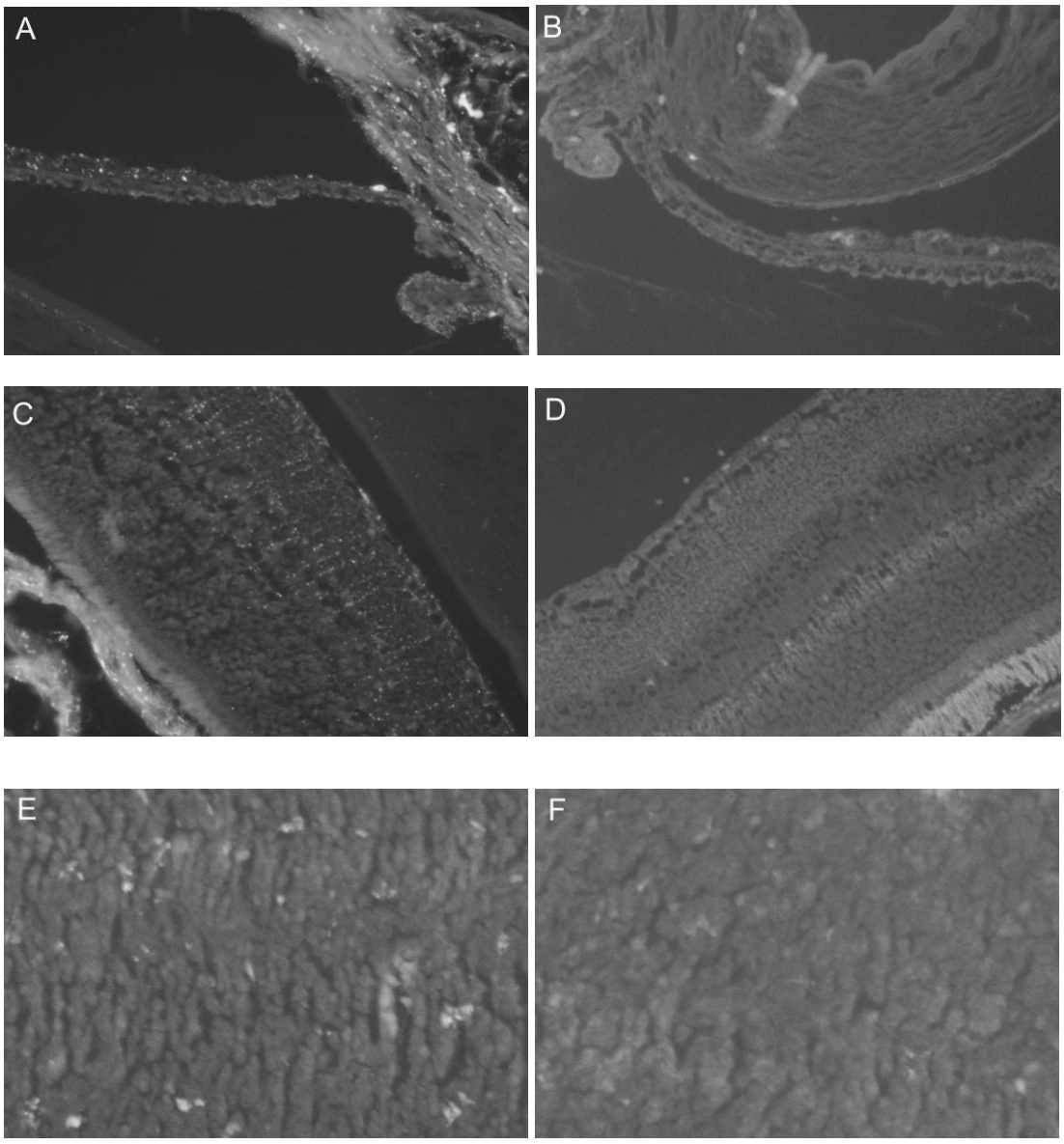

Fig 6 Fluorescence staining of different tissues 1 day after injection of FITC-ASON. After subconjunctival injection of 50μl FITC-TNF-α-ASON, the eyes and regional lymph nodes were harvested and imbedded in paraffin, and 5μm sections were prepared. (A) Subconjunctiva, iris and ciliary body were strongly fluorescent positive.

(B) No fluorescence was found in anterior segment of negative controls. (C) Sclera, choroid, retinal vessels and few cells within the retina were strongly fluorescent positive. (D) No fluorescent was found in the posterior segment of negative controls. (E) A few cells in regional lymph node were fluorescent positive. (F) No fluorescence was found in the lymph nodes of negative controls. (magnification, ×400).

Figure 7

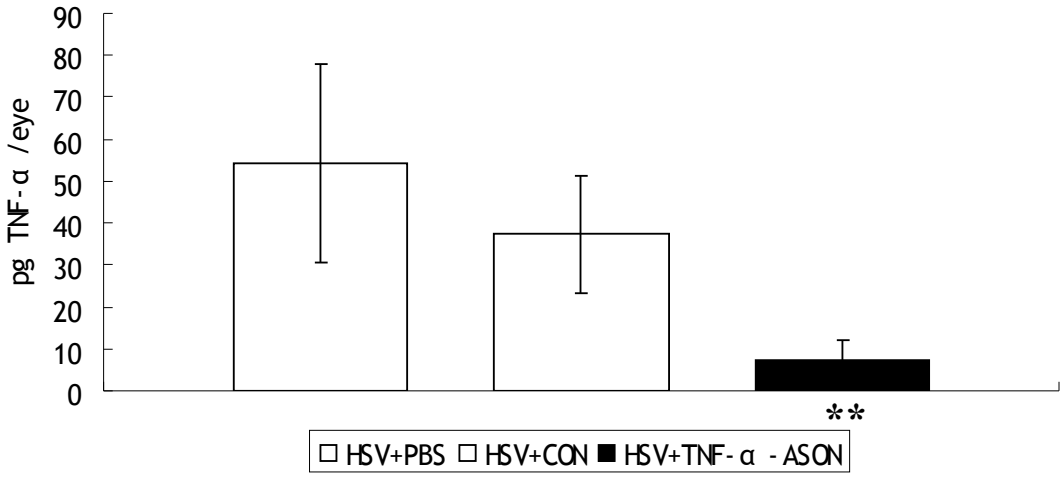

Fig 7 TNF-α content by ELISA assay in the different treatment groups on day 8. Mice were infected with 2×10^4 PFU of HSV into right eyes on day 0. After subconjunctival injection with TNF-α-ASON, CON or PBS, the content of TNF-α in left eye was examined on day 8. The TNF-α-content was significantly reduced after TNF-α-ASON treatment compared with PBS and CON treatment group. ** $P<0.01$ compared with CON and PBS group.

Figure 8

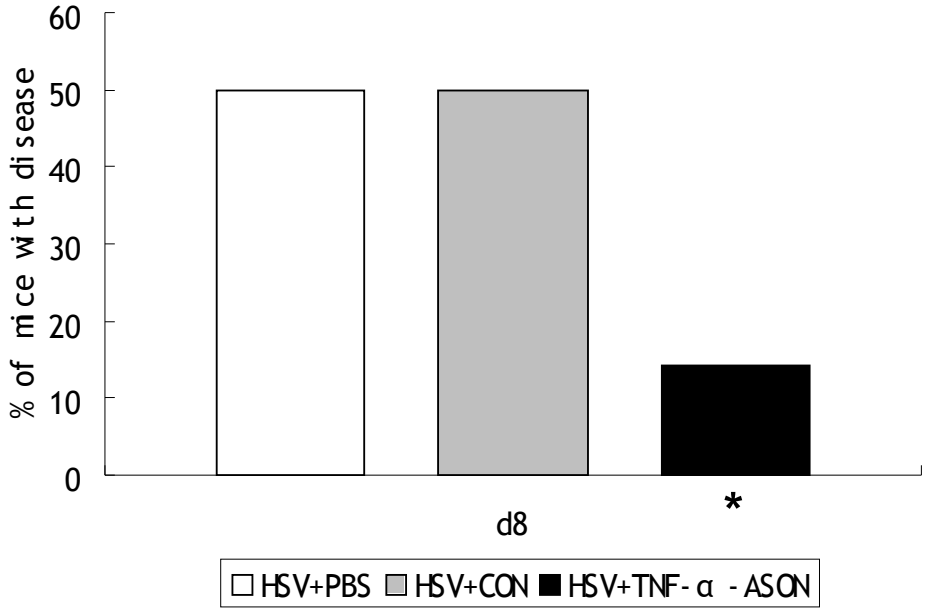

Fig 8 Clinical incidence of retinitis on day 8 after subconjunctival treatment. Mice were infected with 2×10^4 PFU of HSV into right eyes on day 0. After subconjunctival injection with TNF-α-ASON, CON or PBS, the left eyes were examined on day 8. Mice treated with TNF-α-ASON had reduced incidence of retinitis as compared to the CON and PBS treatment group. * $P<0.05$ compared with CON and PBS group.

Figure 9

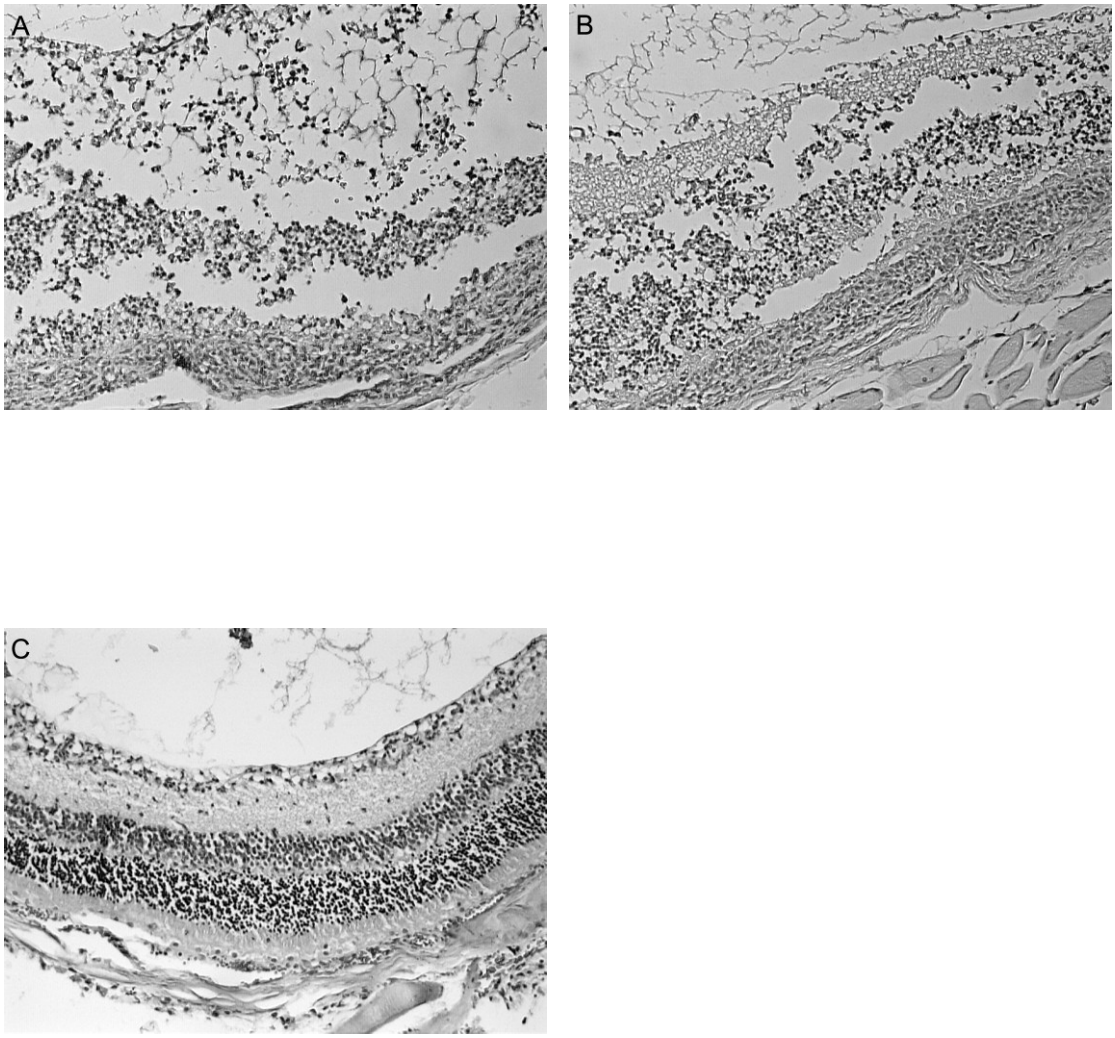

Fig 9 Histological findings in BALB/c mice on day 8 after HSV-1 infection. Mice were infected with 2×10^4 PFU of HSV into right eyes on day 0. After subconjunctival injection with TNF-α-ASON, CON and PBS, the left eyes were obtained by day 8, were sectioned and stained with hematoxylin and eosin (HE). (A) Mice treated with PBS had severe inflammatory cells infiltration and loss of retinal architecture (B)

Treatment with CON (C) Mice treated with TNF-α-ASON had reduced inflammatory cells infiltration and only mild retinitis. (magnification, ×250).

Figure 10

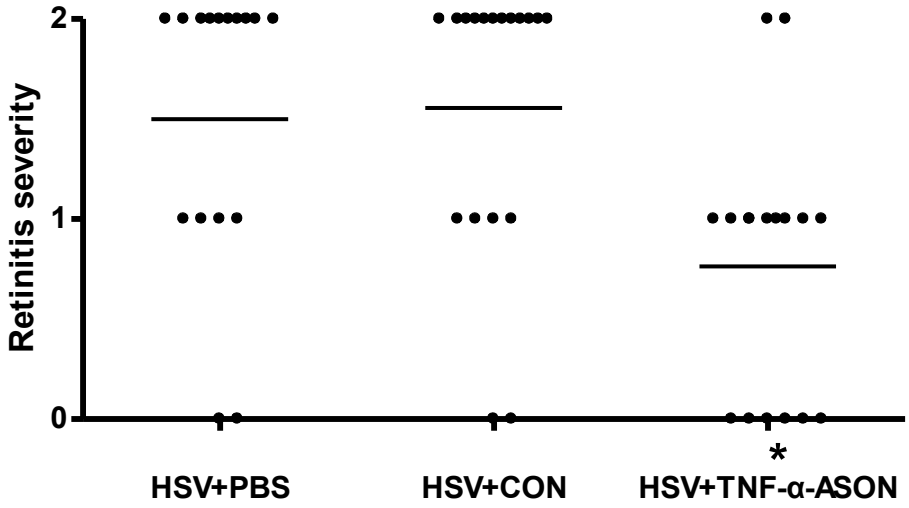

Fig 10 Degree of retinitis on day 8 after infection in the different treatment groups. Mice were infected with 2×10^4 PFU of HSV into right eyes on day 0. After subconjunctival injection with TNF-α-ASON, CON and PBS, the left eyes were harvested by day 8, sectioned and stained with hematoxylin and eosin (HE). The retina was graded from 0 to 2+, depending on the retinitis and necrosis extension. Animals treated with TNF-α-ASON had less severe retinitis than PBS treatment group. ***** $P<0.05$ compared with PBS and CON group. Crossbars indicate the means.

Figure 11

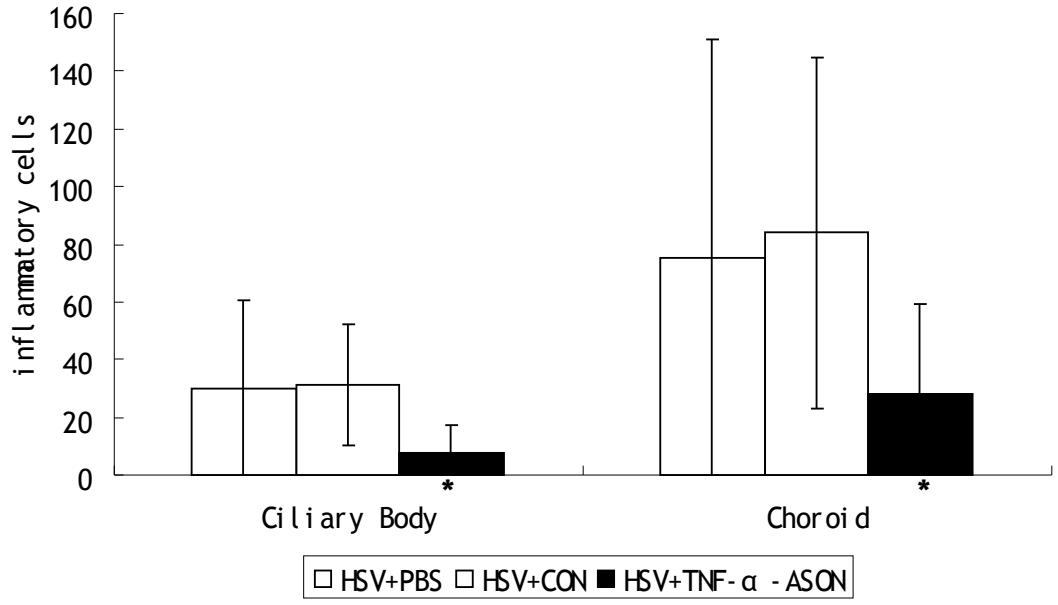

Fig 11 Number of inflammatory cells in ciliary body and choroid on day 8 in the different treatment groups. Mice were infected with 2×10^4 PFU of HSV into right eyes on day 0. After subconjunctival injection with TNF-α-ASON, CON and PBS, the left eyes were cut into sections and stained with hematoxylin and eosin (HE). The number of inflammatory cells was counted in a high-power field. (magnification, ×400). Compared with the control groups, the mice with TNF-α-ASON treatment had less the inflammatory cells in ciliary body and choroid. Data are the mean ± SD. * $P<0.05$ compared with PBS and CON group.

Figure 12

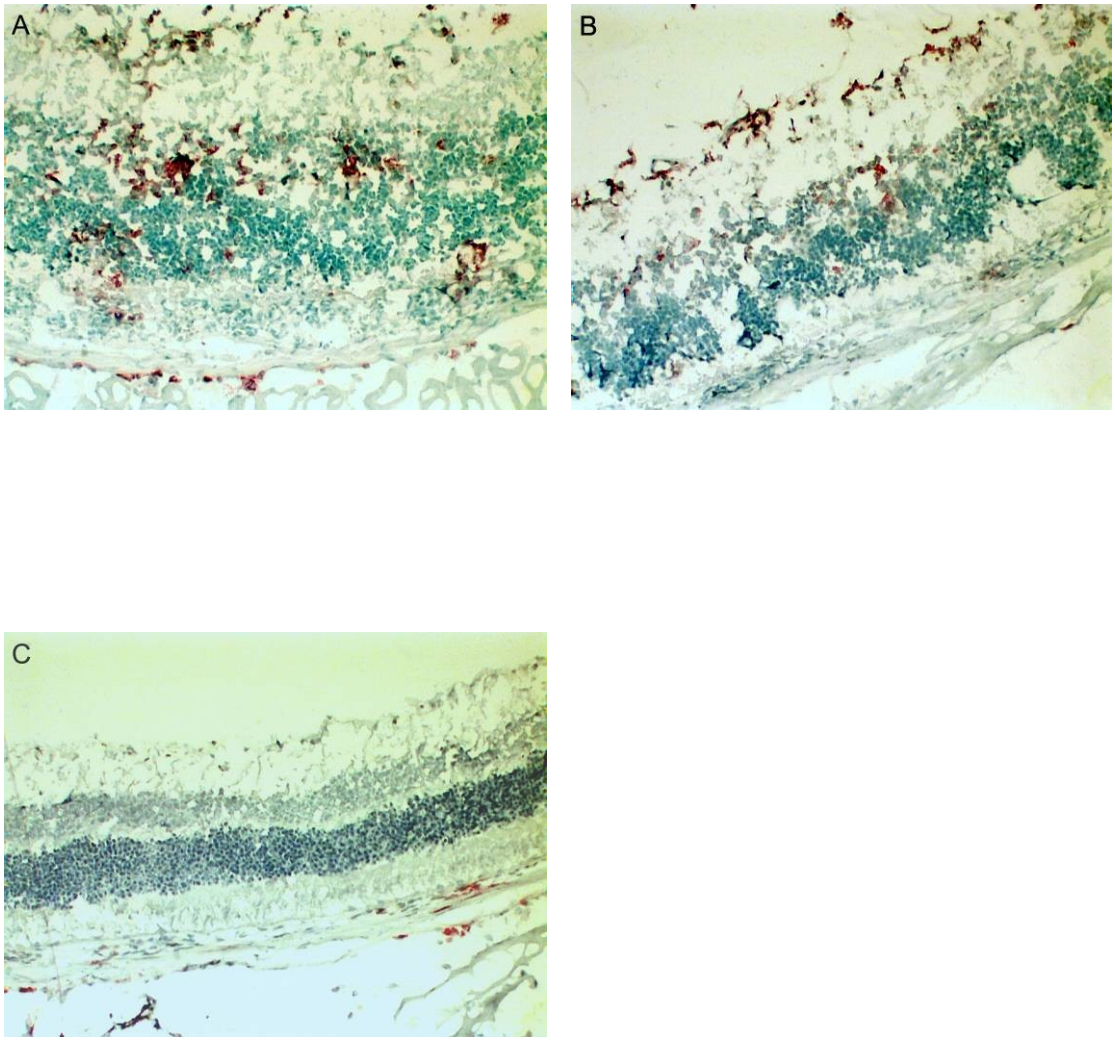

Fig 12 Immunohistochemical findings in BALB/c mice on day 8 after HSV-1 infection. Mice were infected with 2×10^4 PFU of HSV into right eyes on day 0. After subconjunctival injection with TNF-α-ASON, CON and PBS the left eyes were cut into sections and stained by immunohistochemistry (CD11b). (A) Retina of the left eye, treatment with PBS: heavy CD11b positive cell infiltration and loss of normal

retinal architecture. (B) Left eye of mouse with CON treatment had severe CD11b positive cells infiltration and loss of normal retinal architecture. (C) Left retina of mouse after treatment with TNF-α-ASON had fewer CD11b positive cells and only a mild retinitis. (magnification, ×250).

Figure 13

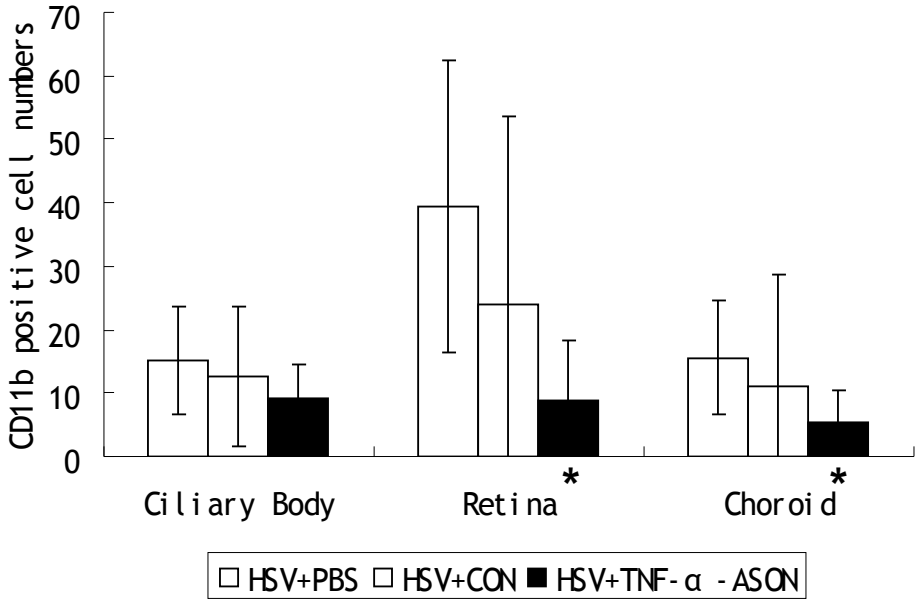

Fig 13 Number of CD11b positive cells in ciliary body, retina and choroid on day 8 with different treatment protocols. Mice were infected with 2×10^4 PFU of HSV into right eyes on day 0. After subconjunctival injection of TNF-α-ASON, CON and PBS, the left eyes were sectioned and processed by immunohistochemistry. The number of

CD11b positive cells was counted in a high-power field (magnification, ×400). Animals treated with TNF-α-ASON had significantly fewer CD11b positive cells than mice on in PBS treatment group. Mean ± SD. ***** $P<0.05$ compared with PBS group.

Figure 14

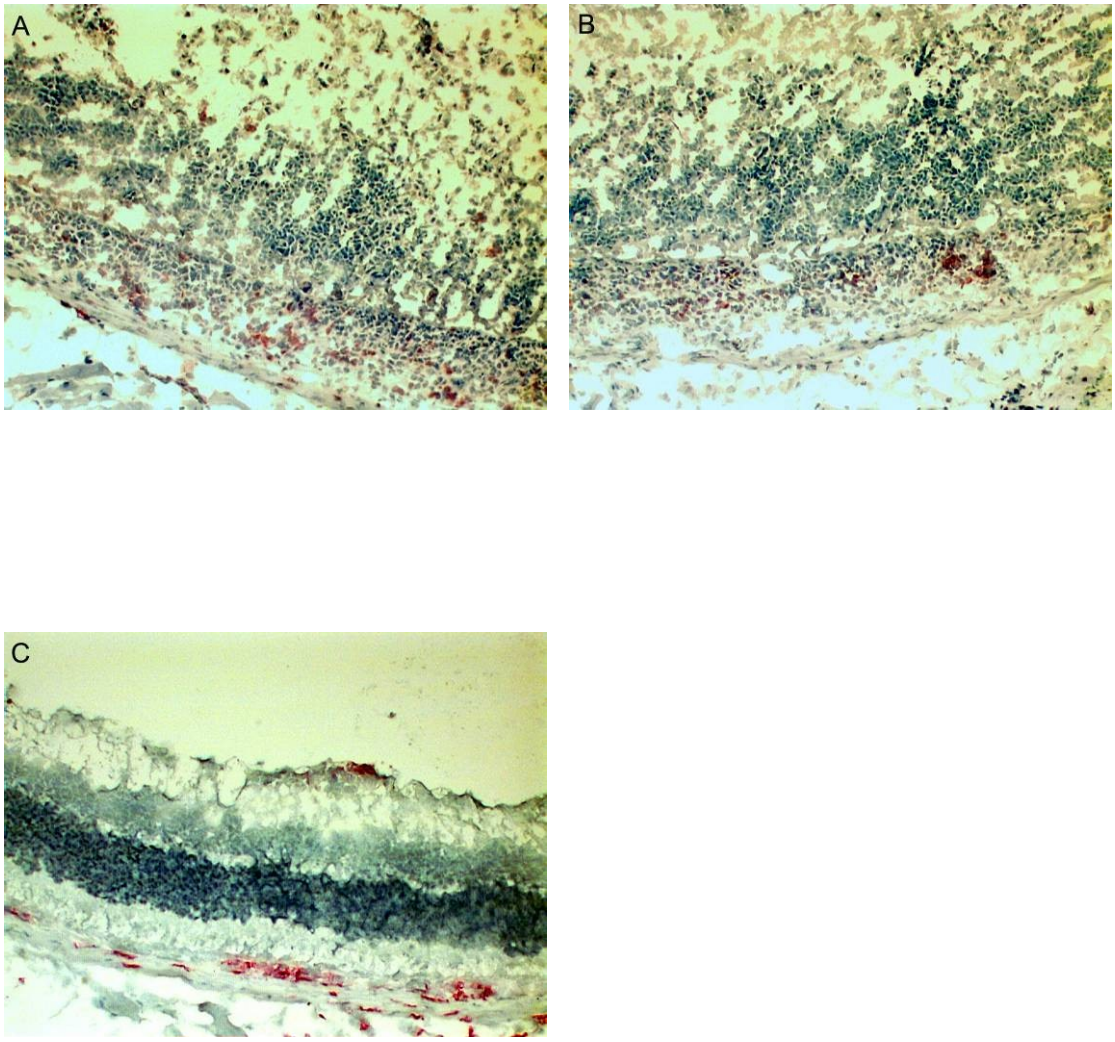

Fig 14 Immunohistochemical findings in BALB/c mice on day 8 after HSV-1 infection. Mice were infected with 2×10^4 PFU of HSV into right eyes on day 0. After subconjunctival injection of TNF-α-ASON, CON and PBS, the left eyes were cut, and sections were stained with mAb directed against CD3. (A) PBS group: severe CD3 cell infiltration in choroid and loss of normal retinal architecture. (B) CON group:

severe CD3 cells infiltration in choroid and loss of normal retinal architecture. (C) TNF-α-ASON treatment: fewer CD3 positive cells and mild retinitis. (magnification, ×250).

Figure 15

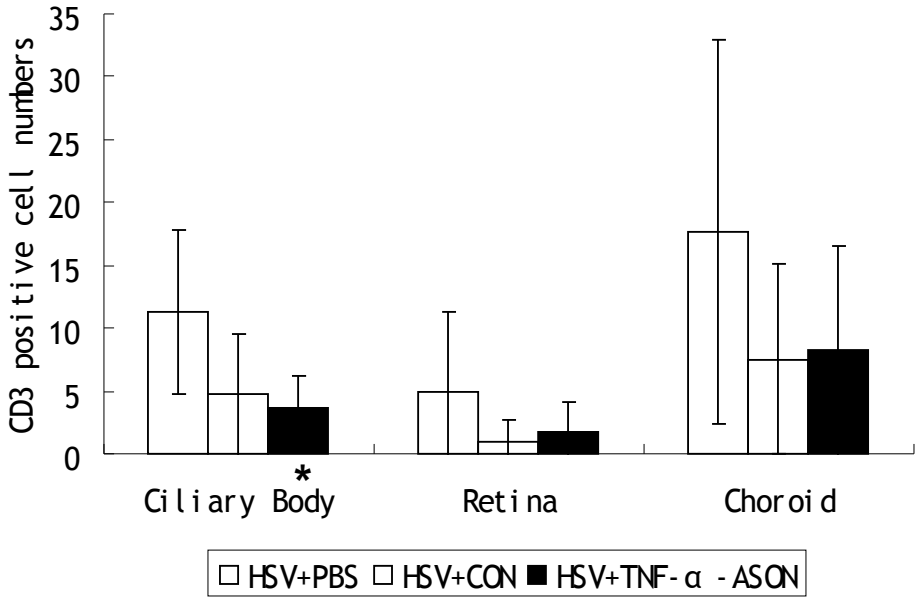

Fig 15 Number of CD3 positive cells in ciliary body, retina and choroid on day 8 in the different treatment groups. Mice were infected with 2×10^4 PFU of HSV into right eyes on day 0. After subconjunctival injection with TNF-α-ASON, CON and PBS, the left eyes were harvested, sectioned and stained by immunohistochemistry. The number of CD3 positive cells was counted in a high-power field. (magnification, ×400). Animals treated with TNF-α-ASON had significantly fewer CD3 positive cells than PBS treatment group in ciliary body. Mean ± SD. * $P<0.05$ compared with PBS group.

Figure 16

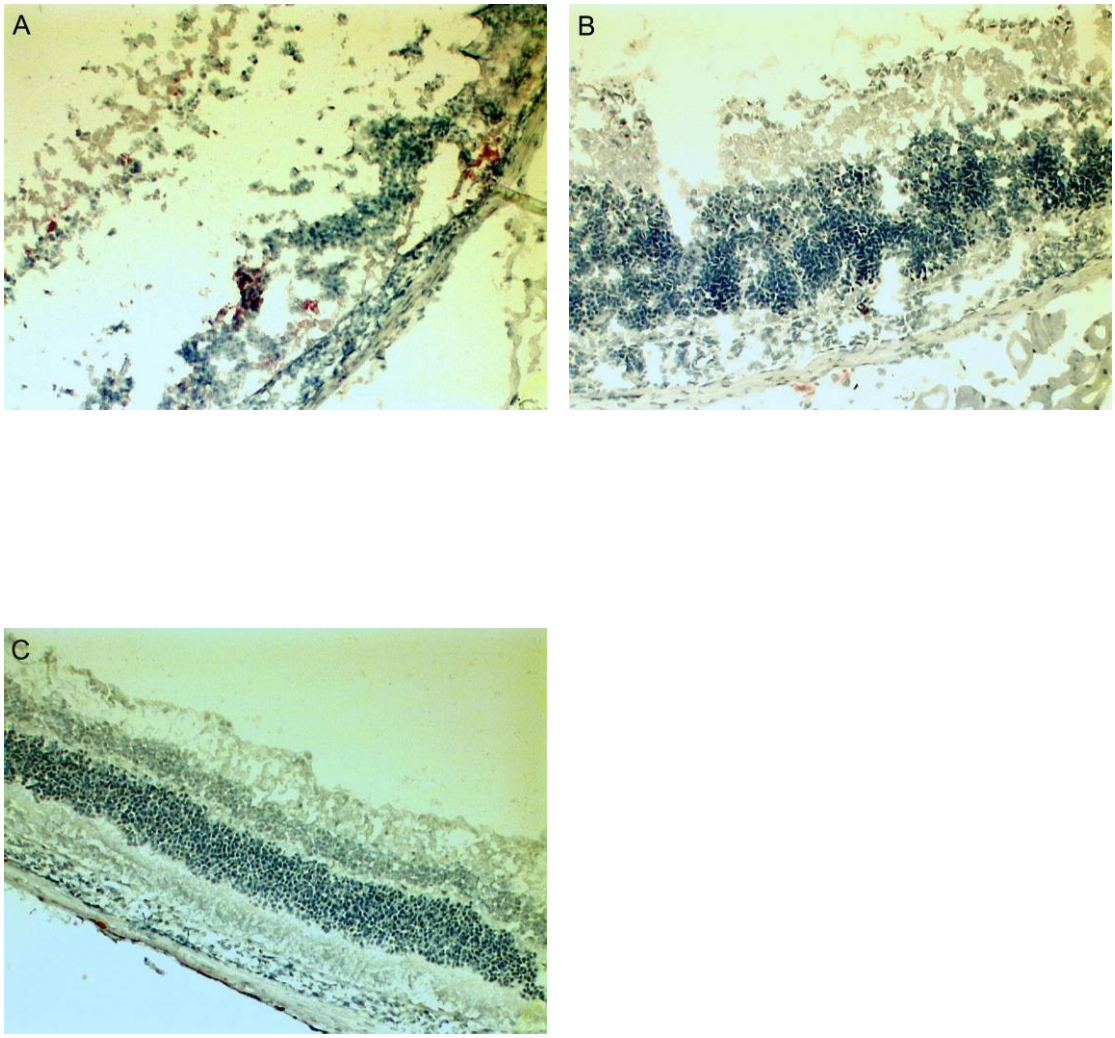

Fig 16 Immunohistochemical findings in BALB/c mice on day 8 after HSV-1 infection. Mice were infected with 2×10^4 PFU of HSV into right eyes on day 0. After subconjunctival injection of PBS, CON and TNF-α-ASON, the left eyes were obtained, sectioned and stained by immunohistochemistry (F4/80). (A) Treatment with PBS: few F4/80 positive cells and loss of normal retinal architecture. (B)

Treatment with CON: few F4/80 positive cells and loss of normal retinal architecture. (C) Treatment with TNF-α-ASON: few F4/80 positive cells and the nearly normal retinal architecture. (magnification, ×250).

Figure 17

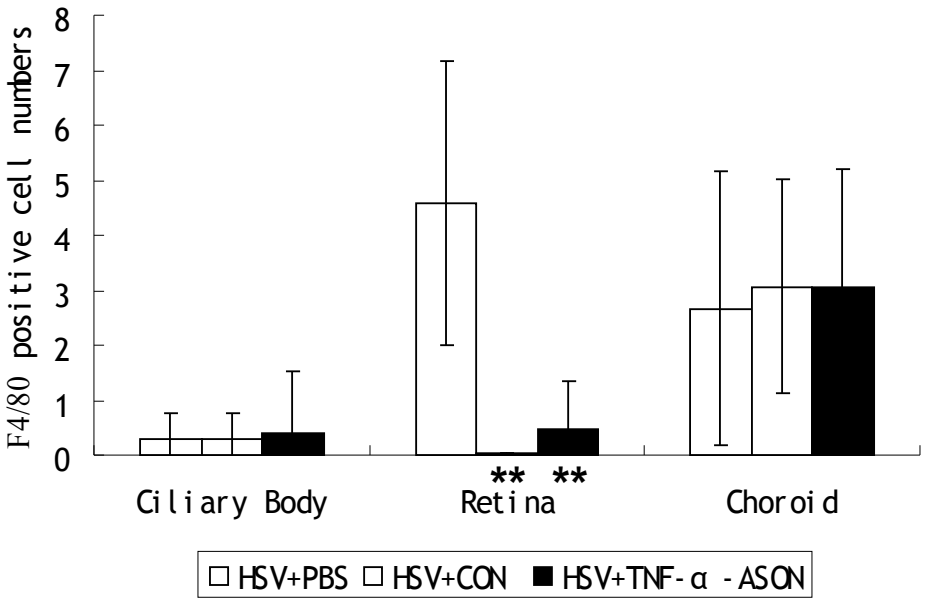

Fig 17 Number of F4/80 positive cells in ciliary body, retina and choroid on day 8 in the different treatment groups. Mice were infected with 2×10^4 PFU of HSV into right eyes on day 0. After subconjunctival injection with TNF-α-ASON, CON and PBS, the left eyes were harvested, sectioned and processed by immunohistochemistry. The number of F4/80 positive cells was counted in a high-power field. (magnification, ×400). Animals treated with TNF-α-ASON and CON had significantly fewer F4/80 positive cells than PBS treatment group in retina. Mean ± SD. ** $P<0.01$ compared with PBS group.

Figure 18

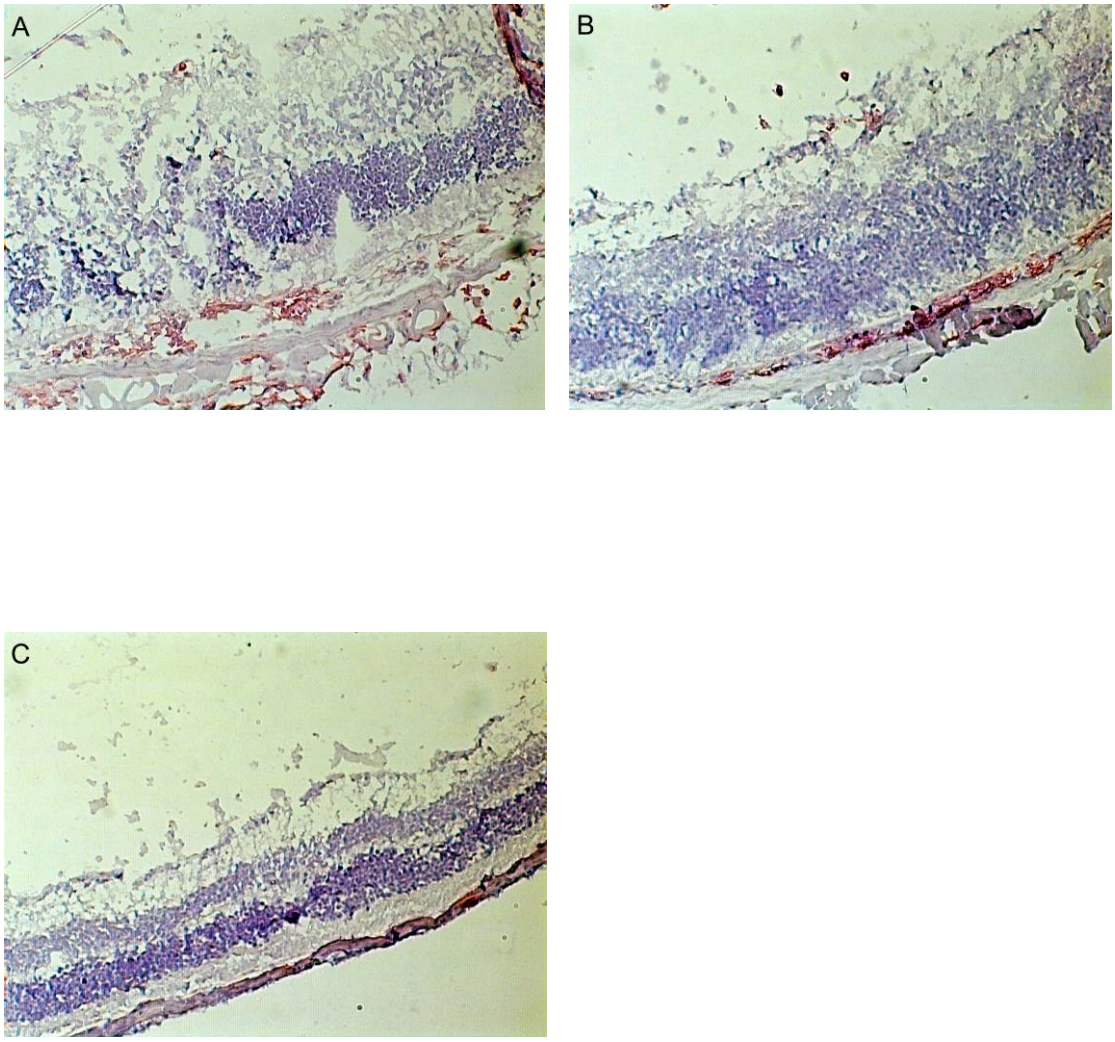

Fig 18 Immunohistochemical findings in BALB/c mice on day 8 after HSV-1 infection. Mice were infected with 2×10^4 PFU of HSV into right eyes on day 0. After subconjunctival injection with TNF-α-ASON, CON and PBS, the left eyes were harvested and cut into sections and stained by immunohistochemistry (IA/IE). (A) Mice treated with PBS had severe IA/IE positive cell infiltration in choroid and loss

normal retinal architecture. (B) Mice treated with PBS had severe IA/IE positive cell infiltration in choroid and loss of normal retinal architecture. (C) Mice treated with TNF-α-ASON had fewer IA/IE positive cells and nearly normal retinal architecture. (magnification, ×250).

Figure 19

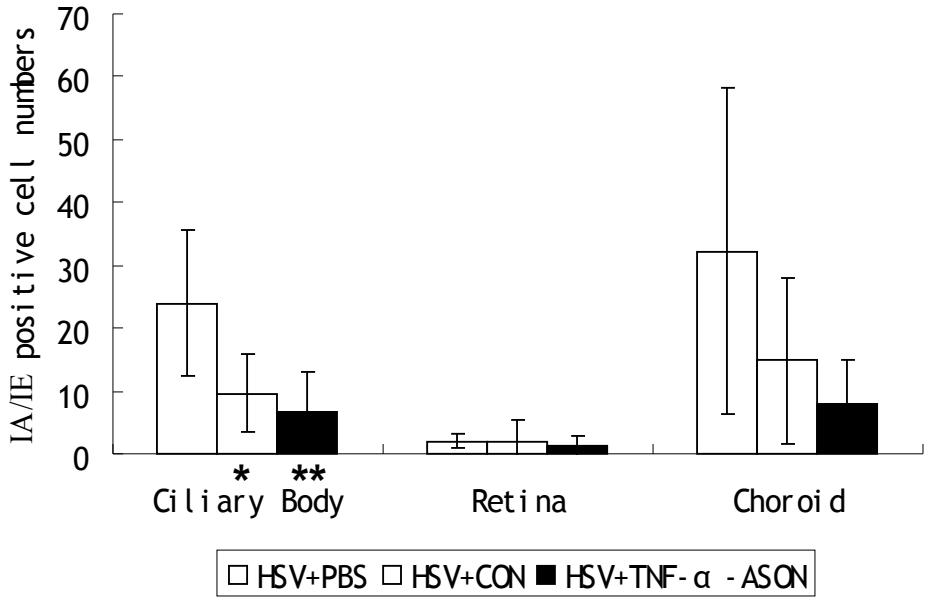

Fig 19 Number of IA/IE positive cells in ciliary body, retina and choroid on day 8 in the different treatment groups. Mice were infected with 2×10^4 PFU of HSV in the right eyes on day 0. After subconjunctival injection with TNF-α-ASON, CON and PBS, the left eyes were obtained, sectioned and assayed with immunohistochemistry. The number of IA/IE positive cells was counted in a high-power field. (magnification, ×400). Animals treated with TNF-α-ASON and CON had significantly fewer IA/IE positive cells than PBS treatment group in ciliary body. Mean ± SD. * $P<0.05$ compared with PBS group.

Figure 20

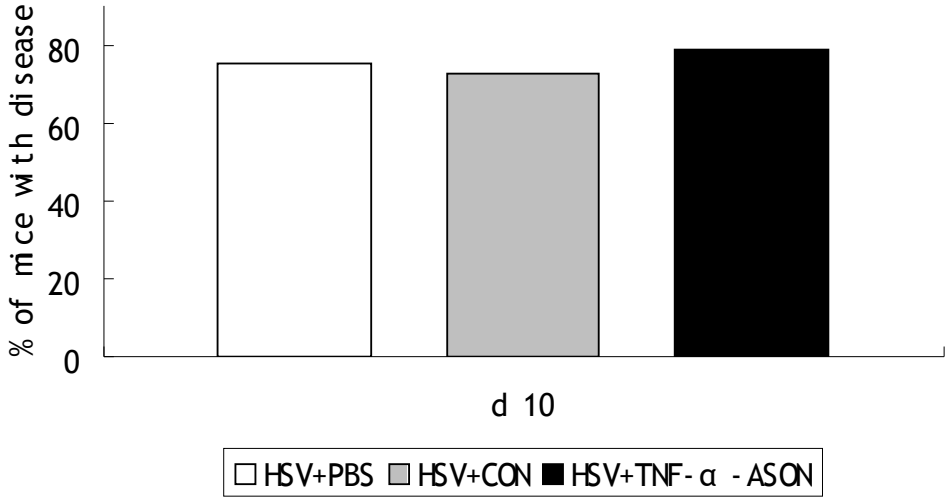

Fig 20 Clinical incidence of retinitis on day 10 after subconjunctival treatment. Mice were infected with 2×10^4 PFU of HSV into right eyes on day 0. After subconjunctival injection with TNF-α-ASON, CON or PBS, the left eyes were examined on day 10. There was no significant difference between TNF-α-ASON, CON and PBS treatment group.

Figure 21

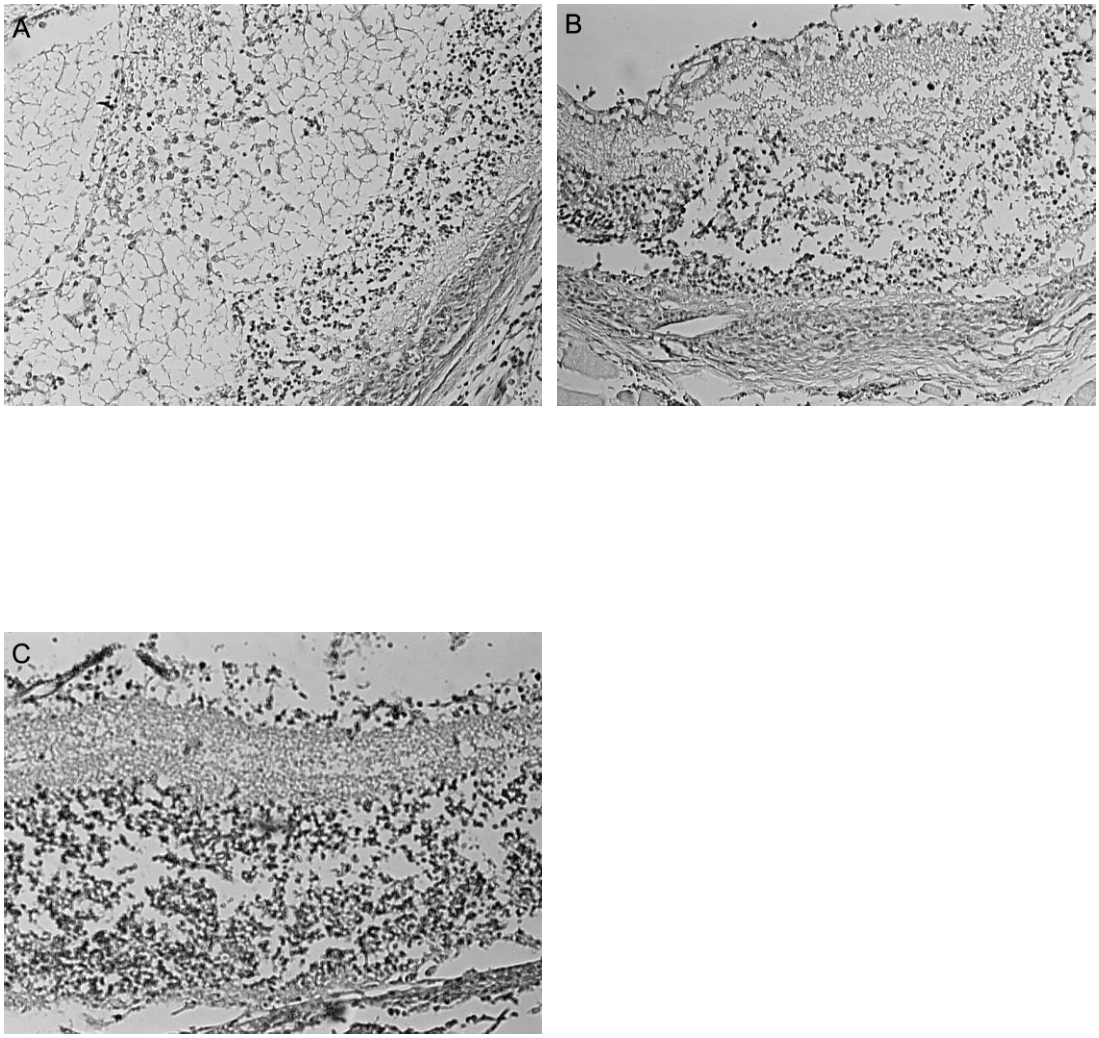

Fig 21　Histological findings in BALB/c mice on day 10 after HSV-1 infection. Mice were infected with 2×10^4 PFU of HSV in the right eyes on day 0. After subconjunctival injection with TNF-α-ASON and PBS, the left eyes were harvested, sectioned and stained with hematoxylin and eosin (HE). (A) Treatment with PBS: severe inflammatory cell infiltration and loss normal retinal architecture. (B) CON

treatment: severe inflammatory cell infiltration and loss of normal retinal architecture (C) Treatment with TNF-α-ASON: severe inflammatory cell infiltration and loss of normal retinal architecture. (magnification, ×250).

Figure 22

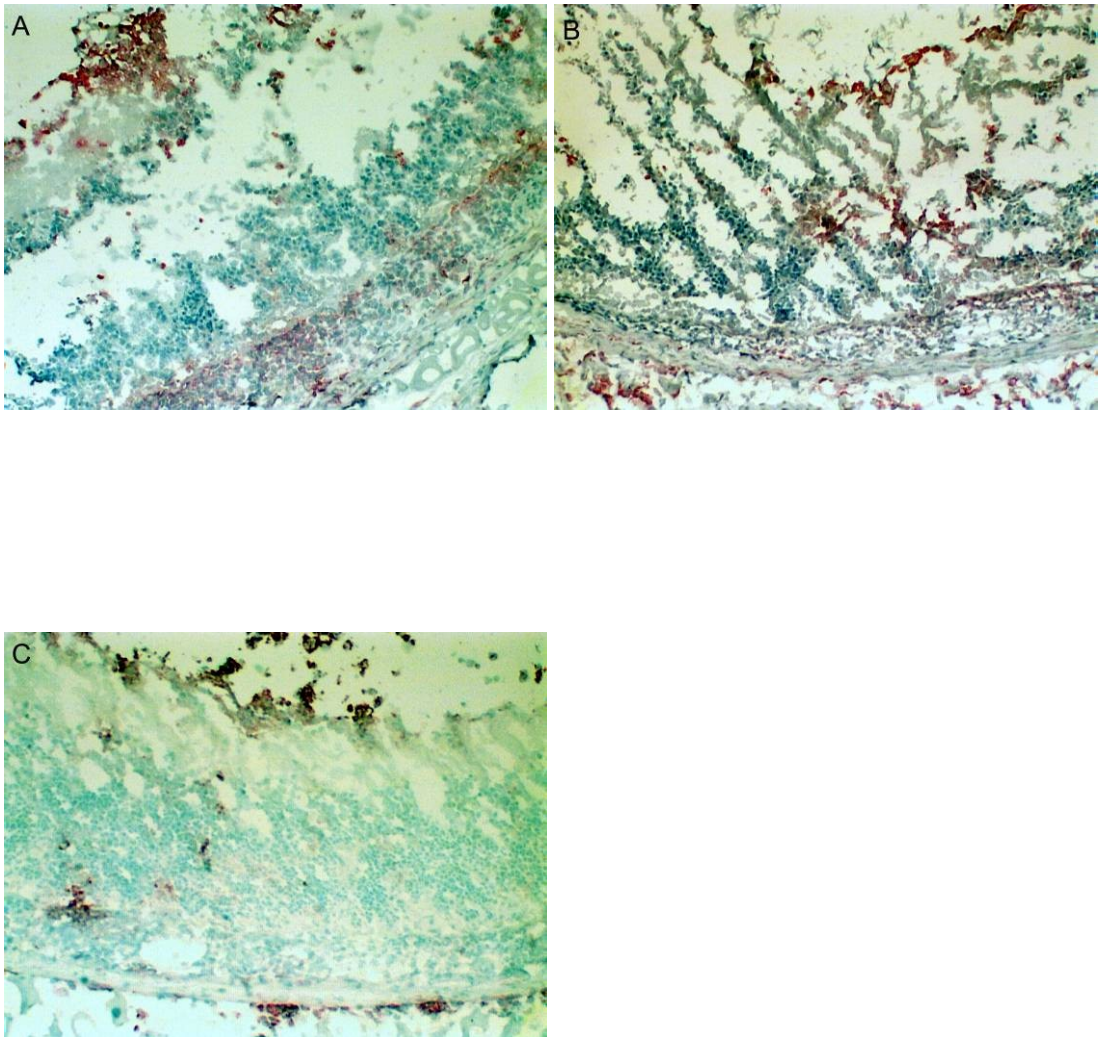

Fig 22 Immunohistochemical findings in BALB/c mice on day 10 after HSV-1 infection. Mice were infected with 2×10^4 PFU of HSV into right eyes on day 0. After subconjunctival injection with TNF-α-ASON, CON and PBS, the left eyes were harvested, cut into sections and stained with mAb directed against CD11b. (A) Mice reated with PBS had severe CD11b positive cell infiltration and loss of normal retinal

architecture. (B) Mice treated with CON had severe CD11b positive cell infiltration and loss of normal retinal architecture. (C) Mice treated with TNF-α-ASON had mild CD11b positive cell infiltration and loss normal retinal architecture. (magnification, ×250).

Figure 23

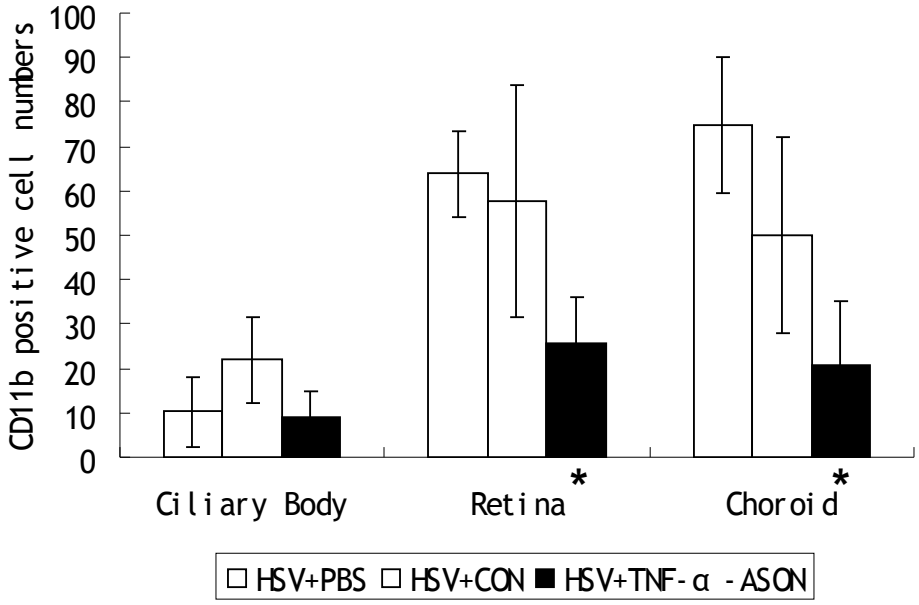

Fig 23 Number of CD11b positive cells in ciliary body, retina and choroid on day 10 in the different treatment groups. Mice were infected with 2×10^4 PFU of HSV in right eyes on day 0. After subconjunctival injection with TNF-α-ASON, CON and PBS, the left eyes were obtained, sectioned and processed by immunohistochemistry. The number of CD11b positive cells was counted in a high-power field. (magnification, ×400). Animals treated with TNF-α-ASON had significantly fewer CD11b positive cells than PBS treatment group in retina and choroid. Mean ± SD. * $P<0.05$ compared with PBS group.

Figure 24

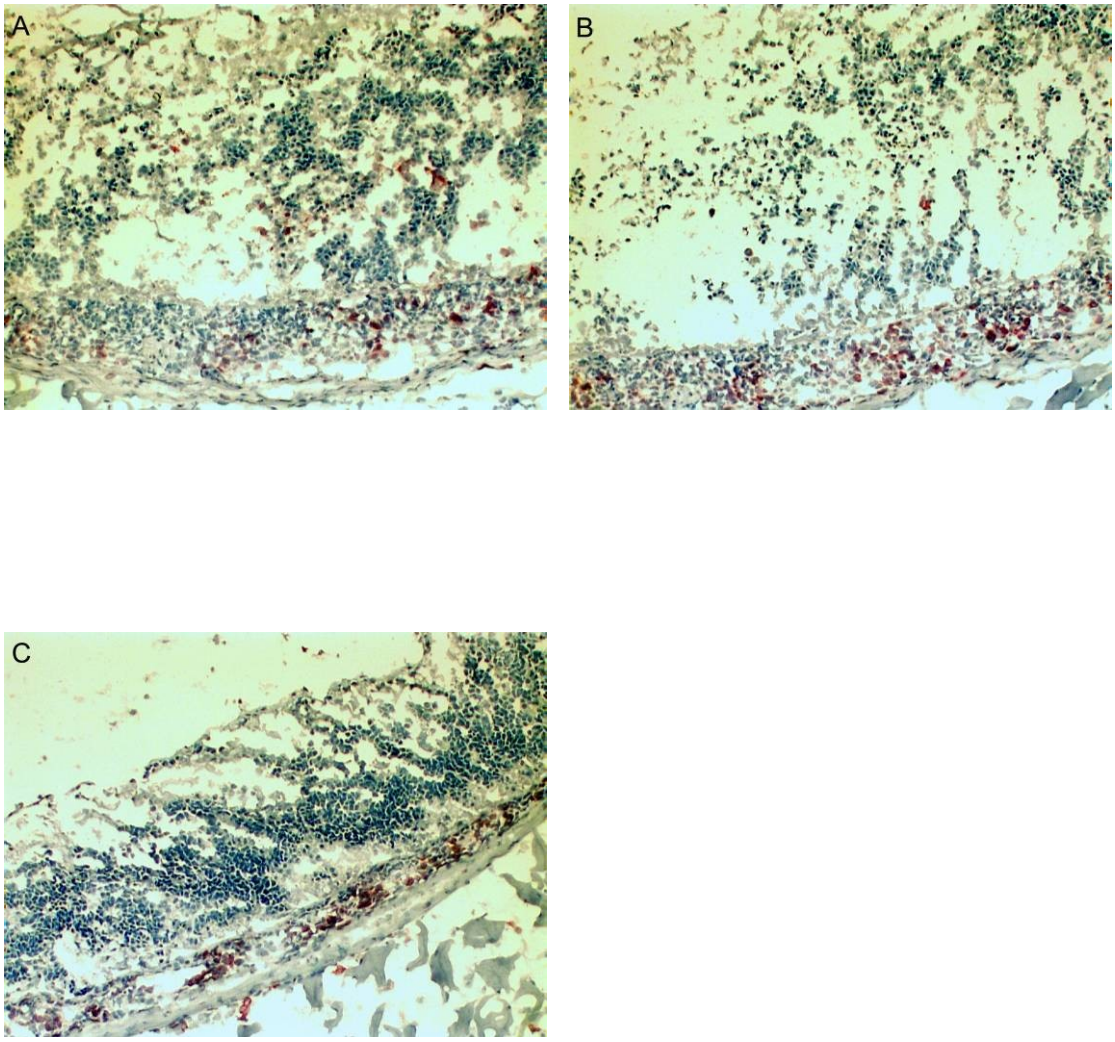

Fig 24 Immunohistochemical findings in BALB/c mice on day 10 after HSV-1 infection. Mice were infected with 2×10^4 PFU of HSV in the right eyes on day 0. After subconjunctival injection with TNF-α-ASON, CON and PBS, the left eyes were harvested, sectioned and stained with mAb directed against CD3. (A) Mice after treatment with PBS had severe CD3 positive cell infiltration. (B) Mice after treatment

with CON had severe CD3 positive cell infiltration in choroid. (C) Mice after treatment with TNF-α-ASON had severe CD3 positive cells infiltration. (magnification, ×250).

Figure 25

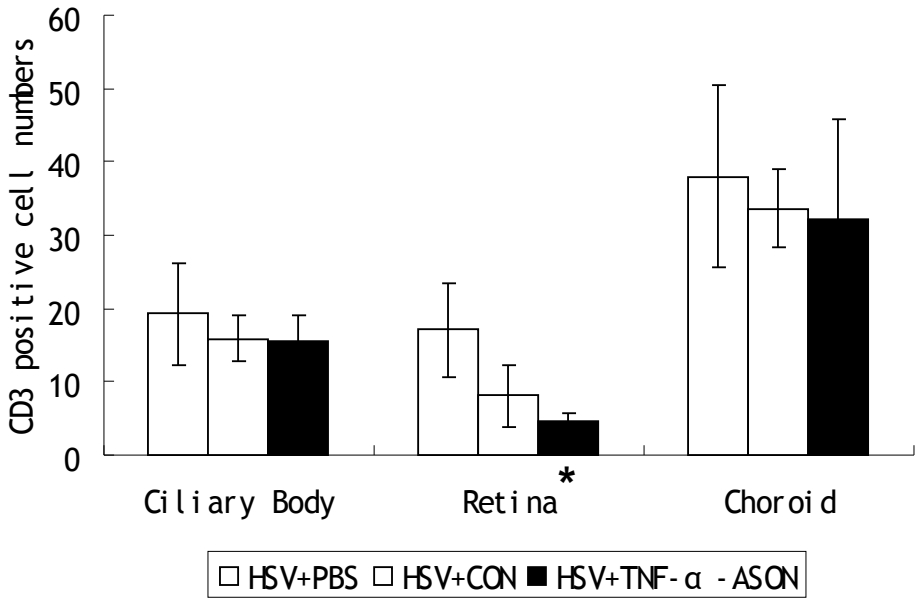

Fig 25 Number of CD3 positive cells in ciliary body, retina and choroid on day 10 in the different treatment groups. Mice were infected with 2×10^4 PFU of HSV in the right eyes on day 0. After subconjunctival injection with TNF-α-ASON, CON and PBS, the left eyes were obtained, sectioned and stained with mAb directed against CD11b. The number of CD11b positive cells was counted in a high-power field. (magnification, ×400). Animals treated with TNF-α-ASON had significantly reduced number of CD3 positive cells in the retina than PBS treatment group. Mean ± SD. * $P<0.05$ compared with PBS group.

Figure 26

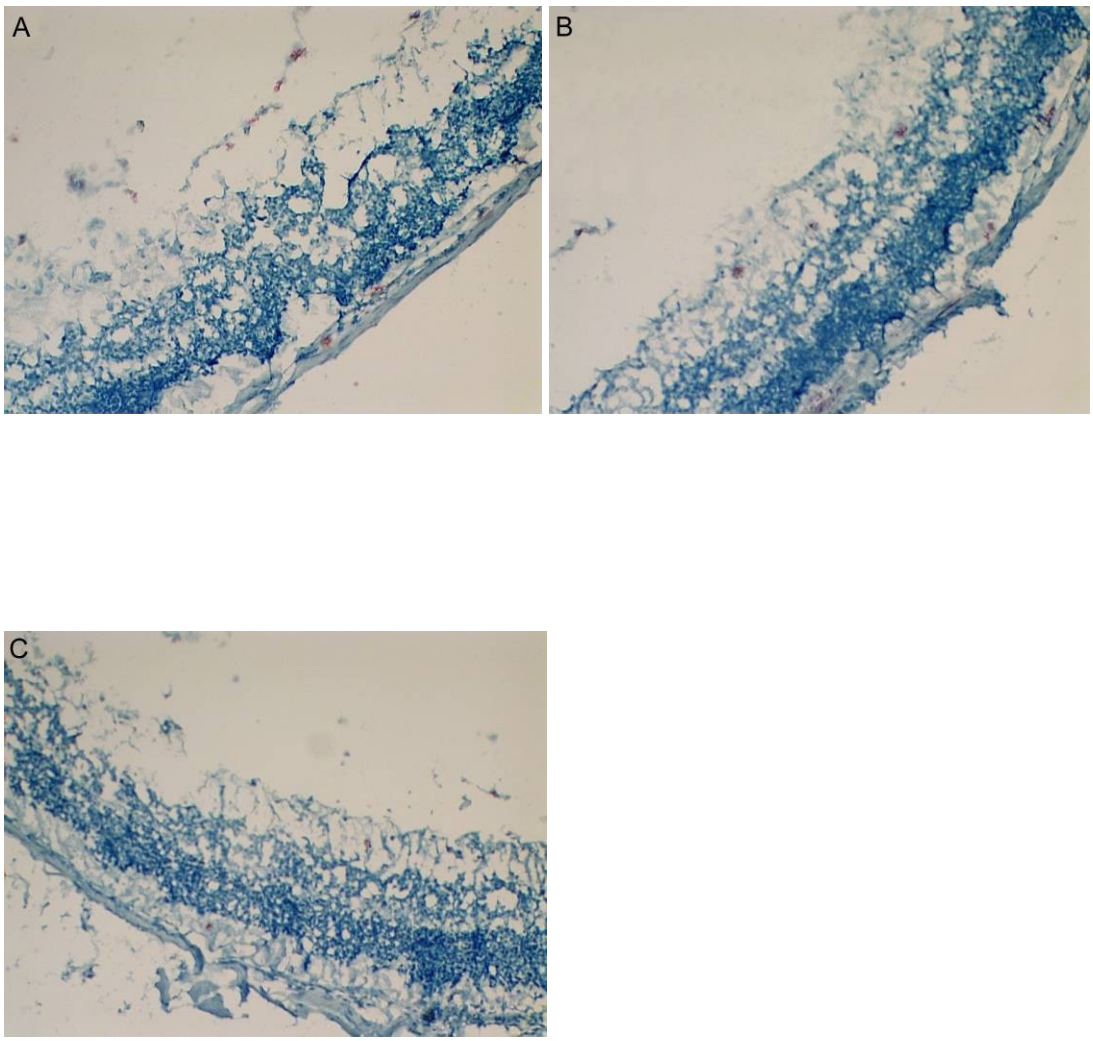

Fig 26 Immunohistochemical findings in BALB/c mice on day 10 after HSV-1 infection. Mice were infected with 2×10^4 PFU of HSV in the right eyes on day 0. After subconjunctival injection with TNF-α-ASON, CON and PBS. mAb against F4/80. (A) After treatment with PBS: severe F4/80 positive cell infiltration. (B) After treatment with CON: mild F4/80 positive cell infiltration. (C) After treatment with

TNF-α-ASON: few F4/80 positive cells. (magnification, ×250).

Figure 27

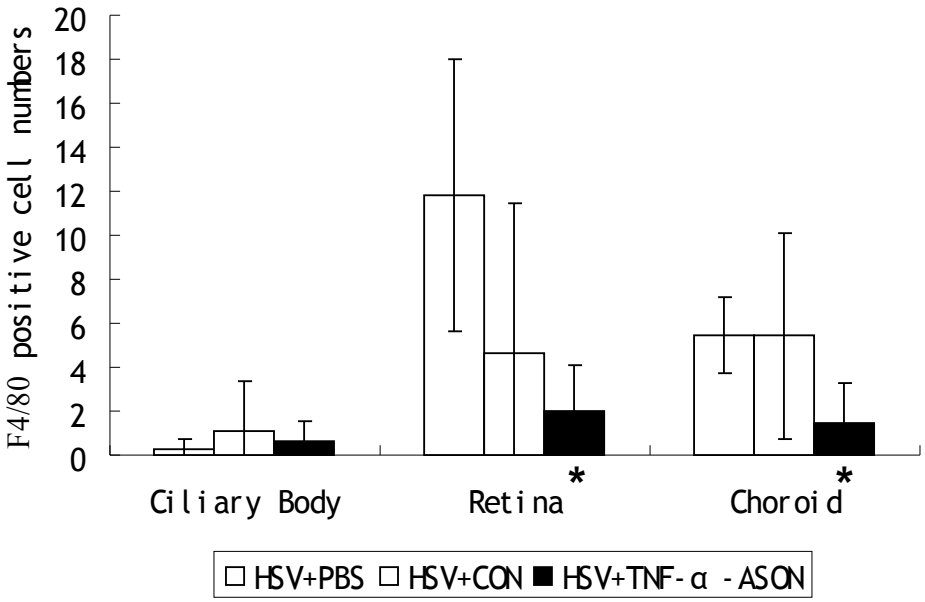

Fig 27 Number of F4/80 positive cells in ciliary body, retina and choroid on day 10 in the different treatment groups. Mice were infected with 2×10^4 PFU of HSV in the right eyes on day 0. Subconjunctival injection with TNF-α-ASON, CON and PBS; day 10. High-power field. (magnification, ×400). Animals treated with TNF-α-ASON had significantly fewer F4/80 positive cells than PBS treatment group in retina and choroid. Mean ± SD. * $P<0.05$ compared with PBS group.

Figure 28

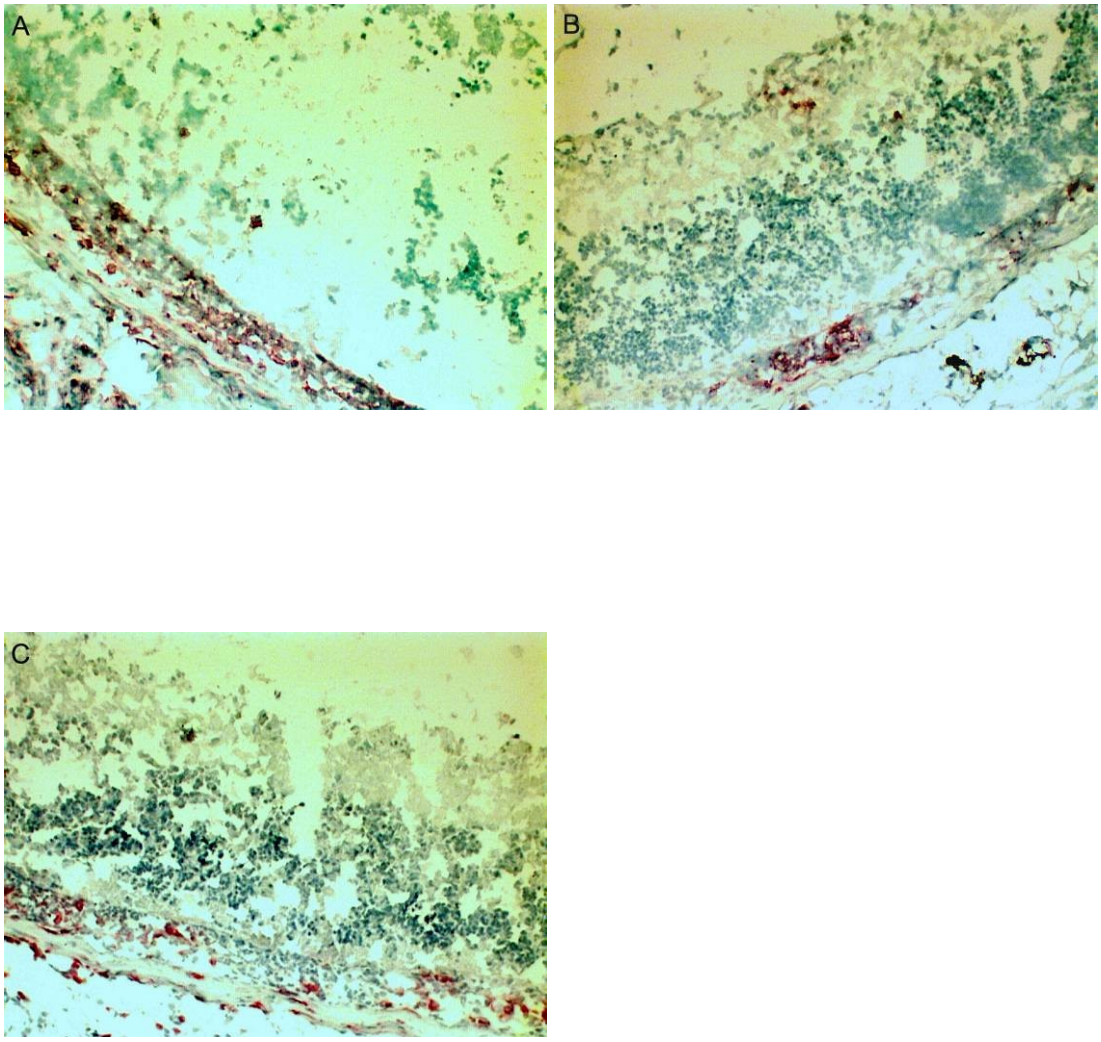

Fig 28 Immunohistochemical findings in BALB/c mice on day 10 after HSV-1 infection. (A) Treatment with PBS: heavy IA/IE positive cell infiltration in choroid. (B) Treatment with PBS: severe IA/IE positive cell infiltration in choroid. (C) Treatment with TNF-α-ASON: severe IA/IE positive cell infiltration in choroid. (magnification, ×250).

Figure 29

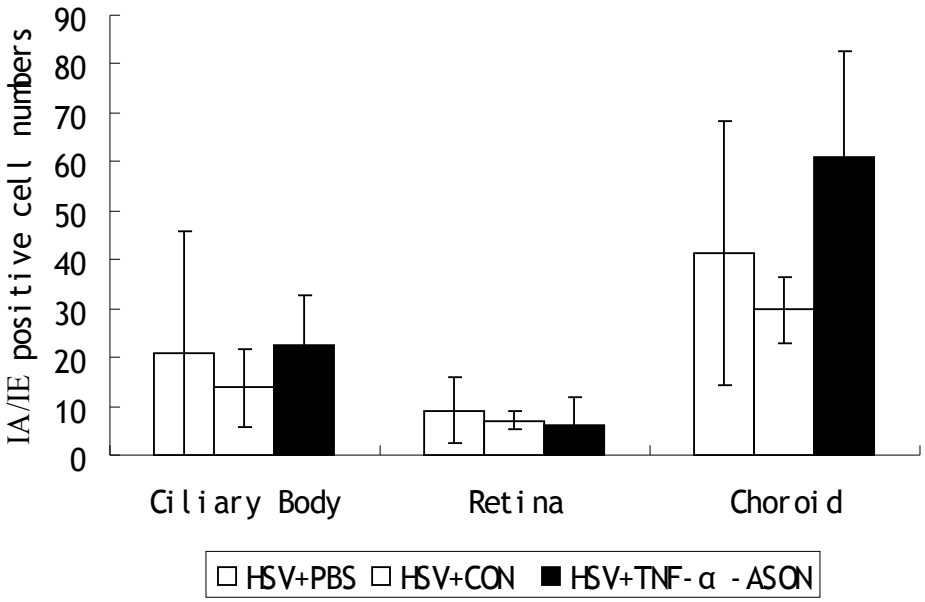

Fig 29 Number of IA/IE positive cells in ciliary body, retina and choroid on day 10 in the different treatment groups. (magnification, ×400). No significant difference between the groups. Mean ± SD.

Figure 30

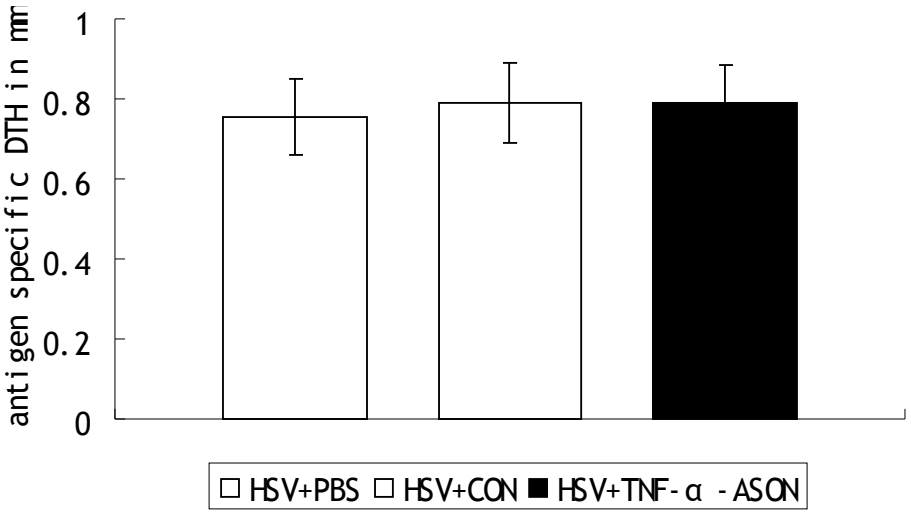

Fig 30 DTH assay in BALB/c mice on day 10 after HSV-1 infection. Mice were infected with 2×10^4 PFU of HSV in the right eyes on day 0. After subconjunctival injection with TNF-α-ASON, CON or PBS, HSV-1-specific DTH was calculated on day 10. No difference between the groups. Mean±SD.

Figure 31

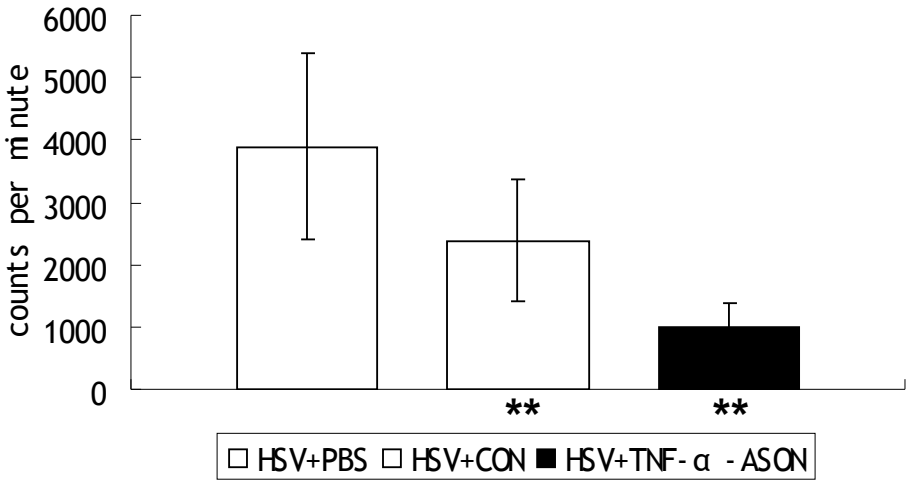

Fig 31 T cell proliferation in BALB/c mice on day 10 after HSV-1 infection. Mice were infected with 2×10^4 PFU of HSV in the right eyes on day 0. After subconjunctival injection with TNF-α-ASON, CON or PBS, the left regional lymph nodes were examined on day 10. Stimulation with UV-inactivated HSV-1, counts per minute measured as uptake of [^{3}H]thymidine. Sc TNF-α-ASON injection reduced HSV-1-specific T cell proliferation. Mean± SD.** $P<0.01$ compared with PBS group.

Figure 32

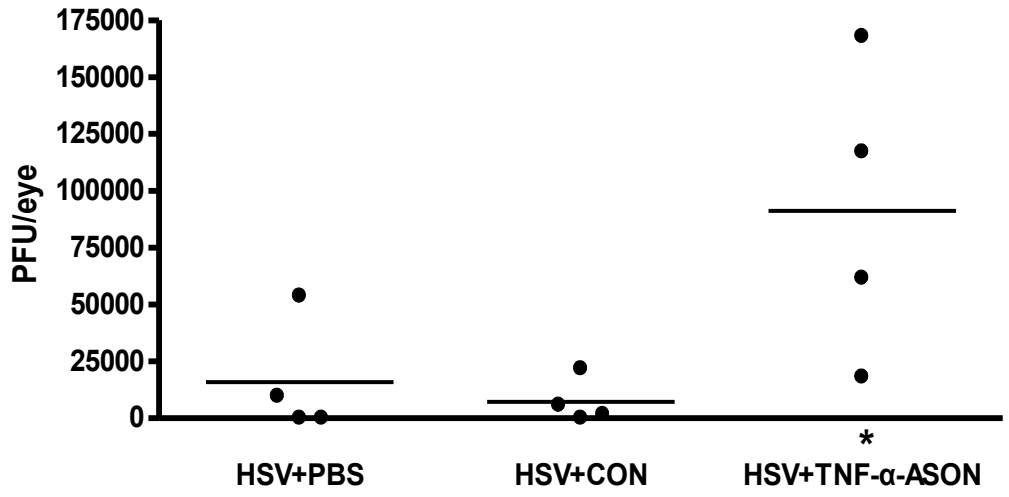

Fig 32 Plaque Forming Unit assay in BALB/c mice on day 10 after HSV-1 infection. Mice were infected with 2×10^4 PFU of HSV in the right eyes on day 0. After subconjunctival injection with TNF-α-ASON, CON or PBS, the PFU in left eye were calculated on day 10. The virus titers were increased in the TNF-α-ASON treatment group. * $P<0.05$ compared with PBS and CON group. Crossbar indicates the mean.

Figure 33

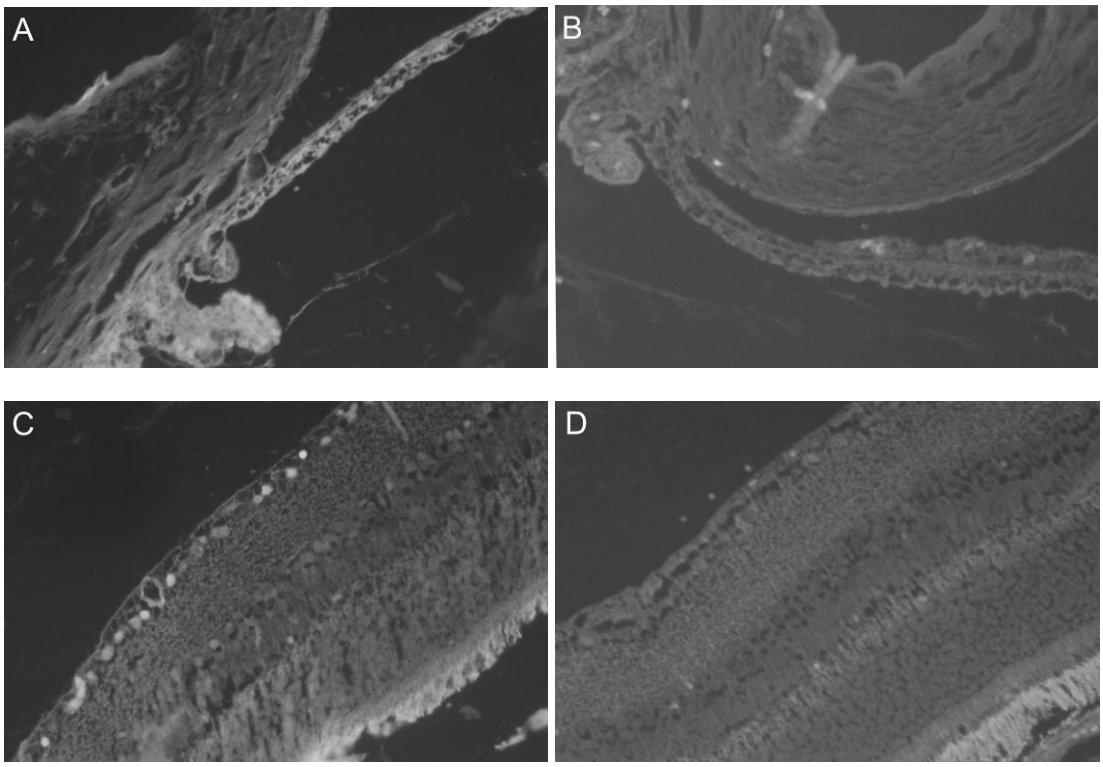

Fig 33 Fluorescence staining of eyes 1 day after intraocular FITC-ASON injection. After 2μl FITC-TNF-α-ASON was injected into the vitreous, the eyes were collected, imbedded in paraffin and 5μm sections were prepared. (A) The endothelium of cornea, iris and ciliary body were strongly fluorescent positive. (B) No fluorescent was found in anterior segment of the negative control. (C) Ganglionic cells of the retina and retinal vessels were strongly fluorescent positive. (D) No fluorescent was found in posterior segment of the negative controls. (magnification, ×400).

Figure 34

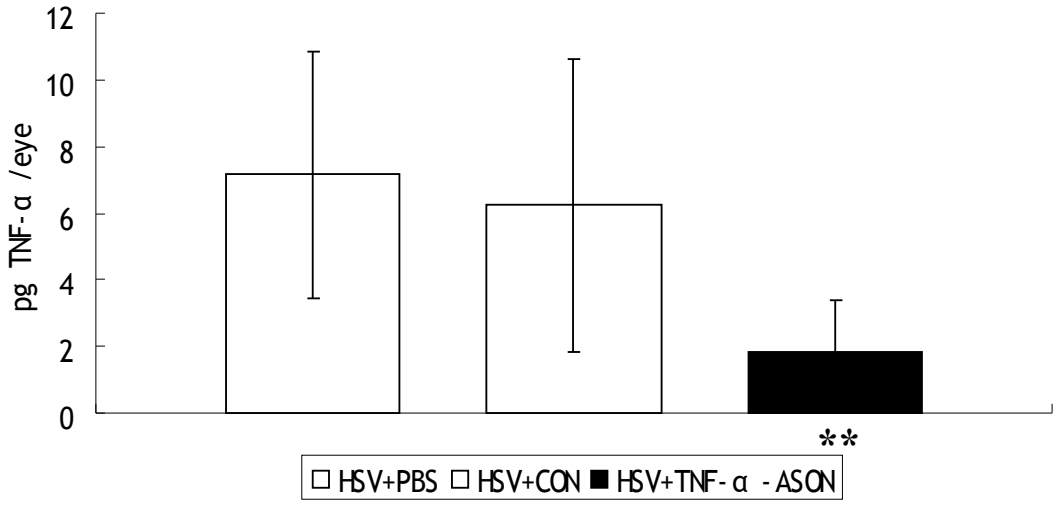

Fig 34 TNF-α content in the eyes by ELISA assay in the different treatment groups on day 8. Mice were infected with 2×10^4 PFU of HSV in the right eyes on day 0. After intraocular injection with TNF-α-ASON, CON or PBS three times, the content of TNF-α in left eye was examined on day 8. The TNF-α content was significantly reduced after TNF-α-ASON treatment as compared to the PBS and CON treatment group. ** $P<0.01$ compared with CON and PBS group.

Figure 35

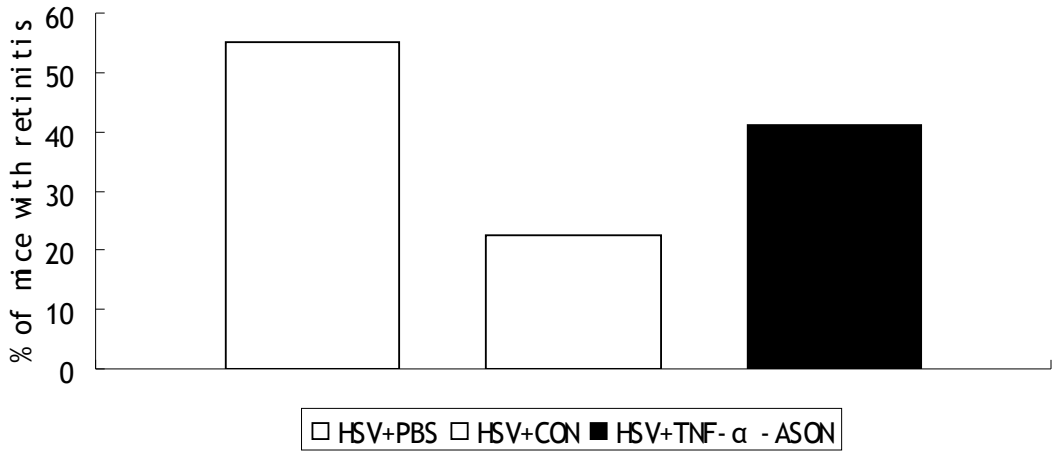

Fig 35 Incidence of retinitis on day 8 after intraocular treatment. Mice were infected with 2×10^4 PFU of HSV into right eyes on day 0. After 3x intraocular injection of TNF-α-ASON, CON or PBS, the left eyes were examined on day 8. There was no significant difference between the groups.

Figure 36

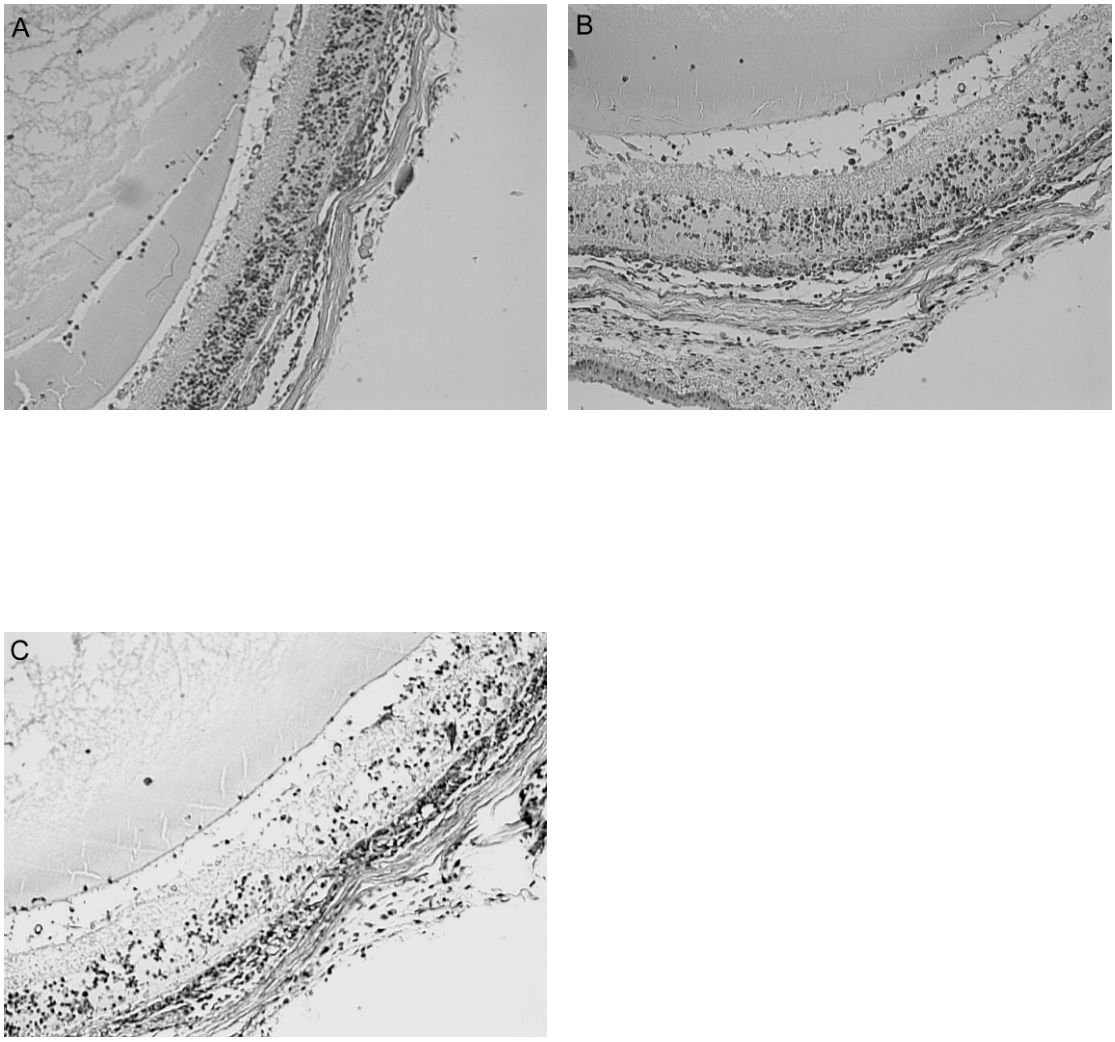

Fig 36 Histological findings in BALB/c mice on day 8 after HSV-1 infection. 3x intraocular injection with TNF-α-ASON, CON and PBS the left eyes. (A) PBS: had severe inflammatory cell infiltration and loss of normal retinal architecture. (B) CON: severe inflammatory cell infiltration and loss of normal retinal architecture. (C) TNF-α-ASON: severe inflammatory cell infiltration and loss normal retinal architecture.

(magnification, ×250).

Figure 37

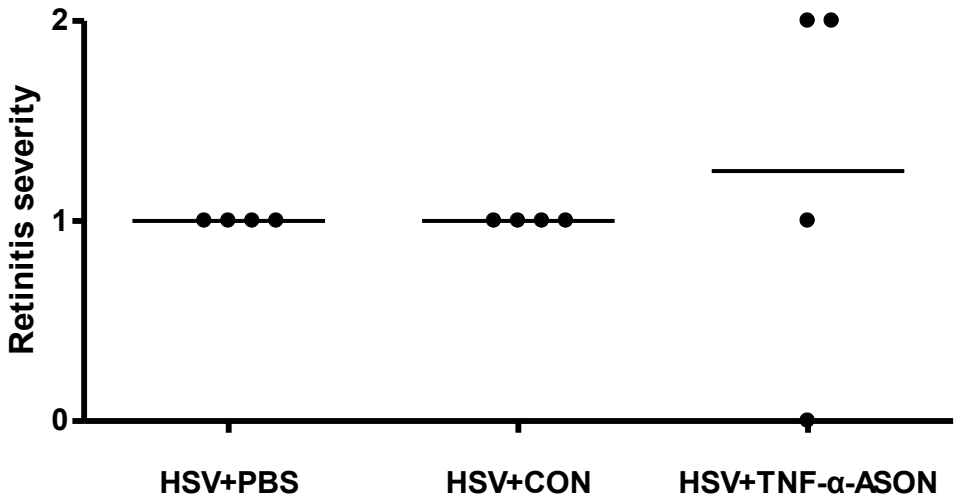

Fig 37 Degree of retinitis on day 8 in the different treatment groups. Mice were infected with 2×10^4 PFU of HSV into right eyes on day 0. 3x intraocular injection with TNF-α-ASON, CON and PBS. Hematoxylin and eosin (HE). The retina was graded from 0 to 2+, depending on the retinitis and necrosis extension. There was no significant difference between the treatment groups. Crossbar indicated the means.

Figure 38

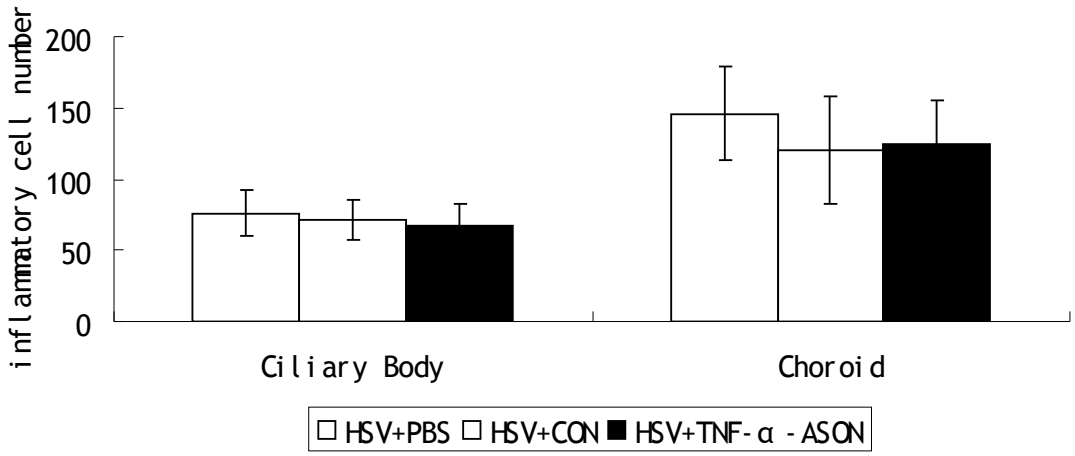

Fig 38 Number of inflammatory cells in ciliary body and choroid on day 8 in the different treatment groups. Mice were infected with 2×10^4 PFU of HSV in the right eyes on day 0. After 3x intraocular injection with TNF-α-ASON, PBS and CON. Hematoxylin and eosin (HE). The number of inflammatory cells was counted in a high-power field. (magnification, ×400). The number of inflammatory cells in ciliary body and choroid were not significantly different in the treatment groups. Data are the mean ± SD.

Figure 39

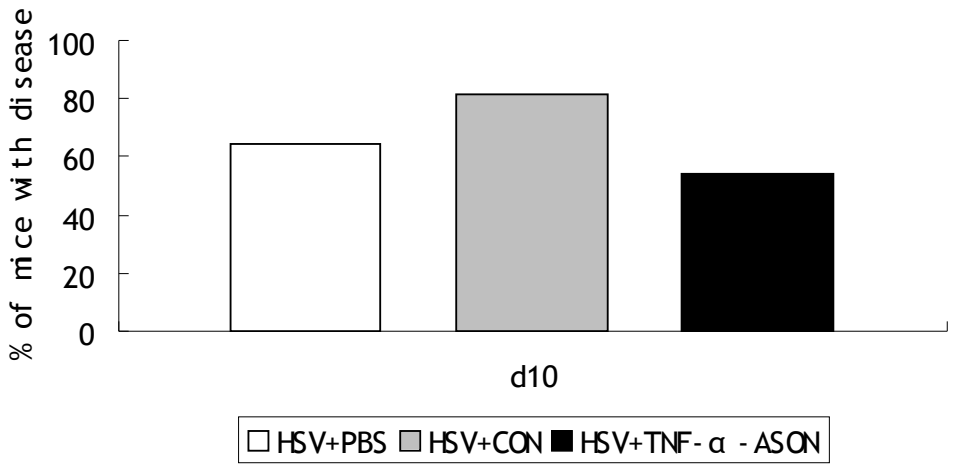

Fig 39 Incidence of retinitis on day 10 after 3x intraocular treatment. Mice were infected with 2×10^4 PFU of HSV in the right eyes on day 0. After 3x intraocular injection with TNF-α-ASON, CON or PBS, the left eyes were examined on day 10. There was no significant difference between TNF-α-ASON, CON and PBS treatment groups.

Figure 40

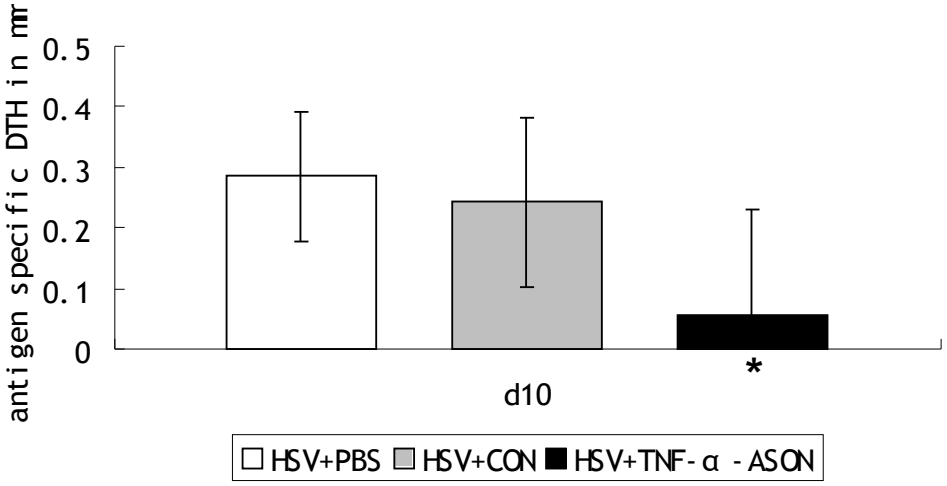

Fig 40 DTH assay in BALB/c mice on day 10 after HSV-1 infection. Mice were infected with 2×10^4 PFU of HSV into right eyes on day 0. After 3x intraocular injection with TNF-α-ASON, CON or PBS, the HSV-1-specific DTH was determined on day 10. The mice in TNF-α-ASON group had significantly reduced DTH reaction as compared to control groups. Mean±SD. * $P<0.05$ compared with PBS group.

Figure 41

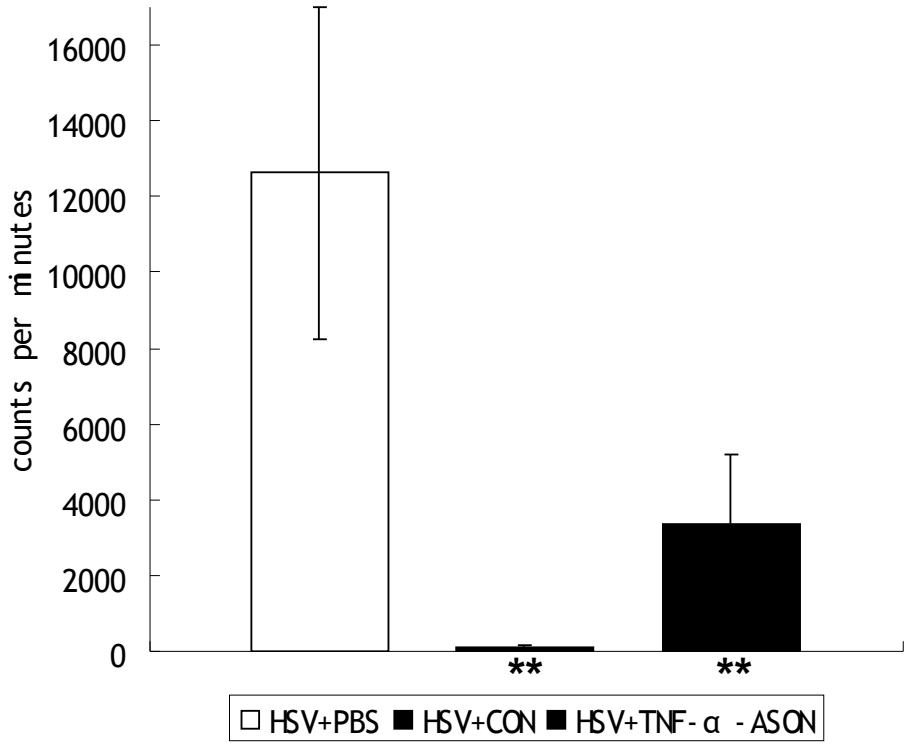

Fig 41 HSV-1 T cell proliferation assay in BALB/c mice on day 10 after HSV-1 infection. Mice were infected with 2×10^4 PFU of HSV in the right eyes on day 0. After 3x intraocular injection with TNF-α-ASON, CON or PBS, the left regional lymph nodes were examined on day 10. Stimulation with UV-inactivated HSV-1, counts per minute measured as uptake of [^{3}H]thymidine. TNF-α-ASON injection reduced the T cell proliferation. Mean± SD.** P<0.01 compared with PBS group.

8. Abbreviations

AC	anterior chamber
ACAID	anterior chamber-associated immune deviation
AH	anterior hypothalamic nucleus
ARN	acute retinal necrosis
APC	antigen presenting cell
APES	3-aminopropyltriethoxysilane
ASON	antisense oligonucleotides
BARN	bilateral acute retinal
CB	ciliary body
CG	ciliary ganglion
CMV	cytomegalovirus
CNS	central nervous system
CON	control oligonucleotides
DNA	deoxyribonucleic acid
DTH	delayed type hypersensitivity
EAU	experimental autoimmune uveoretinitis
EW	Edinger-Westphal nucleus
FCS	fetal calf serum
FITC	fluorescein isothiocyanate
GCL	ganglion cell layer
HRP	horseradish peroxidase
HSK	herpetic stromal keratitis
HSV	herpes simplex virus
IFN	interferon
LGN	lateral geniculate nucleus
IL	interleukin
LN	lymph node
MIP	macrophage inflammatory protein
MMP	matrix metalloproteinase
MPA	medial pretectal area
NK	nature kill cells
NO	nitric oxide
NOS2	nitric oxide synthase
OC	optic chiasm
OM	nucleus of the oculomotor nerve
ON	optic nerve
PBS	phosphate buffered saline
PFU	plaque forming units
PH	paraventricular hypothalamic nucleus
PI	post inoculation
PMN	polymorphonuclear leukocytes
PVR	proliferative vitreoretinopathy
RNA	ribonucleic acid
ROS	reactive oxygen species
RPE	retinal pigment epithelium

S.C.	subconjunctival
SCN	suprachiasmatic nucleus
siRNA	short interfering RNA
TNF-α	tumor necrosis factor alpha
UV	ultraviolet
VZV	varicella zoster virus

9. Acknowledgement

This thesis was finished under the guide of Prof. Dr. Arnd Heiligenhaus. I do appreciate his fastidiously teaching and strictly guide to the scientific research during the period of my study, it will be useful forever in my career. Also I thank him for his kindly supports to my study in Germany, it is an excellent opportunity for me to learn many new techniques and study in the novel fields.

I am very grateful for my parents, my relationship in my big family and Ji. Without their sustained supports, it would be unimaginable for me to finish the work during two years.

I further thank my colleagues, Dr. Dirk Bauer, Ms. Pia Hermans, Dr. Susanne Wasmuth and Ms. Hanna Baehler. They gave me kind help and instructions in my work.

Additionally, I present a lot of appreciations to all my friends in China, Germany and other countries who helped and encouraged me to perform my work in Germany.

10. Curriculum vitae

Name:	Jin Li
Sex:	Male
Date of birth:	July 28,1973
Place of birth:	Wuhan, Hubei, China
Nationality:	China
Marital status:	Single
Corresponding address	Münster
Email:	blackli@hotmail.com

Education:

1985-1991	Wuhan 26th Middle School, Wuhan
1991-1996	Undergraduate student at Tongji Medical University. Bachelor's degree was granted in July, 1996.
1999-2002	Graduate student at Tongji Medical University. Master's degree was granted in July, 2002.
2004-present	Postgraduate student of Porf. Dr. Arnd Heiligenhaus, Department of Ophthalmology, University of Duisburg-Essen, Germany.

Professional experience:

1995-1996	Intern, Tongji Hospital, Wuhan
1996-2001	Resident, Department of Ophthalmology, Tongji Hospital, Wuhan
2001-2004	Attending Physician, Department of Ophthalmology, Tongji Hospital, Wuhan